

High Gradient Structures and RF Systems for High Brightness Electron Linacs

Marco Diomede

Sapienza University (Rome, Italy)

INFN-LNF (Frascati, Italy)

Advisor

Massimo Ferrario (INFN-LNF)

Co-Advisor

David Alesini (INFN-LNF)

PhD in Accelerator Physics - Final Exam

Rome, Italy

18/02/2020

OUTLINE

- High brightness linacs
 - The EuPRAXIA@SPARC_LAB project
 - The CompactLight project
- Design and optimization of accelerating structures and power distribution network
 - EuPRAXIA@SPARC_LAB
 - CompactLight
 - Joining the projects

OUTLINE

- High brightness linacs
 - The EuPRAXIA@SPARC_LAB project
 - The CompactLight project
- Design and optimization of accelerating structures and power distribution network
 - EuPRAXIA@SPARC_LAB
 - CompactLight
 - Joining the projects

SPARC_LAB: A MULTI-DISCIPLINARY TEST FACILITY

⇒ **SPARC_LAB** is a multi-disciplinary test facility of the **INFN Frascati Labs** based on 2 pillars:

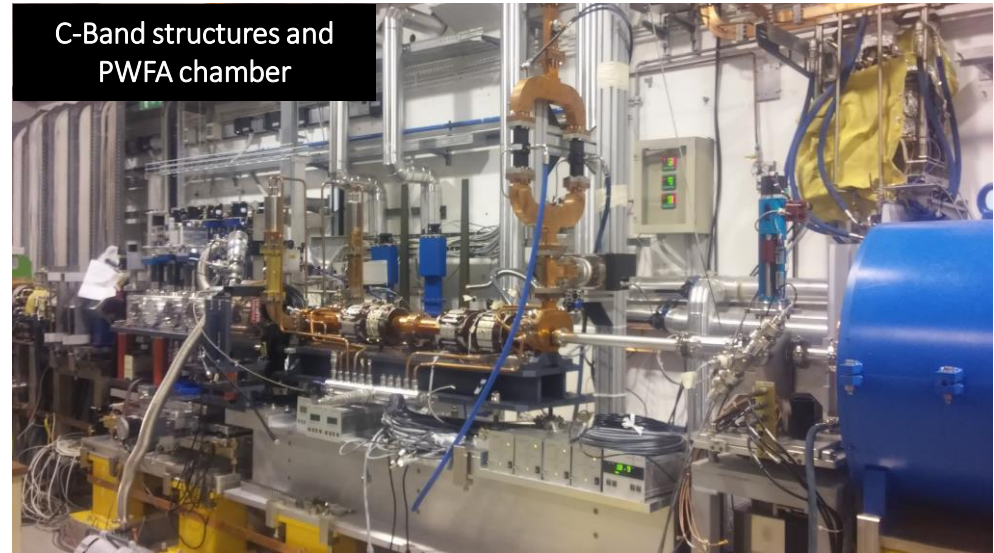
- a conventional **RF photo-injector (SPARC)**
- a **multi-hundred TW laser system (FLAME)**

⇒ The experimental activities cover various fields such as **FEL, THz radiation production, Thomson scattering, beam dynamics** and **beam diagnostics** studies.

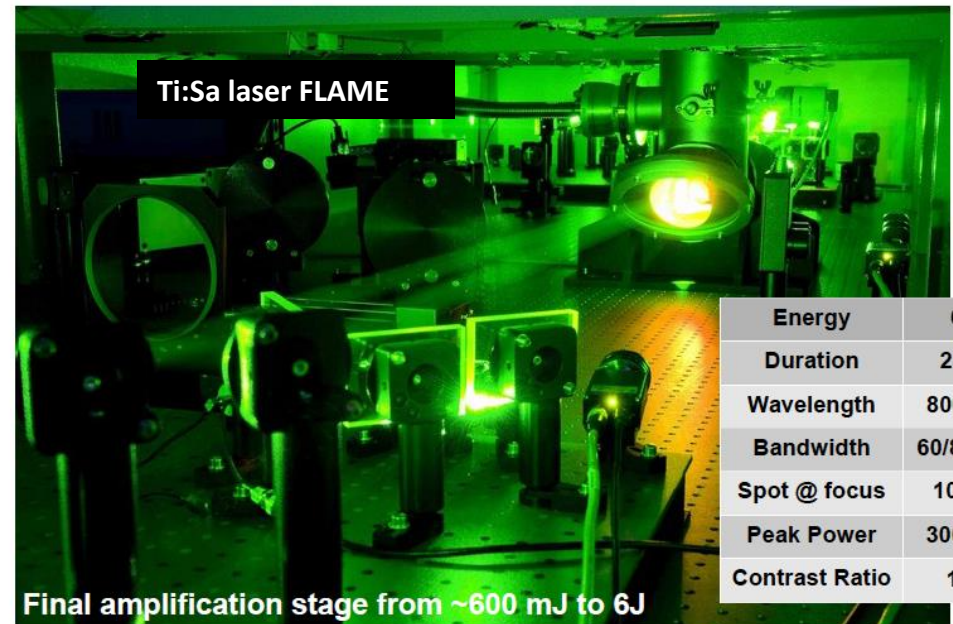
⇒ In the last years **plasma acceleration** research, in the **self-injection and external injection (both particle and laser driven)** modalities, has become a relevant part of the **SPARC_LAB** scientific program.



Capillary Discharge
at SPARC_LAB



C-Band structures and
PWFA chamber



Ti:Sa laser FLAME

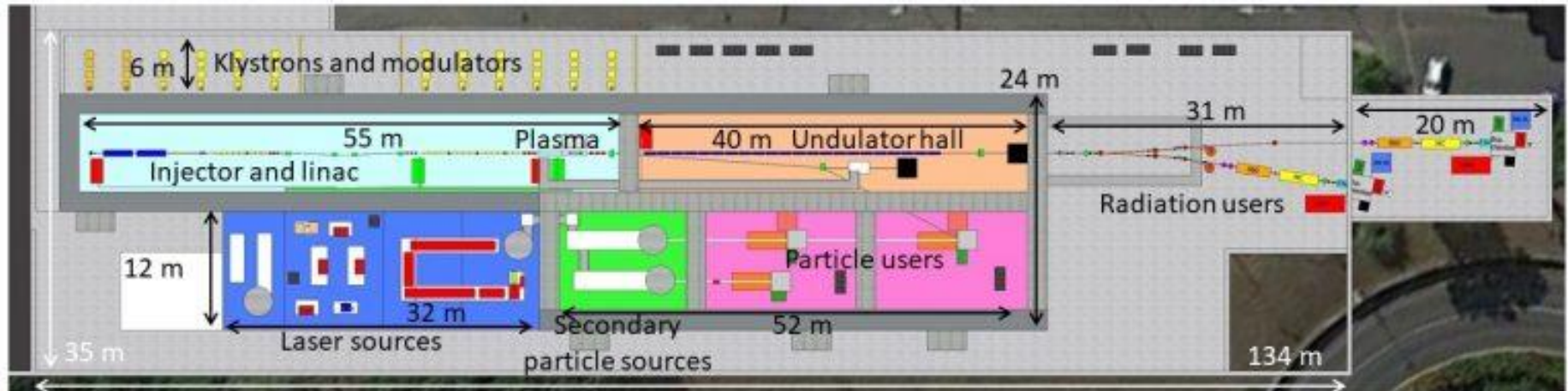
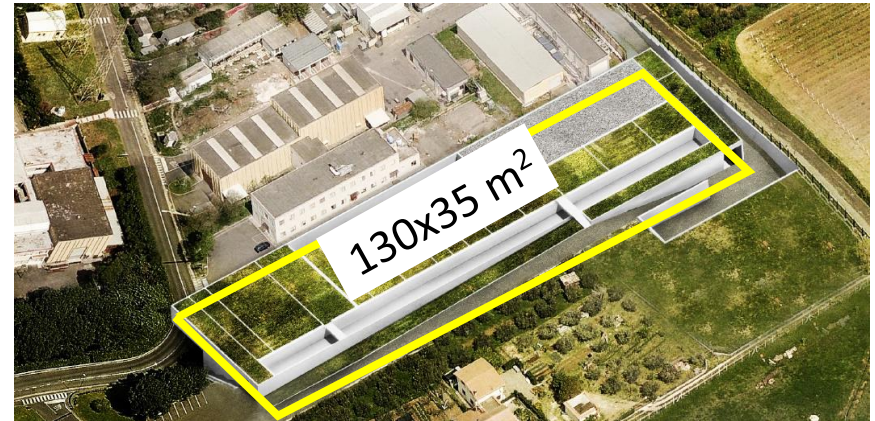
Final amplification stage from ~600 mJ to 6J

Energy	6 J
Duration	23 fs
Wavelength	800 nm
Bandwidth	60/80 nm
Spot @ focus	10 μ m
Peak Power	300 TW
Contrast Ratio	10^{10}

EuPRAXIA@SPARC_LAB: A COMPACT FEL SOURCE

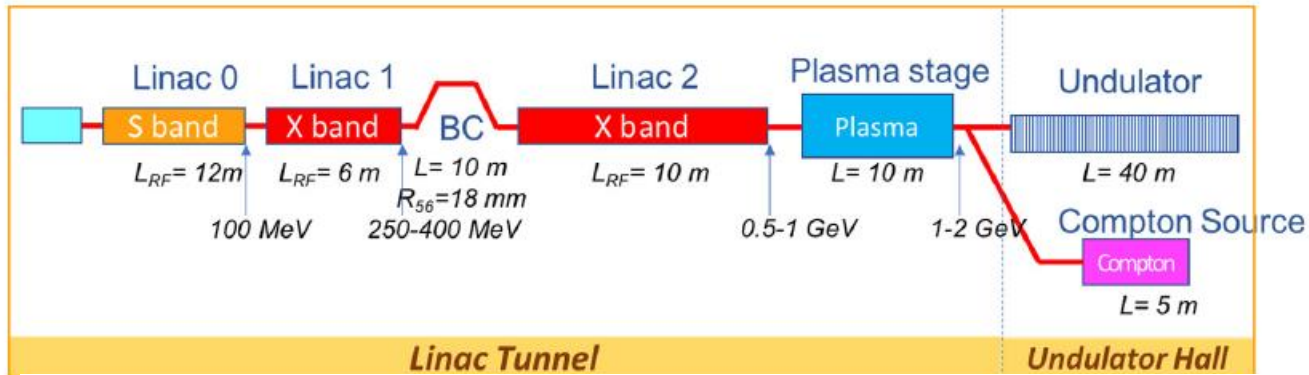
EuPRAXIA@SPARC_LAB project is a proposal for a new national facility as an expansion of the SPARC_LAB activities, based on the combination of a **high gradient compact linac and high-power lasers for plasma acceleration oriented to FEL with user beam line at 3 nm wavelength**, synergic with the EU EuPRAXIA Design study.

EuPRAXIA is a design study which goal is to demonstrate the feasibility to **drive an FEL** with a beam accelerated in a **plasma stage**.



M. Ferrario et al., EuPRAXIA@SPARC_LAB Design study towards a compact FEL facility at LNF, NIM A 909 (2018) 134–138

EuPRAXIA@SPARC_LAB: LAYOUT AND PARAMETERS



	Units	Full RF case	LWFA case	PWFA case
Electron Energy	GeV	1	1	1
Repetition Rate	Hz	10	10	10
RMS Energy Spread	%	0.05	0.025	??
Peak Current	kA	1.79	2.26	2.0
Bunch charge	pC	200	30	30
RMS Bunch Length	μm (fs)	16.7 (55.6)	2.14 (7.1)	3.82 (12.7)
RMS normalized Emittance	mm mrad	0.5	0.47	??
Slice Length	μm	1.66	0.5	1.2
Slice Charge	pC	6.67	18.7	8
Slice Energy Spread	%	0.02	0.015	0.034
Slice normalized Emittance (x/y)	mm mrad	0.35/0.24	0.45/0.465	0.57/0.615
Undulator Period	mm	15	15	15
Undulator Strength $K(a_w)$		0.978 (0.7)	1.13 (0.8)	1.13 (0.8)
Undulator Length	m	30	30	30
ρ (1D/3D)	$\times 10^{-3}$	1.55/1.38	2/1.68	2.5/1.8
Radiation Wavelength	nm (keV)	2.87 (0.43)	2.8 (0.44)	2.98 (0.42)
Photon Energy	μJ	177	40	6.5
Photon per pulse	$\times 10^{10}$	255	43	10
Photon Bandwidth	%	0.46	0.4	0.9
Photon RMS Transverse Size	μm	200	145	10
Photon Brilliance per shot	$(s\,mm^2\,mrad^2\,bw(0.1\%))^{-1}$	1.4×10^{27}	1.7×10^{27}	0.8×10^{27}

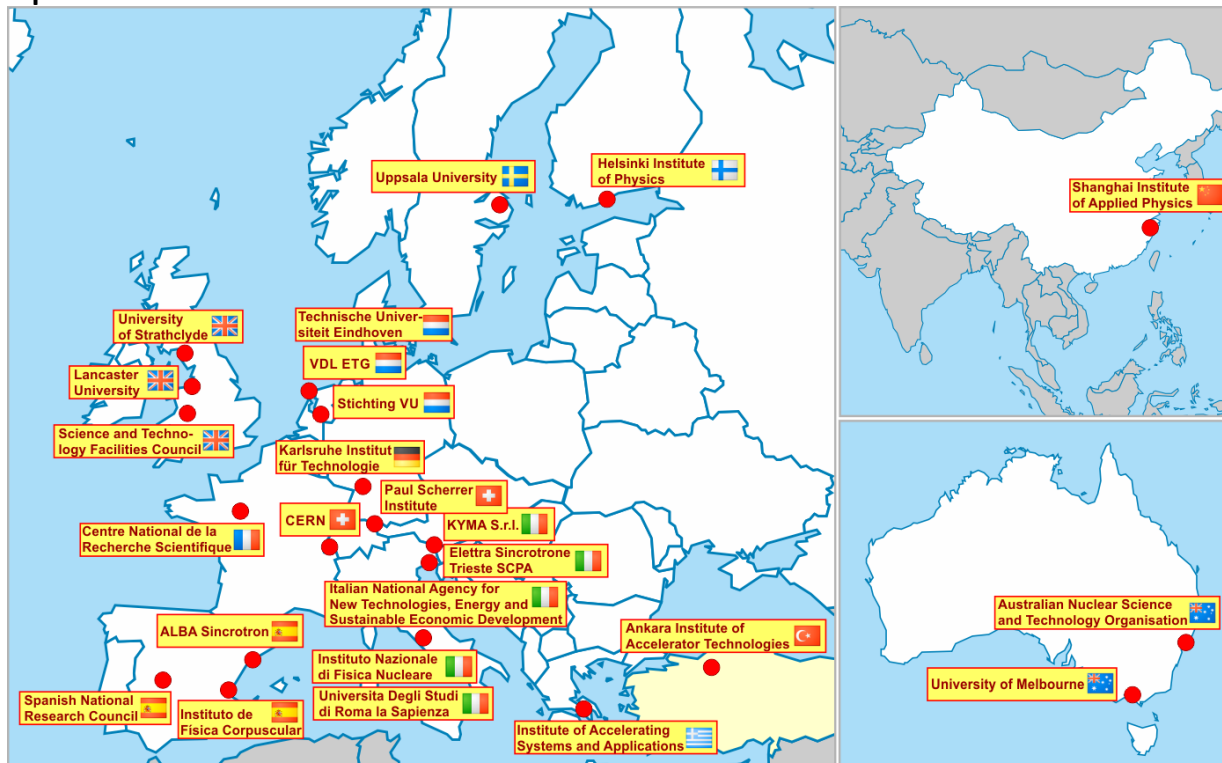
C. Vaccarezza et al., EUPRAXIA@SPARC_LAB: Beam dynamics studies for the X-band Linac, NIM A 909 (2018) 314–317
 EuPRAXIA@SPARC_LAB Conceptual Design Report, Tech. Rep. INFN -18-03/LNF, 2018

CompactLight: a compact & cost effective FEL facility

The key objective of the EU CompactLight Design Study is to demonstrate, through a **conceptual design**, the feasibility of an **innovative, compact and cost effective FEL facility** suited for **user demands** identified in the science case.

The goal is to design a **Hard X-ray Facility** using the very latest **concepts** for:

- High brightness electron photoinjectors
- Very high gradient accelerating structures
- Novel short period undulators



<http://www.compactlight.eu>

CompactLight: PARAMETERS AND PRELIMINARY LAYOUT

Main Parameters of the CompactLight FEL

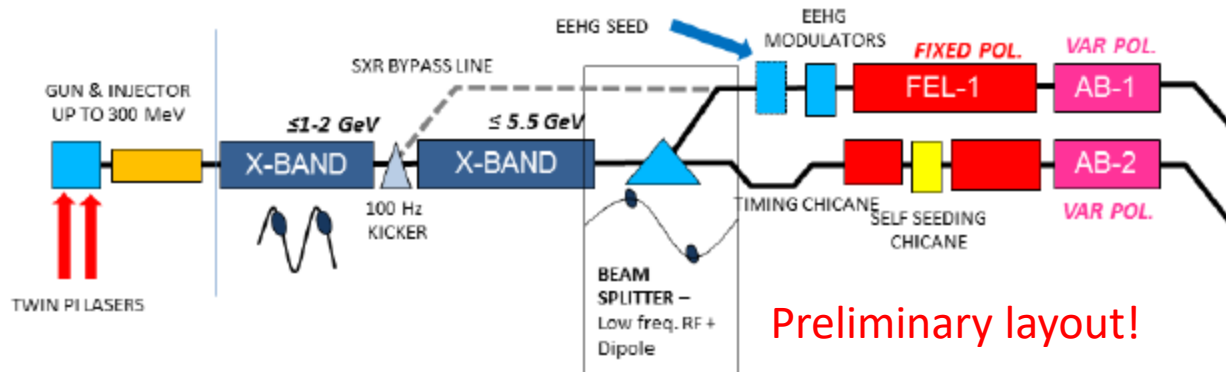
Parameter	Unit	Soft X-ray	Hard X-ray
Photon energy	keV	0.25 – 2.0	2.0 – 16.0
Wavelength	nm	5.0 – 0.6	0.6 – 0.08
Repetition rate	Hz	1000	100
Pulse duration	fs	0.1 – 50	1 – 50
Polarization		Variable, selectable	
Two-pulse delay	fs	± 100	± 100
Two-colour separation	%	20	10
Synchronization	fs	< 10	< 10

Main Electron Beam and FEL Parameters

Parameter	Value
Max energy	5.5 GeV @ 100 Hz
Peak current	5 kA
Normalised emittance	0.2 mm.mrad
Bunch charge	< 100 pC
RMS slice energy spread	10^{-4}
Max photon energy	16 keV
FEL tuning range at fixed energy	$\times 2$
Peak spectral brightness @ 16 keV	10^{33} ph/s/mm ² /mrad ² /0.1%bw

Preliminary RF Parameters

Parameter	Unit	Value
Frequency	GHz	11.9942
Phase advance	rad	$2\pi/3$
Average iris radius $\langle a \rangle$	mm	3.5
Total length	m	0.9
RF pulse	μ s	1.5
Average gradient	MV/m	65
Group velocity	%	4.5 – 1.0
Filling time	ns	140
Input power per structure	MW	9.8
Structures per module	-	4



Task in **WG4** (RF systems): design and optimization of an **X-band SLED + accelerating sections system**.

G. D'Auria et al., CompactLight DESIGN STUDY, JACoW-IPAC2019-TUPRB032 (2019)

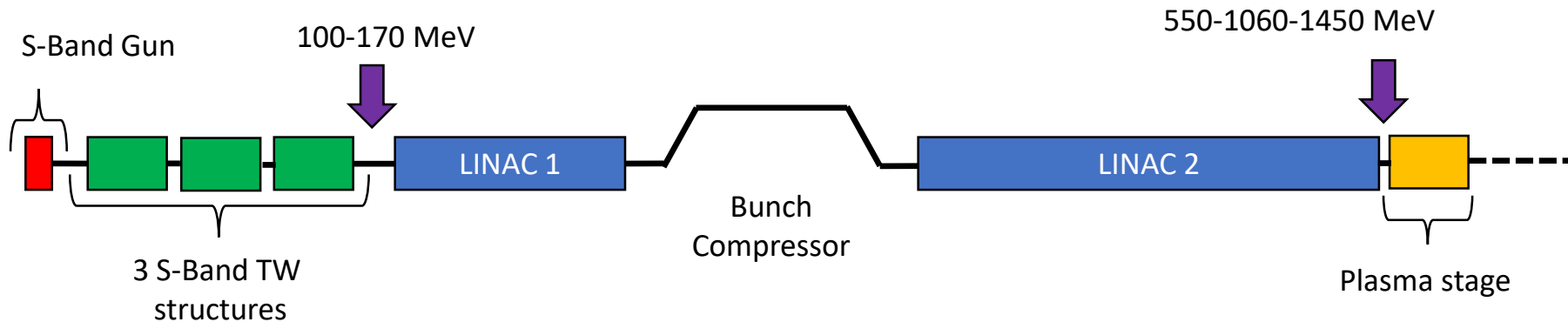
OUTLINE

- High brightness linacs
 - The EuPRAXIA@SPARC_LAB project
 - The CompactLight project
- Design and optimization of accelerating structures and power distribution network
 - EuPRAXIA@SPARC_LAB
 - CompactLight
 - Joining the projects

RF MODULE DESIGN WORKFLOW

- Define the **average accelerating gradient**
- **Average iris radius** (determined by beam dynamics calculations and simulations)
- **RF sources** and pulse compressor characteristics
- Electromagnetic parametric study of the TW cell
- Analytical design of the structure to have the highest effective shunt impedance (constant impedance and constant gradient)
- **Effective shunt impedance optimization** by a 2D numerical scan of the total length and the iris tapering
- Check the expected Breakdown rate (modified Poynting vector values @ nominal gradient)
- Design a realistic **RF module** (including power distribution network)
- Design the input and output couplers
- **Wakefields and BBU** calculations
- EM simulation of the whole structure
- Mechanical drawings and thermo-mechanical simulations of the structure
- ...

X-BAND LINAC PARAMETERS



The RF X-band linac layout is based on **klystrons with SLEDs** that feed several **TW accelerating structures**. The operating mode is the **$2\pi/3$** mode at **11.9942 GHz**.

X-Band LINAC parameters				
L_t [m]	16			
	PWFA	LWFA	Full RF	Ultimate
E_0 [MeV]	100	170	170	170
E_L [MeV]	550	550	1060	1450
E_{gain} [MeV]	450	380	890	1280
$\langle G \rangle$ [MV/m]	20(L1)-36(L2)	20(L1)-27(L2)	57	80
Charge [pC]	200(D)-30(W)	30	200	
σ_z [μm]	3.82 (W)	2.14	16.7	
ε [mm mrad]	0.47 (W)	0.47	0.5	

Klystron parameters (CPI VKX-8311A)	
Frequency [GHz]	11.9942
P_k [MW]	50
t_k [μs]	1.5

PWFA: particle driven plasma acceleration

LWFA: laser driven plasma acceleration

Full RF: no plasma acceleration, only RF

Ultimate: Full RF with double power (a factor of $\sqrt{2}$ in terms of gradient)

MINIMUM AVERAGE IRIS RADIUS OF THE STRUCTURE

The **critical part** is the **LINAC1**, where beta is high and the gradient is low.

The **minimum average iris radius** has been calculated fixing the growth rate of the **beam breakup instabilities due to wakefield kick from head to tail**.

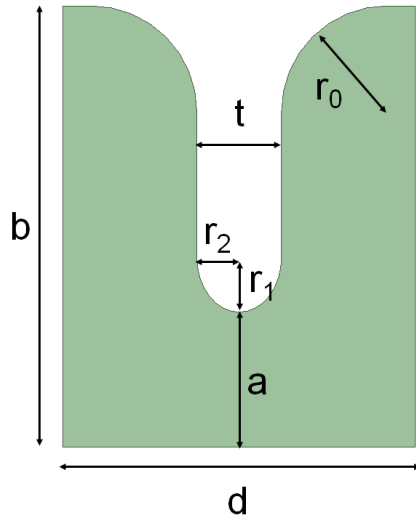
	PWFA	Full rf
$\langle G \rangle$ [MV/m]	20	57
$\langle \beta \rangle$ [m]	~ 30	~ 30
E_0 [MeV]	102	171
E_{L1} [MeV]	222	502
σ_z [μm]	50	112
Charge [pC]	200	200
Y	2	2
$\langle a \rangle$ [mm]	3.2	

Alex Chao, "Physics of collective beam instabilities in high energy accelerators", 1993

Karl Bane, "Short-range Dipole Wakefields in Accelerating structures for the NLC", SLAC-PUB-9663, 2003

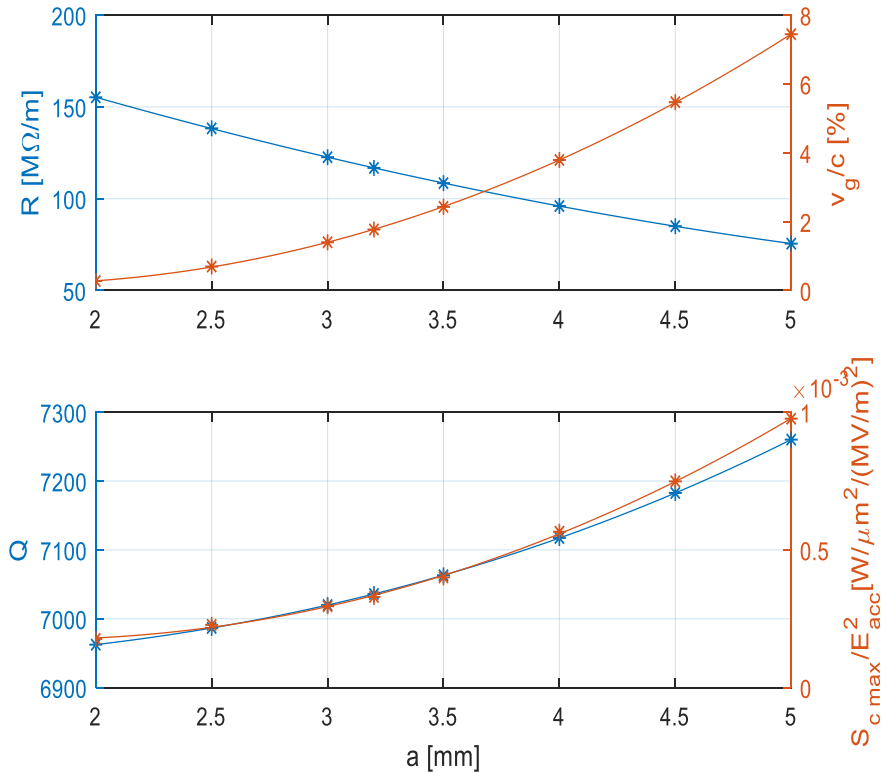
Alexej Grudiev, talk at INFN-LNF, Frascati, December 2016

DESIGN OF THE CELLS



Geometrical parameters

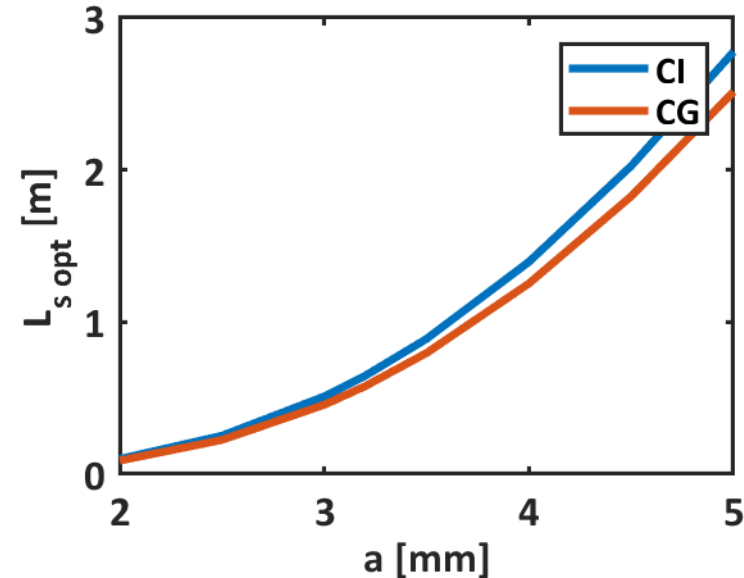
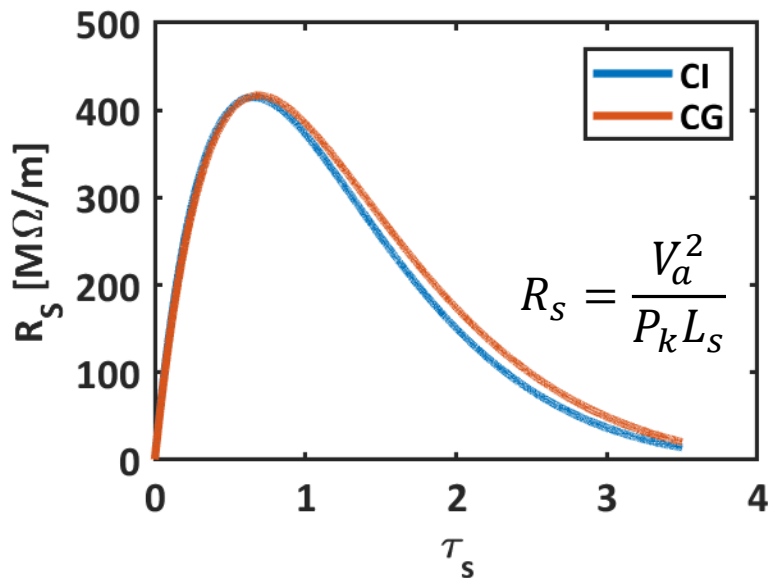
a [mm]	2 ÷ 5
b [mm]	10.155 ÷ 11.215
d [mm]	8.332 (2 π /3 mode)
r ₀ [mm]	2.5
t [mm]	2
r ₁ /r ₂	1.3 (Min S _{c max} for a=3.2 mm)



Single cell parameters (R , v_g/c , Q , $S_{c \max}/E^2_{acc}$) as a function of the iris radius calculated with HFSS for structure design. The iris has been designed with an **elliptical shape** to minimise $S_{c \max}/E^2_{acc}$.

ANALYTICAL STRUCTURE LENGTH OPTIMIZATION

Assuming constant values for Q , R/Q , we calculated the structure **attenuation constant** (τ_s) that maximises the **effective shunt impedance** R_s (CI and CG cases). This allows to calculate the **structure length** L_s (for a given iris aperture).



$$\tau_s = \int_0^L \alpha(z) dz$$

$$\alpha(z) = f(\omega, R/Q, v_g, Q)$$

$$\langle a \rangle = 3.2 \text{ mm}$$



$$L_{\text{opt_CI}} = 0.65 \text{ m}$$

$$L_{\text{opt_CG}} = 0.58 \text{ m}$$

The obtained results are used as a **reference guideline** in a **numerical optimization**.

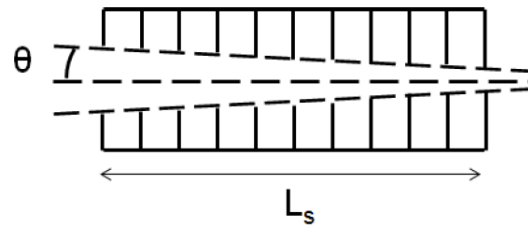
B. Spataro, INFN-LNF technical report, L-87 (1986)

P. M. Lapostolle, A. L. Septier, Linear Accelerators, North-Holland, Amsterdam (1970)

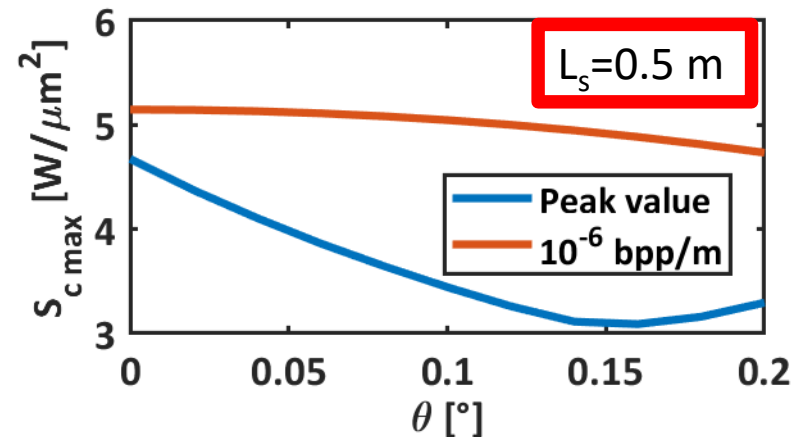
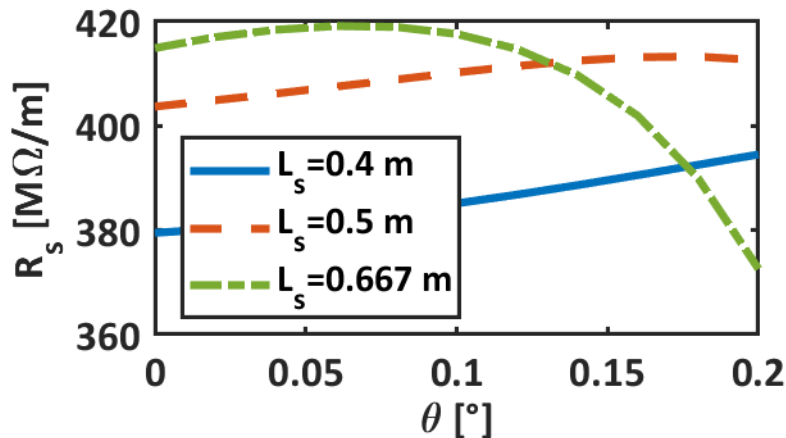
T. P. Wangler, RF Linear Accelerators, John Wiley & Sons (2008)

NUMERICAL EFF. SHUNT IMPEDANCE OPTIMIZATION

R/Q variation with iris aperture is not negligible and CG concept does not apply for not-flat RF pulses (SLED). For this reason we have developed a **numerical tool** able to calculate the main **structure parameters** (effective shunt impedance, modified Poynting vector, E_z field profile) **with an arbitrary cell-by-cell iris modulation along the structure itself**.



linear iris tapering



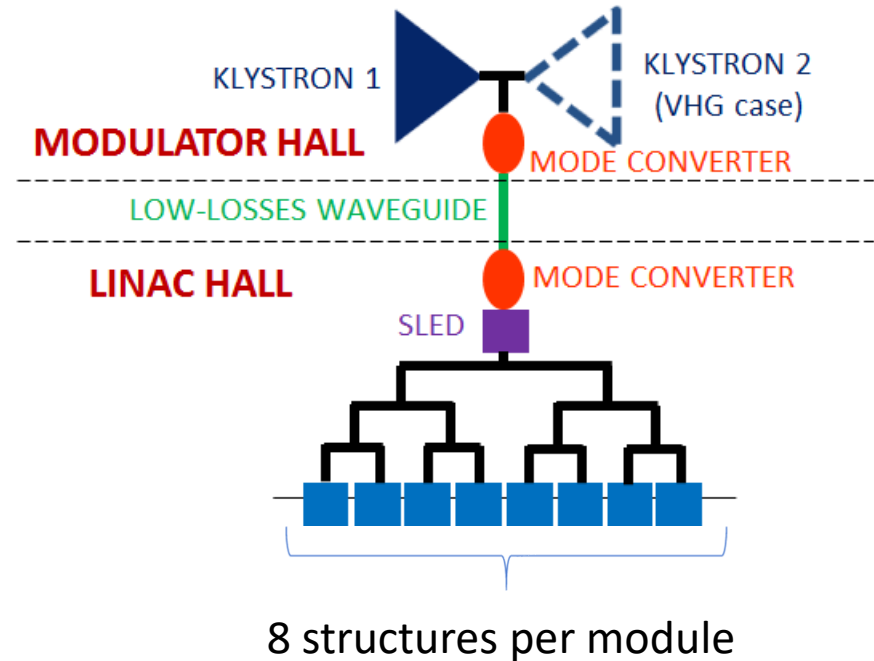
As a reference design of the structure, we have considered **0.5 m long structures with 0.1 deg tapering** as a good compromise between modularity, R_s and iris tapering.

M. Diomede et al, Preliminary RF design of an X-band linac for the EuPRAXIA@SPARC_LAB project, NIM A 909 (2018) 243–246

M. Diomede et al., RF DESIGN OF THE X-BAND LINAC FOR THE EUPRAXIA@SPARC_LAB PROJECT, JACoW-IPAC2018-THPMK058 (2018)

RESULTS OF RF MODULE OPTIMIZATION

X-band booster parameters		
a first-last cell [mm]	3.629 – 2.771	
L_s [m]	0.5	
No. of cells N_c	60	
L_t [m]	16	
No. of structures N_s	32	
Klystron pulse length t_k [μ s]	1.5	
SLED Q_0 (SLEDX)	180000	
SLED Q_e	19300	
v_g/c [%]	2.76 – 1.03	
t_p [ns]	100	
Section attenuation τ_s	0.534	
Shunt impedance R [$M\Omega/m$]	105-130	
R_s [$M\Omega/m$]	410	
Net kly. power [MW]	≈ 40	
	Full RF	Ultimate
$\langle G \rangle$ [MV/m]	57	80
E_{gain} [MeV]	912	1280
P_{RF} [MW]	127	250
Peak input power [MW]	30	58
Input power averaged over the pulse [MW]	21	42
No. of klystrons N_k	4	8

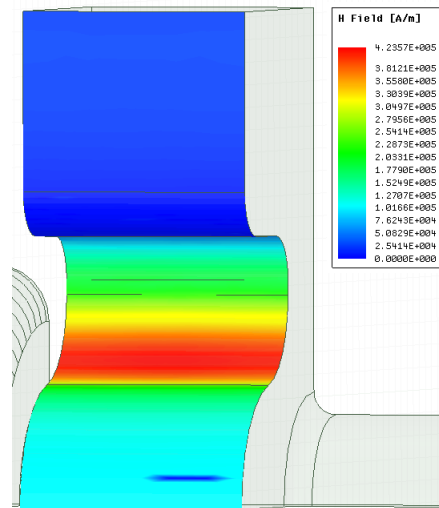
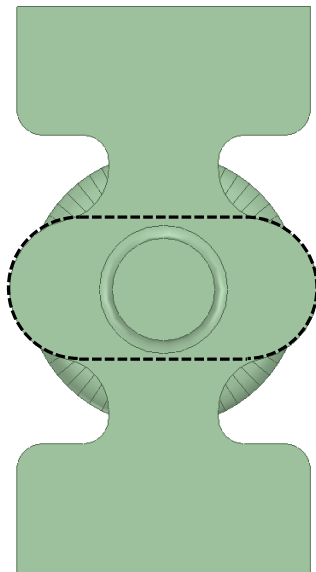


The **basic RF module** of the EuPRAXIA@SPARC_LAB X-band linac can be conveniently composed by a group of **8 TW sections** assembled on a single girder and fed by **one or two klystrons** by means of **one pulse compressor system** and a **waveguide network** splitting and transporting the RF power to the input couplers of the sections.

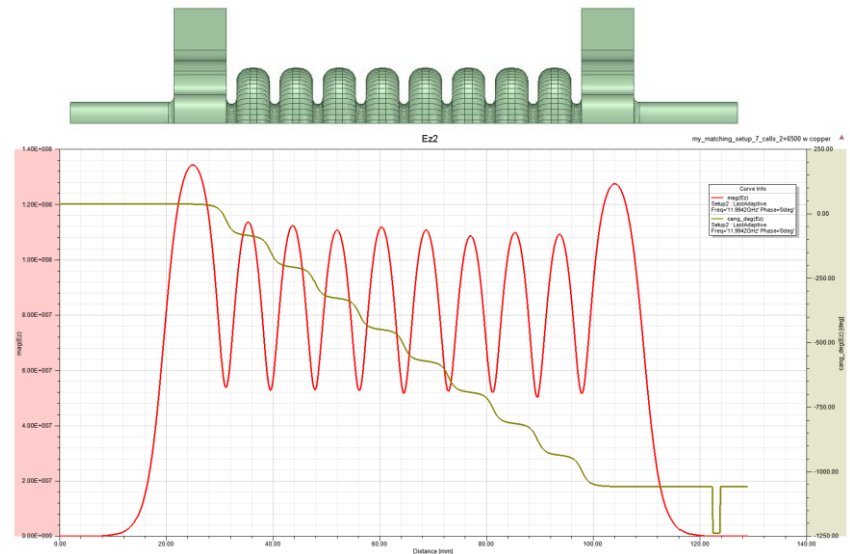
RF POWER COUPLERS DESIGN

As first case, we have considered a **z-type coupler** because of its compactness with respect to the waveguide and mode launcher ones. A **dual feed** allows to completely avoid the dipole magnetic field component. **Racetrack geometry** has been implemented in order to compensate the residual quadrupole field components.

The calculated **pulsed heating** on the input coupler is **<25 °C** (in the 80 MV/m case), the obtained **reflection coefficient** is **<-30 dB**.



7 cells model

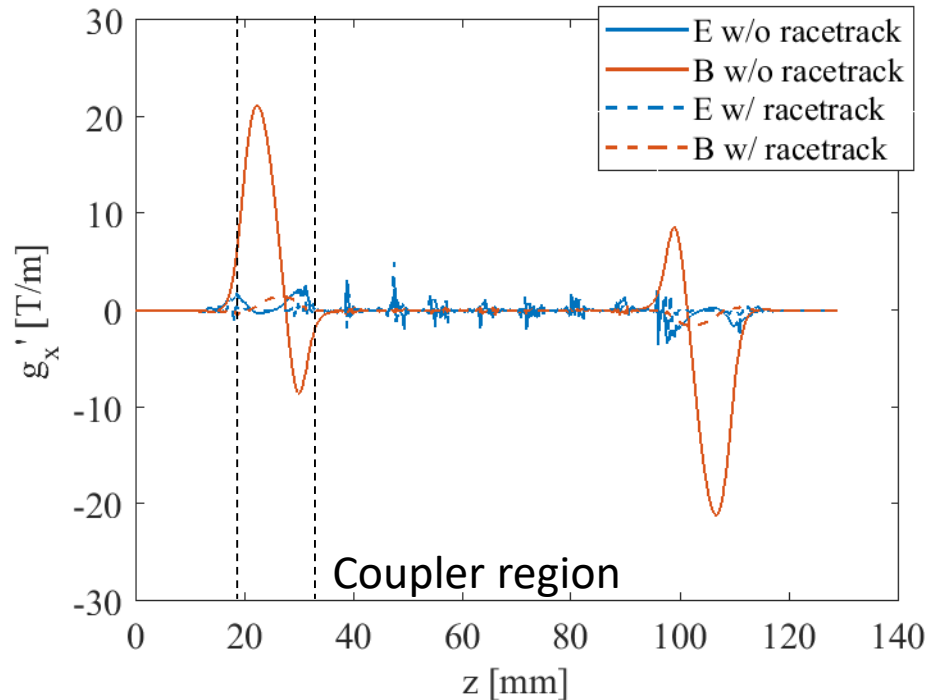


V. A. Dolgashev, High magnetic fields in couplers of X-band accelerating structures (2003)

L. Laurent, Experimental study of rf pulsed heating (2011)

Slot coupler (z-type, input, a1=3.629 mm)

Equivalent focusing/defocusing quadrupole kicks on the x plane along the coupler:



$$G'_{coupler} = \int_{coupler} (g'_B + g'_E) dz [T]$$

w/o racetrack: $G=0.0554$ T

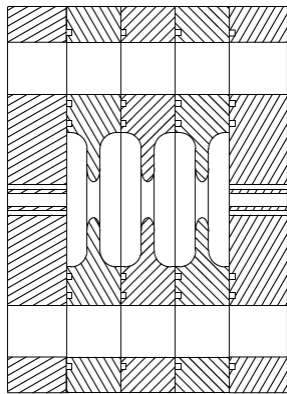
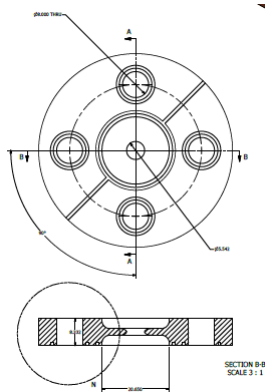
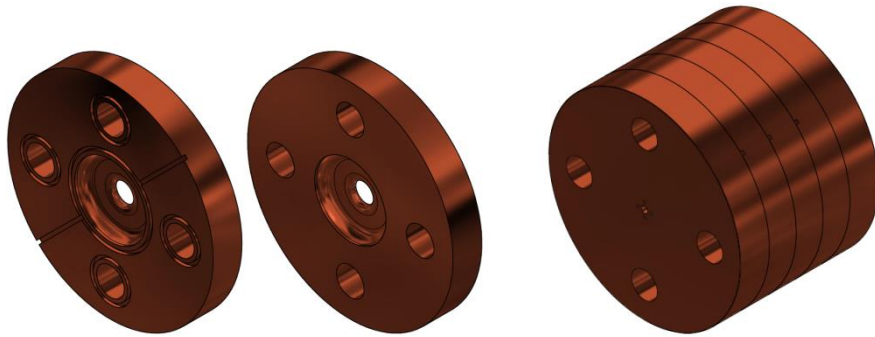
w/ racetrack: $G=0.0051$ T (a factor 10 less)

D. Alesini et al., 10.1103/PhysRevAccelBeams.20.032004 (2017).

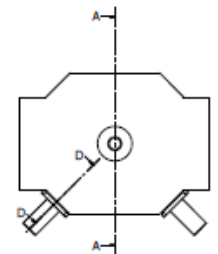
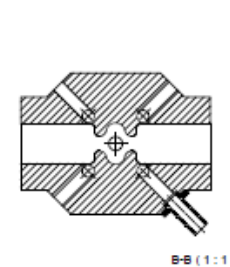
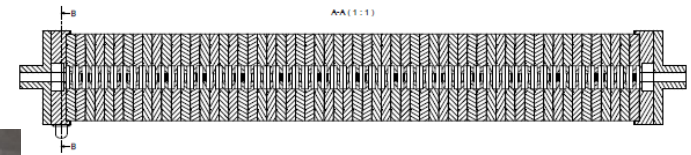
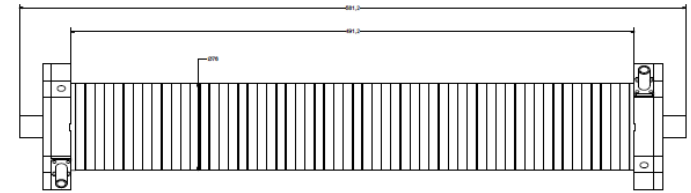
3 CELLS AND STRUCTURE PROTOTYPE

A **mechanical design** activity has been started. The cells will integrate four symmetric cooling channels.

RF prototype



Structure prototype



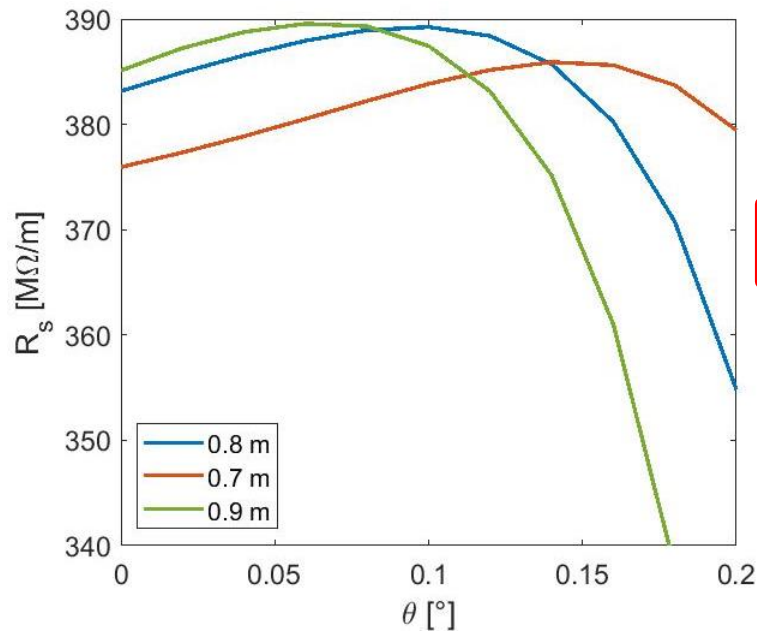
Collaboration with Valerio Lollo (INFN-LNF)

OUTLINE

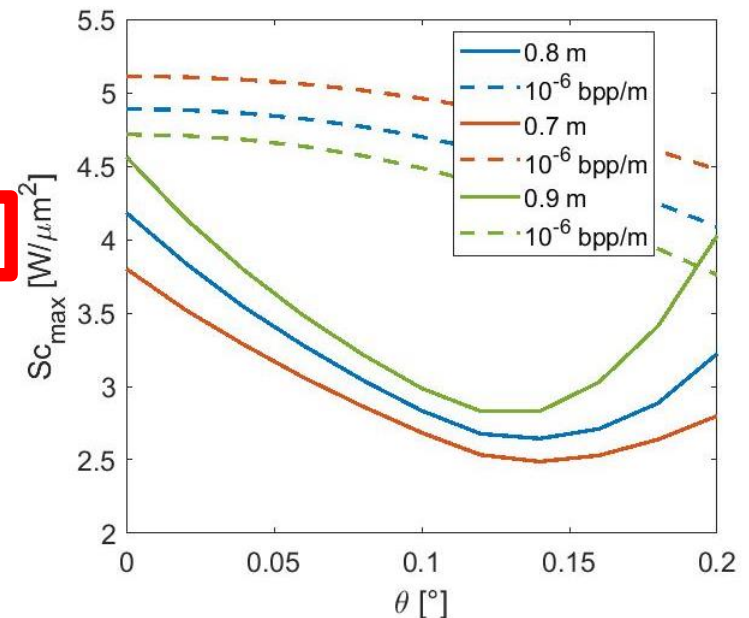
- High brightness linacs
 - The EuPRAXIA@SPARC_LAB project
 - The CompactLight project
- Design and optimization of accelerating structures and power distribution network
 - EuPRAXIA@SPARC_LAB
 - CompactLight
 - Joining the projects

STRUCTURE OPTIMIZATION

Initial main parameters are an **average accelerating gradient of 65 MV/m** and an **energy gain of 5.2 GeV**. Starting from the work already done for EuPRAXIA@SPARC_LAB, the preliminary **optimal structure length** and the **irises cell-by-cell tapering** have been calculated. In this case, the **average iris radius** has been fixed equal to **3.5 mm** for beam dynamics considerations.



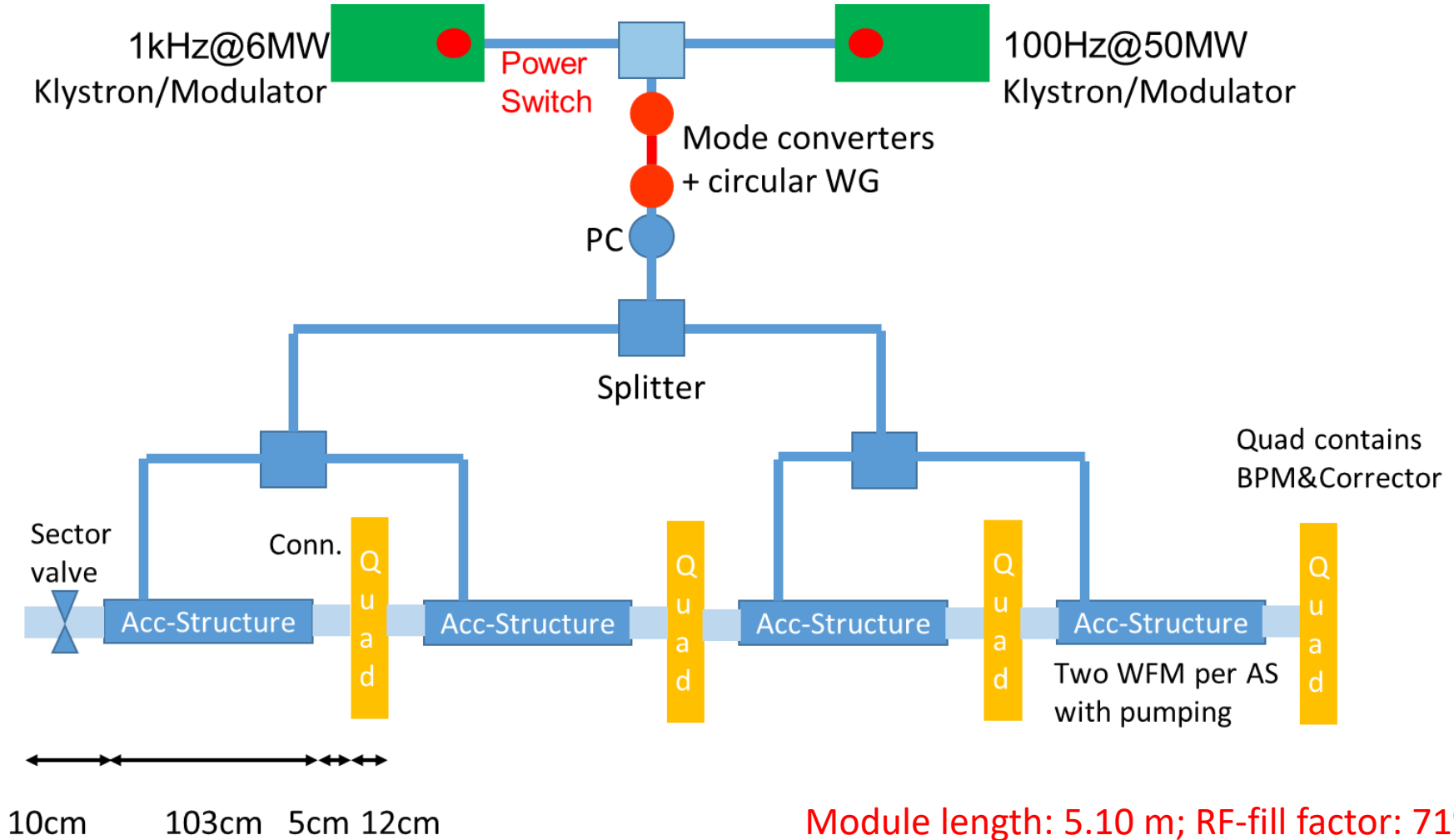
$\langle a \rangle = 3.5$ mm



The **0.9 m solution with 0.1 deg tapering** allows to have a **good power distribution in a 4-structure module**.

Low-Energy RF MODULE (up to 300 MeV)

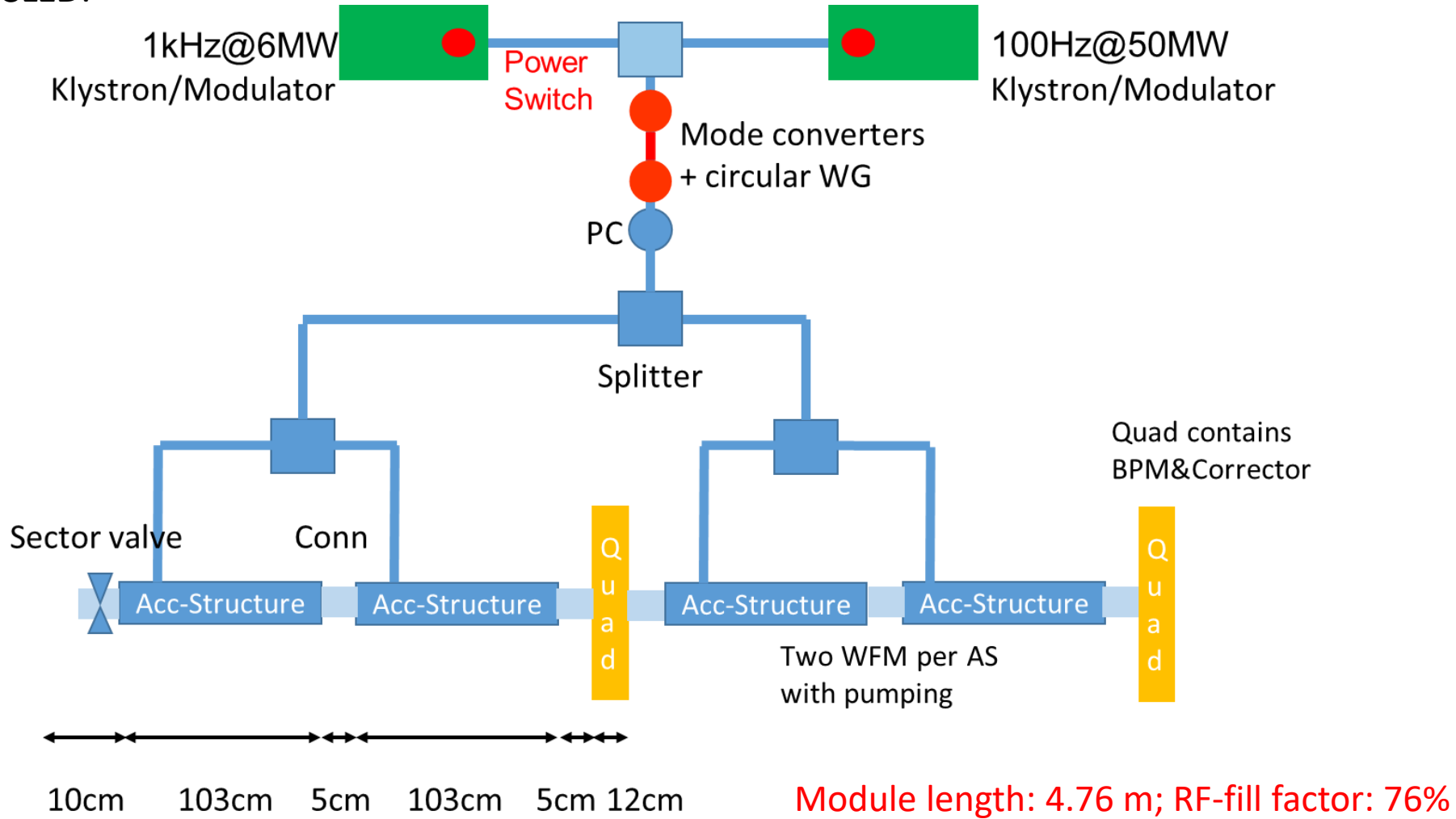
The preliminary **RF module** is then made up of **4 TW structures** fed by **1 klystron** with **1 SLED**.



Collaboration with Markus Aicheler (HIP)

Medium-Energy RF MODULE (up to 1.7 GeV)

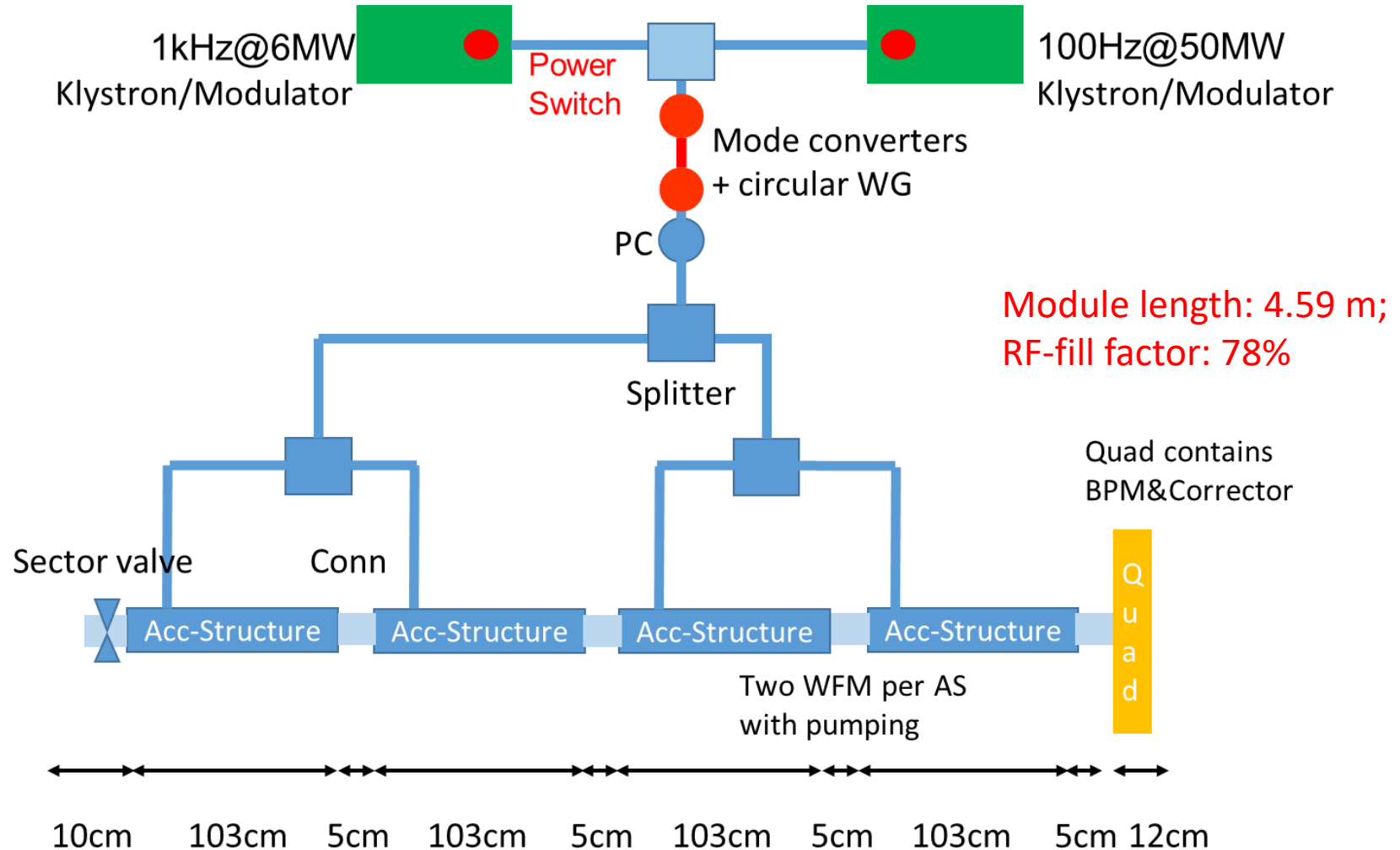
The preliminary **RF module** is then made up of **4 TW structures** fed by **1 klystron** with **1 SLED**.



Collaboration with Markus Aicheler (HIP)

High-Energy RF MODULE (up to 5.5 GeV)

The preliminary **RF module** is then made up of **4 TW structures** fed by **1 klystron** with **1 SLED**.

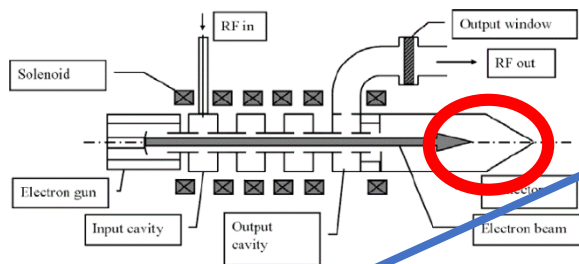


Collaboration with Markus Aicheler (HIP)

HIGH REPETITION RATE OPERATION

The high repetition rate operation is limited by two effects:

The **main limitation** for the rep rate increasing comes from the **power released** on the **tube collector** P_{coll} which can **not exceed** a **limit value** corresponding to the **nominal working point** (with some margin).



$$P_{coll} \simeq \frac{P_{RFsat}}{\eta} (\tau_{flat\ top} + \tau_{trans}) f_{rep}$$

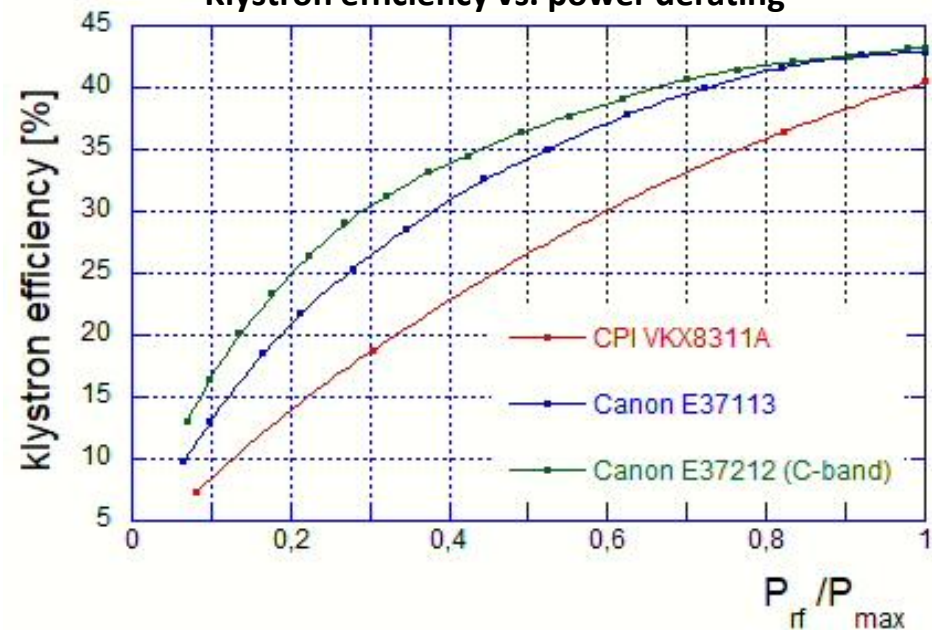
The klystron operational **rep rate** can be **increased** at expenses of the **saturated RF power** (by decreasing the tube HV) and/or the **pulse duration**

The amount of rep rate increase obtainable by **reducing the HV** and the RF saturation power P_{RFsat} is limited by the **tube efficiency decrease**.

The **average dissipated power** in the structure: is something manageable.

The amount of rep rate increase obtained by **reducing the pulse duration** depends very much on the actual value of the **dead time** τ_{trans} , which is a **characteristics of the modulator**.

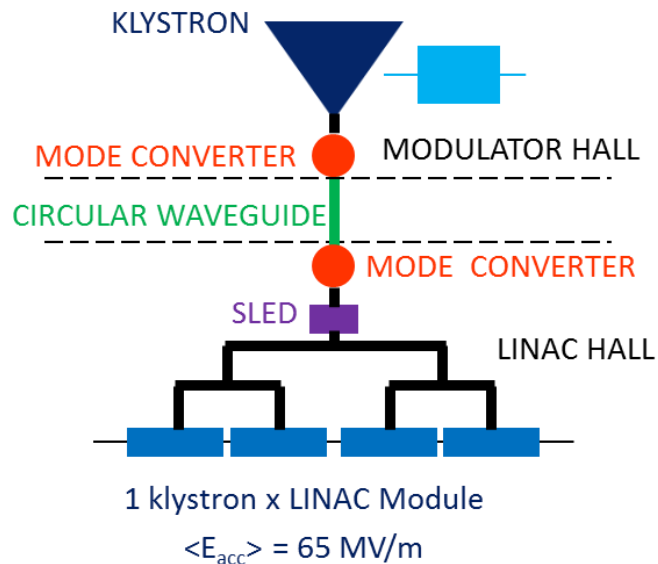
Klystron efficiency vs. power derating



HIGH REP. RATE 1st SCENARIO: PULSE SHORTENING WITH HIGH PEAK POWER KLYSTRONS

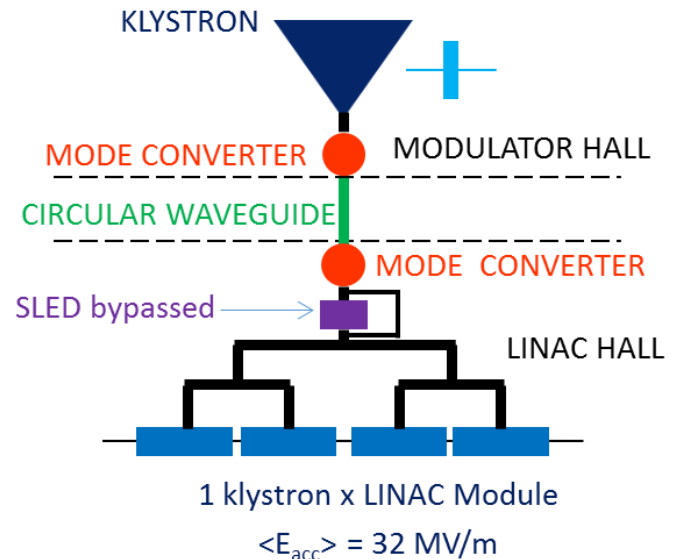
Ref. CPI VKX-8311A

50 MW, 1.5 μ s, 100 Hz



Operation probably possible with an optimization of the modulator rise/fall times

50 MW, 150 ns, 250 Hz



- Accelerating gradient and Linac energy reduced by a factor ~ 2 @ 250 Hz rep rate;
- The SLED has to be bypassed;
- Klystron operated always at its nominal working point (good!);
- Max rep rate very much dependent on modulator rise/fall times τ_{trans}

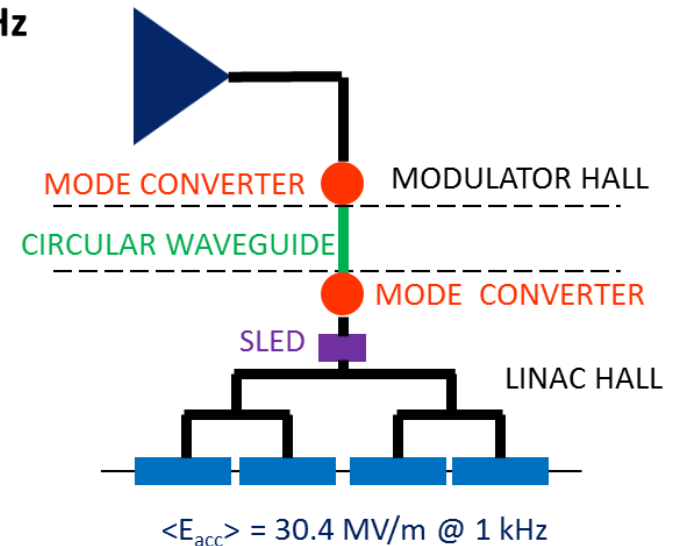
HIGH REP. RATE 2nd SCENARIO: LOW POWER HIGH REP. RATE KLYSTRONS

Reference RF source CANON
Commercially available

Parameters	Specifications	units
	E37113	
RF Frequency	11.9942	GHz
Peak RF power	6	MW
RF pulse length	5	μ s
Pulse repetition rate	400	Hz
Klystron voltage	150	kV
Micro perveance	1.5	

*10 MW, 1.5 μ s, 1 kHz, operation
probably possible in the near future*

10 MW, 1.5 μ s,
1 kHz



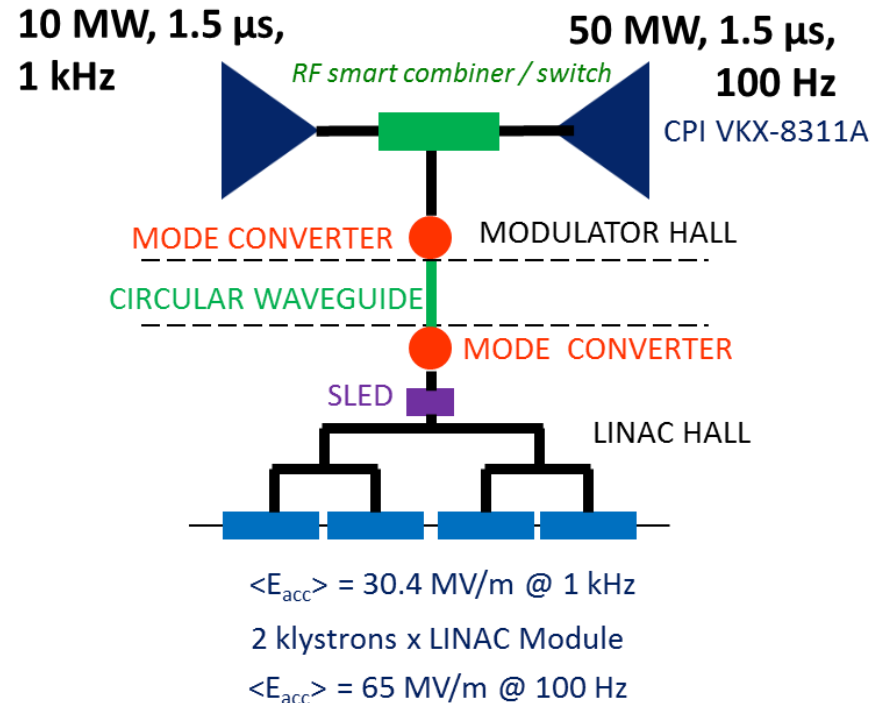
- 1 kHz rep rate capability, with linac energy up to $\approx 47\%$ of the max value;
- R&D activity in progress @CANON and CPI on high rep. rate klystrons towards 10 MW, 1.5 μ s, 1 kHz

HIGH REP. RATE 3rd SCENARIO: COMBINATION OF HIGH REP. RATE AND LOW REP. RATE KLYSTRONS

Reference RF source CANON

Parameters	Specifications	units
	E37113	
RF Frequency	11.9942	GHz
Peak RF power	6	MW
RF pulse length	5	μ s
Pulse repetition rate	400	Hz
Klystron voltage	150	kV
Micro perveance	1.5	

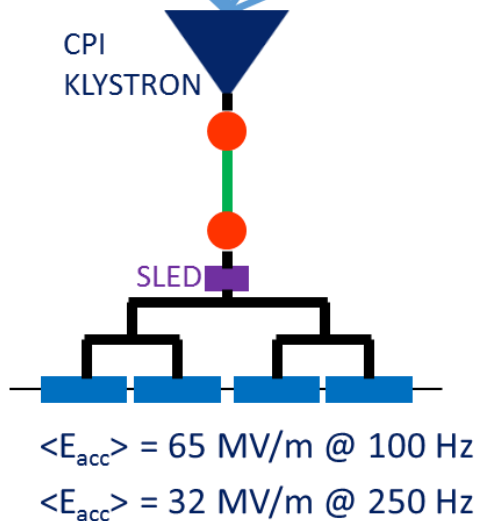
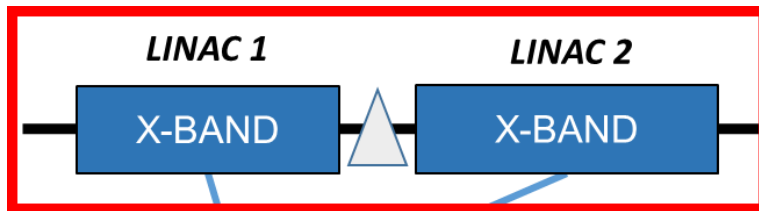
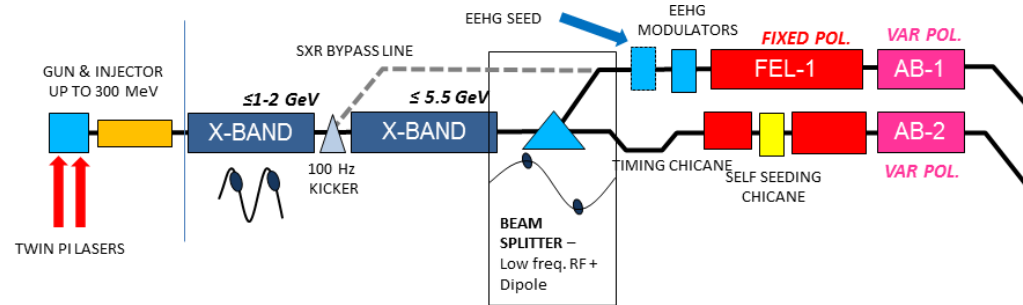
***10 MW, 1.5 μ s, 1 kHz, operation
probably possible in the near future***



- Switching 2 sources would preserve **high gradient at low rep rate**;

BASELINE: DUAL MODE

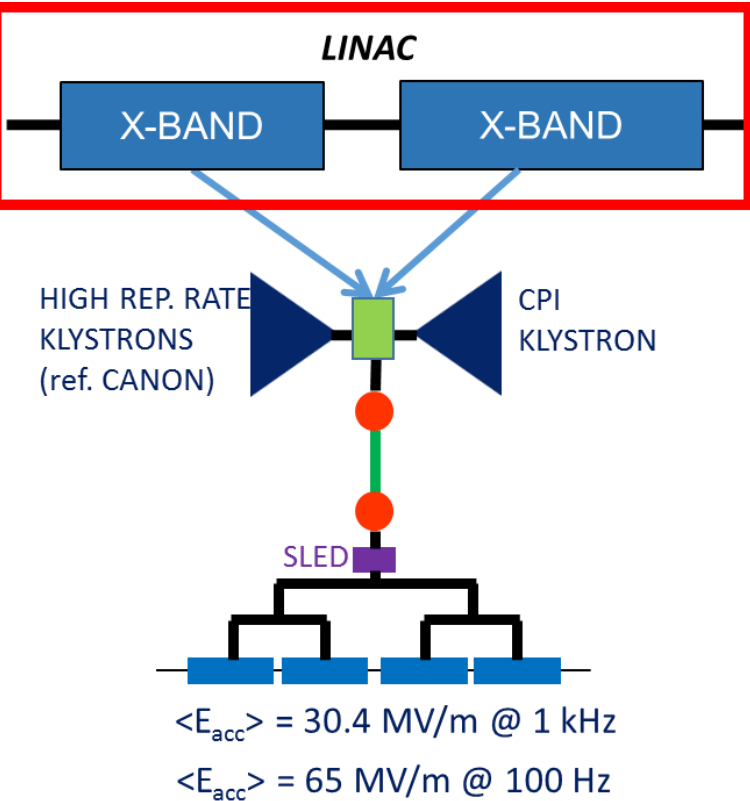
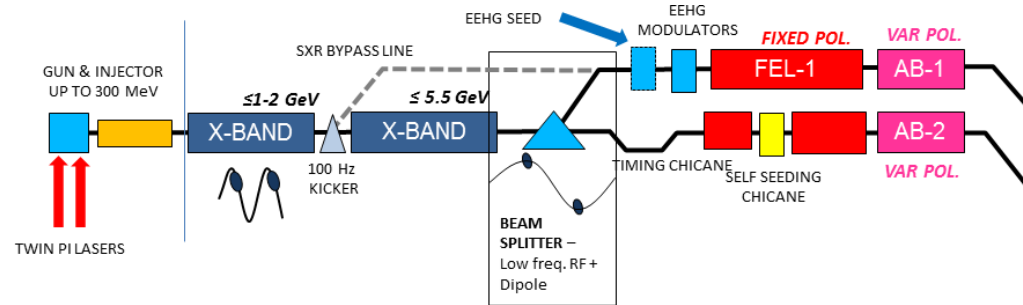
- Single rf source
- single linac run in two operating modes
- Cheapest
- Limited increase in repetition rate (SLED bypassed)
- Linac optics needs to operate at two gradient



Parameter	LINAC 1	LINAC 2	TOTAL
Number of structures	32	60	92
Number of modules	8	15	23
Number of klystrons	8 (CPI)	15 (CPI)	23
Linac active length [m]	29	54	83
Rep. rate [Hz]	100 (250)		
$\langle E_{\text{acc}} \rangle$ per struct. [MV/m]	65 (32)		
Energy gain per module [MeV]	234 (115)		
Max. Energy gain [MeV]	1872 (921)	3510 (1728)	5382 (2649)

UPGRADE-1: DUAL SOURCE

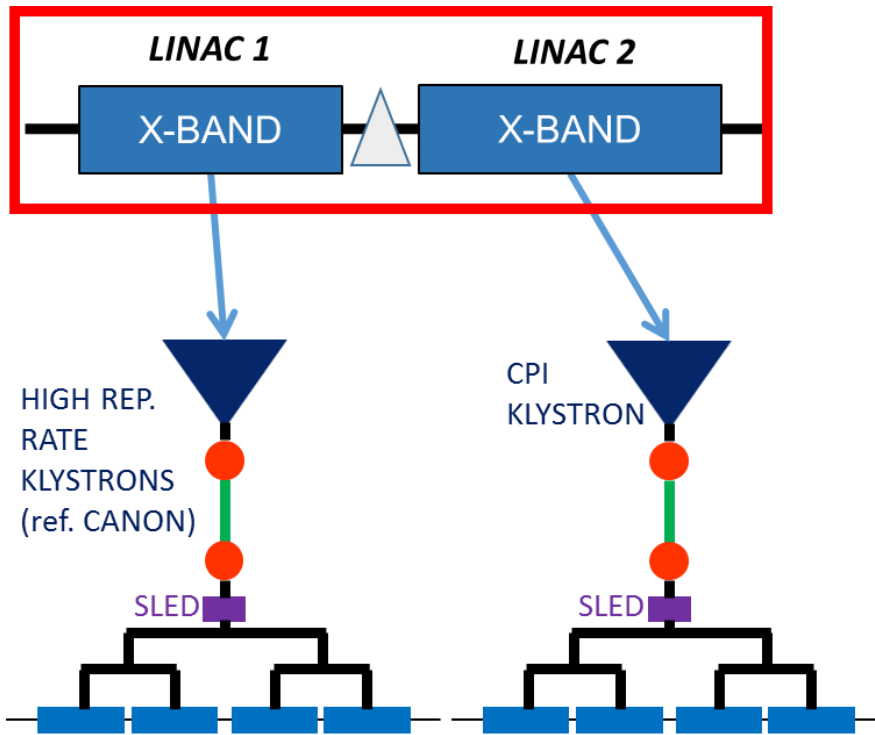
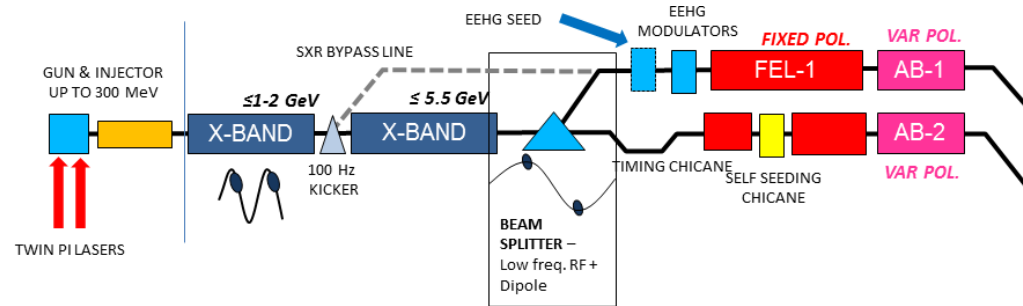
- Single linac with two sources
- SXR@ 1 kHz
- HXR@ 100 Hz
- SXR and HXR CANNOT run in parallel



Parameter	LINAC
Number of structures	92
Number of modules	23
Number of klystrons	23 (HRR) + 23 (CPI)
Linac active length [m]	83
$\langle E_{acc} \rangle$ per struct. [MV/m]	30.4 (@1 kHz), 65 (@ 100 Hz)
Rep. rate [Hz]	100-1000
Energy gain per module [MeV]	109 (@1 kHz), 234 (@ 100 Hz)
Max. Energy gain [MeV]	2507 (@1 kHz), 5382 (@ 100 Hz)

UPGRADE-2: DUAL LINAC

- two distinct linacs with different rf sources
- SXR@ 1 kHz
- HXR@ 100 Hz
- SXR@ 900 Hz and HXR@ 100 Hz running in parallel



$\langle E_{acc} \rangle = 30.4$ MV/m @ 1 kHz $\langle E_{acc} \rangle = 65$ MV/m @ 100 Hz

Parameter	LINAC 1	LINAC 2	TOTAL
Number of structures	68	60	128
Number of modules	17	15	32
Number of klystrons	17 (HRR)	15 (CPI)	32
Linac active length [m]	61	54	137
$\langle E_{acc} \rangle$ per struct. [MV/m]	30.4	65	-
Rep. rate [Hz]	1000	100	-
Energy gain per module [MeV]	109	234	-
Max. Energy gain [MeV]	1853	3510	5363

OUTLINE

- High brightness linacs
 - The EuPRAXIA@SPARC_LAB project
 - The CompactLight project
- Design and optimization of accelerating structures and power distribution network
 - EuPRAXIA@SPARC_LAB
 - CompactLight
 - Joining the projects

COMPARISON BETWEEN EuPRAXIA@SPARC_LAB AND CompactLight

	EuPRAXIA@SPARC_LAB	CompactLight
Frequency [GHz]	11.9942	
RF pulse [μ s]	1.5	
Net kly. power [MW]	≈ 40	
Average iris radius $\langle a \rangle$	3.2	3.5
Iris radius a [mm]	3.6-2.8	4.3-2.7
Average gradient $\langle G \rangle$ [MV/m]	80 MV/m	65 MV/m
Linac Energy gain E_{gain} [GeV]	1.3	5.4
Structure length L_s [m]	0.5	0.9
Linac active length L_{act} [m]	16	86
Unloaded SLED Q-factor Q_0	180000	
External SLED Q-factor Q_E	19300	23000
Shunt impedance R [$M\Omega/m$]	105-130	90-131
Effective shunt Imp. R_s [$M\Omega/m$]	410	387
Structures per module N_m	8	4
Klystron power per module P_{k_m} [MW]	54	39
Peak input power [MW]	58	68
Input power averaged over the pulse [MW]	42	44
Total number of structures N_{tot}	32	96
Total number of klystrons N_k	8	24

Using the CompactLight accelerating section for EUPRAXIA@SPARC_LAB

The X-band linac baseline shown in the EUPRAXIA@SPARC_LAB Conceptual Design Report is based on **4 modules hosting 8 x 50 cm long TW cavities** each (**16 m of active length**), powered by **4 or 5 klystrons in total**. We are proposing to change this baseline for a new one based on **5 RF modules** of the type designed for Compact Light, hosting **4 x 90 cm long TW cavities (18 m of active length)**.

The proposal has been approved in a recent collaboration meeting @ LNF

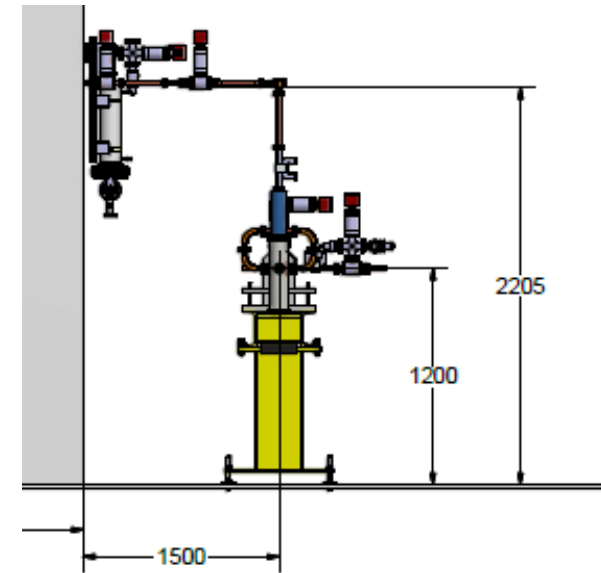
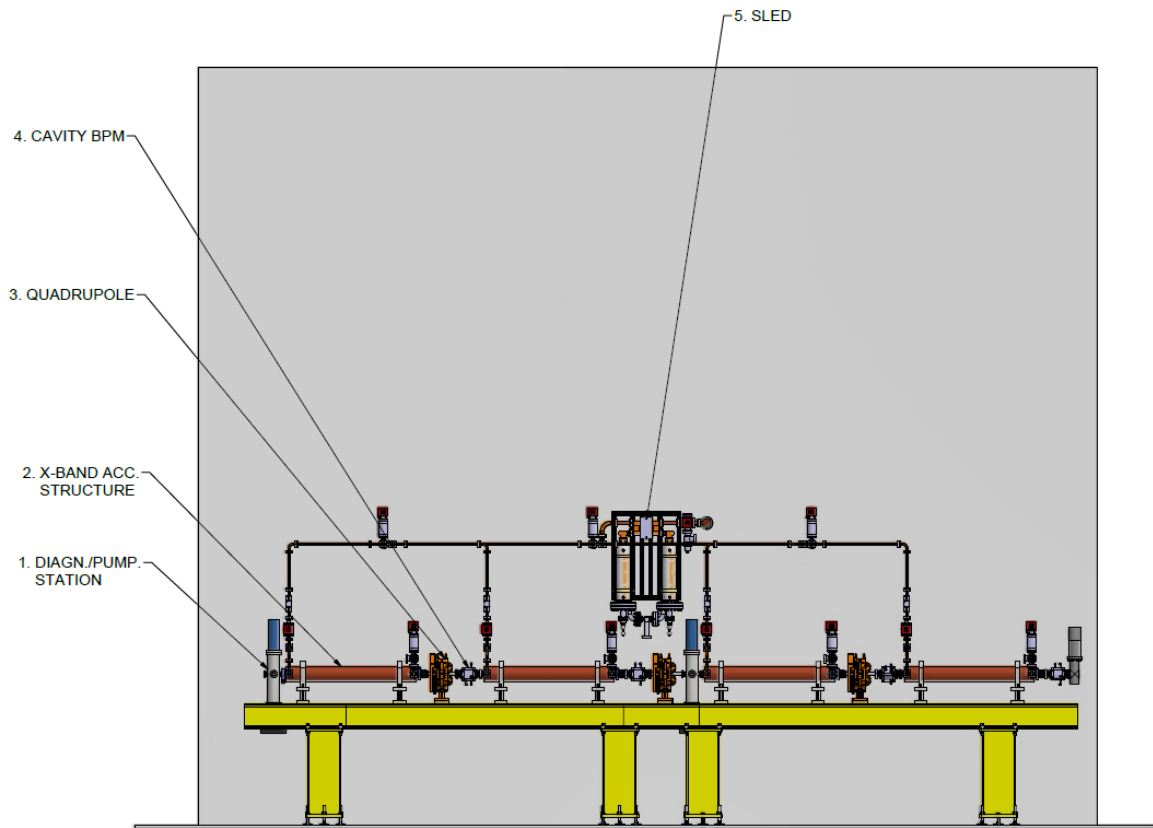
Potential **advantages** are:

- Simplified waveguide distribution network (less accelerating sections per module)
- Linac filling factor improvement (active length / real length)
- Wider average iris radius (3.5 mm vs. 3.2 mm, better beam stay-clear)
- Higher operational gradient (65 MV/m vs 57 MV/m)
- Higher final energy (1170 MeV vs. 1102 MeV)
- Fully synergic with CompactLight design study

Potential **Drawbacks** are:

- Longer active length (18 m vs 16 m)

EUPRAXIA@SPARC_LAB RF MODULE LAYOUT



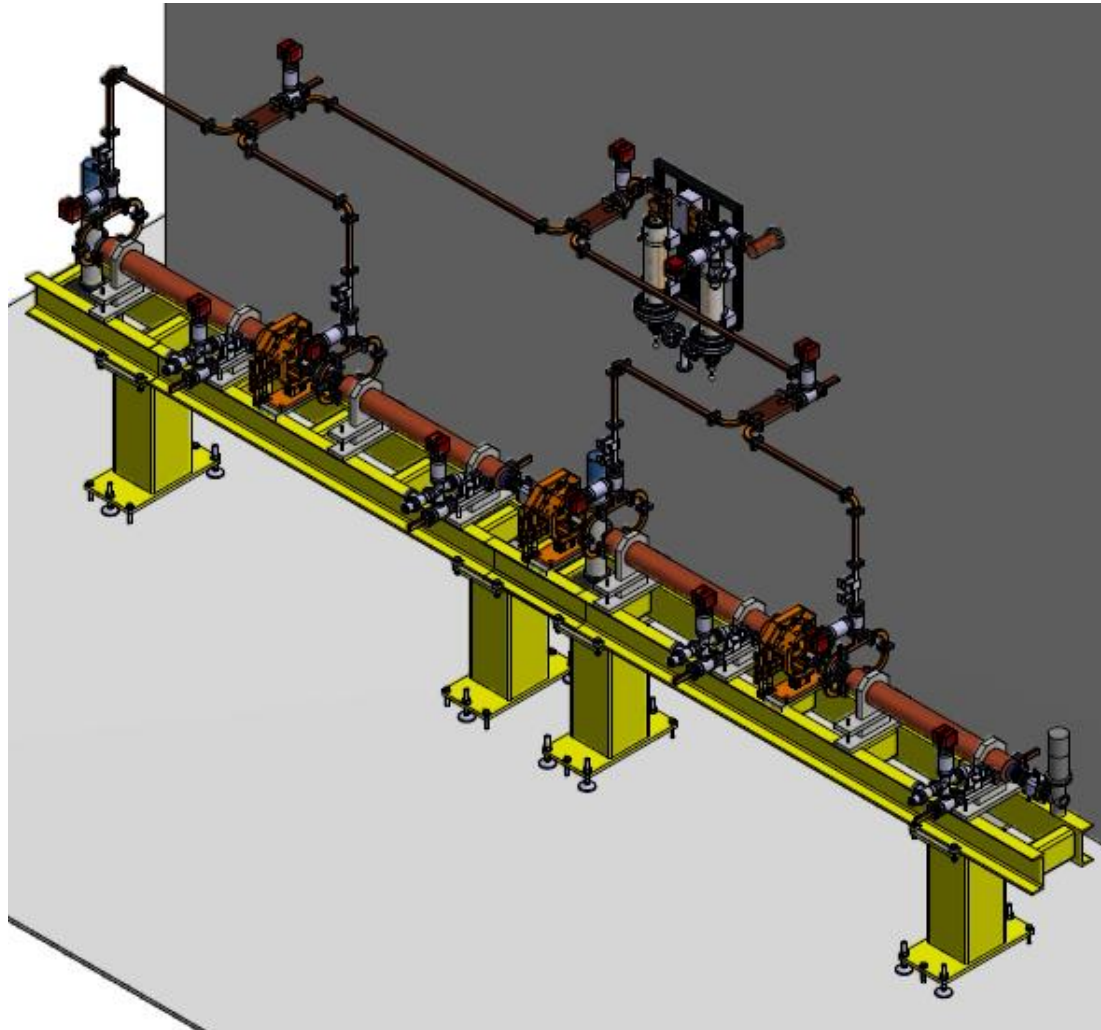
Estimated power (including overmoded waveguide): **11%**

waveguide
attenuation
circular
waveguide):

Preliminary layout of the **RF module** (collaboration with CERN)

Collaboration with Gianluca Di Raddo (INFN-LNF)

EUPRAXIA@SPARC_LAB RF MODULE LAYOUT

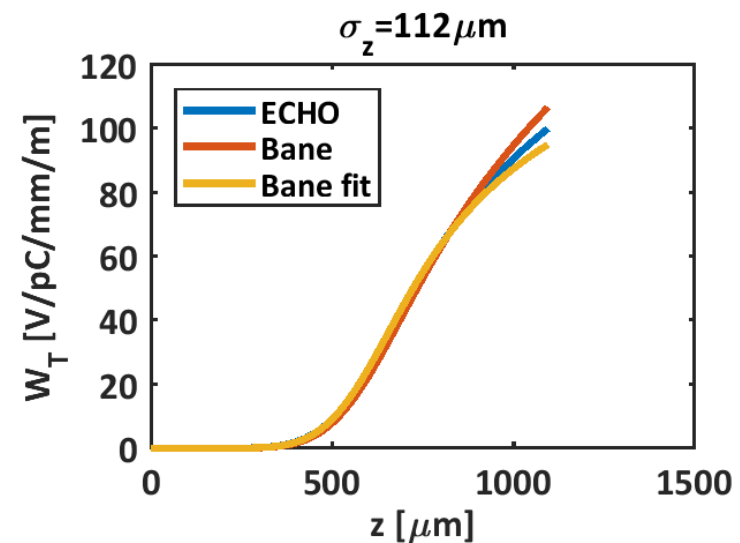
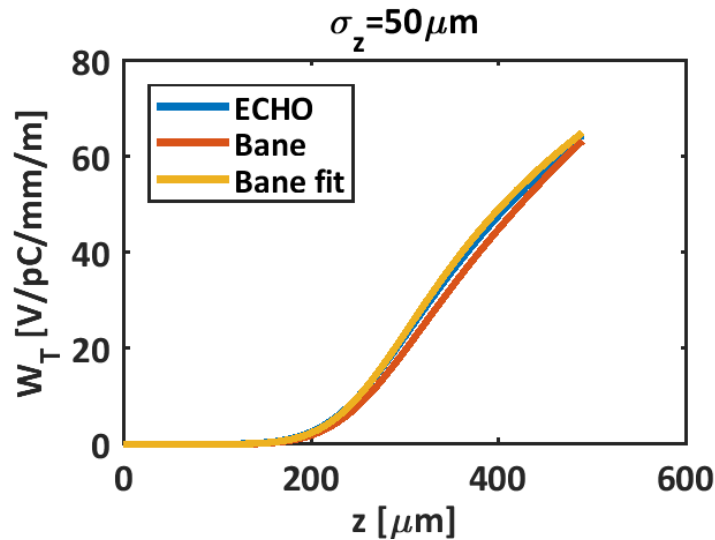


Collaboration with Gianluca Di Raddo (INFN-LNF)

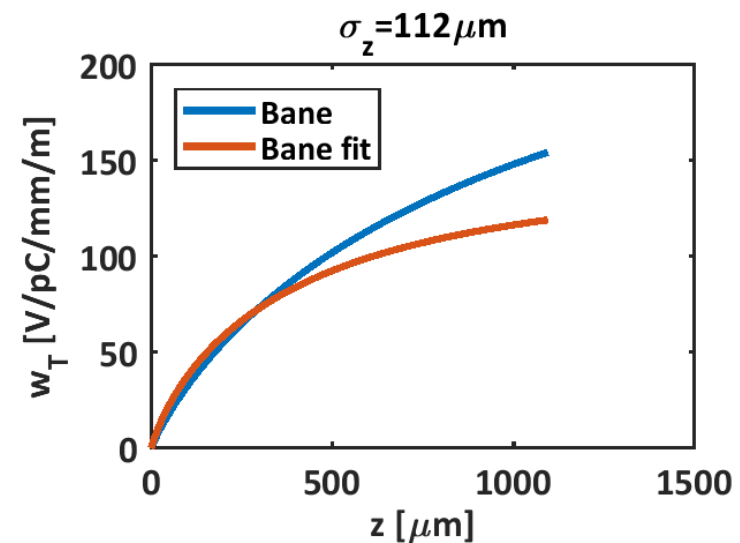
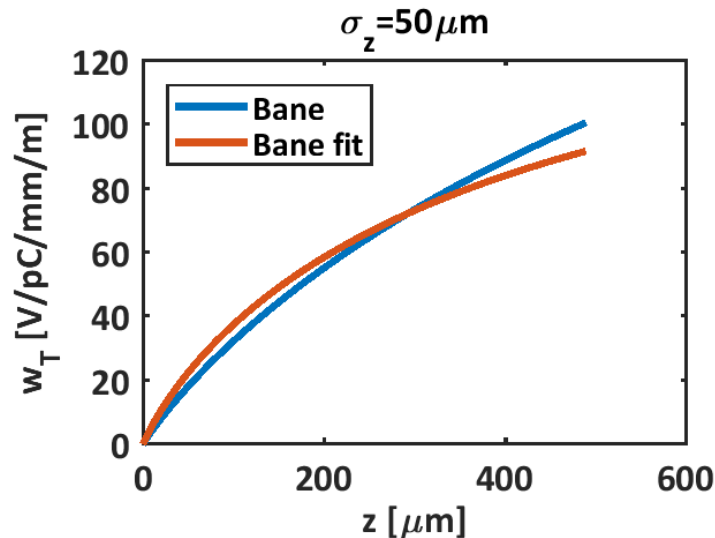
WAKEFIELDS IN THE 90 CM LONG STRUCTURE

Using the ECHO code , the structure wakefield has been found fitting the Bane's formula

Wake potential



Wake function



WAKEFIELDS IN THE 90 CM LONG STRUCTURE

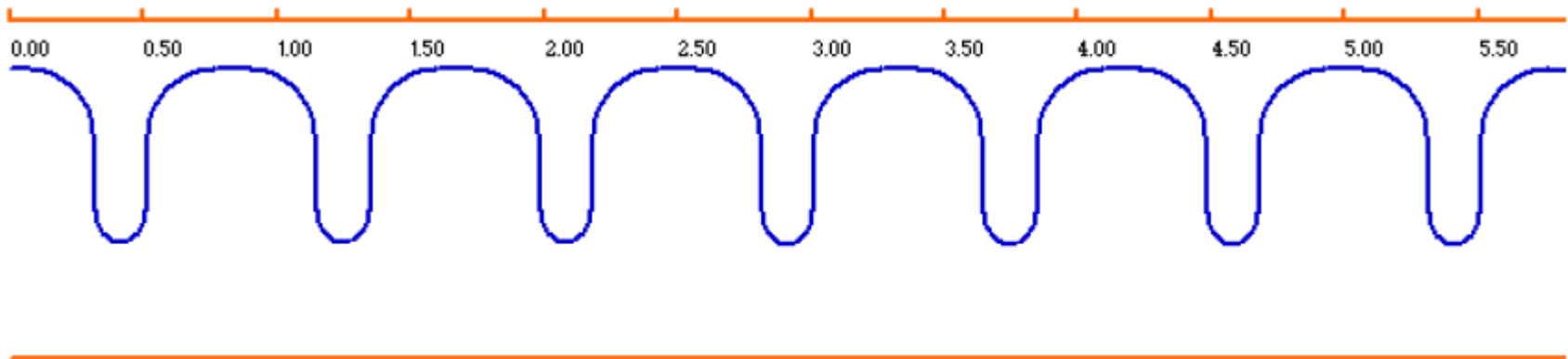
Fitted formula

$$w_{\perp}(z) = \frac{4Z_0cs_2A}{\pi a^4} \left[1 - \left(1 + \sqrt{\frac{z}{s_2}} \right) e^{-\sqrt{\frac{z}{s_2}}} \right]$$

$$a=3.5\text{mm}$$

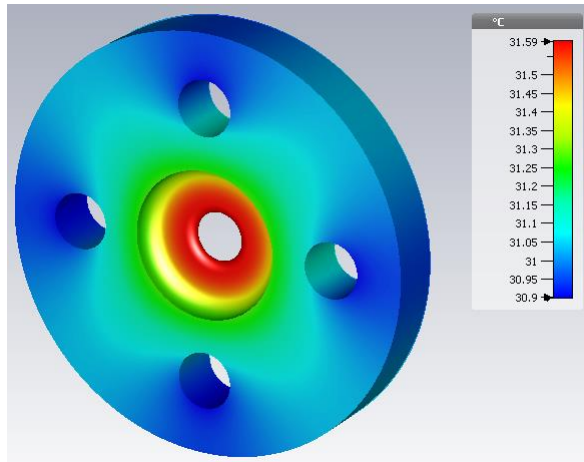
$$A=1.48$$

$$s_2=9.948 \times 10^{-5}$$



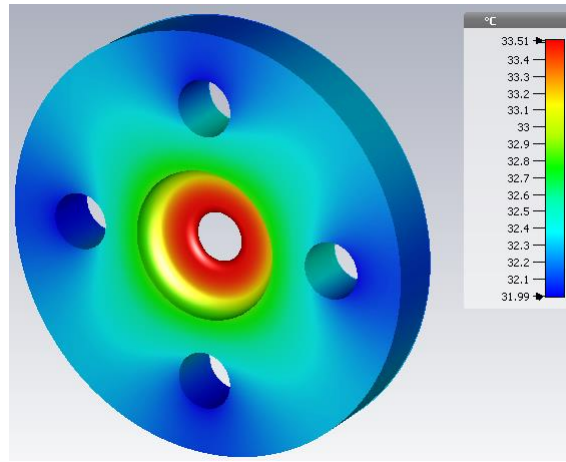
THERMAL ANALYSIS WITH CST CODE

$P_{\text{diss}}=9 \text{ W}$



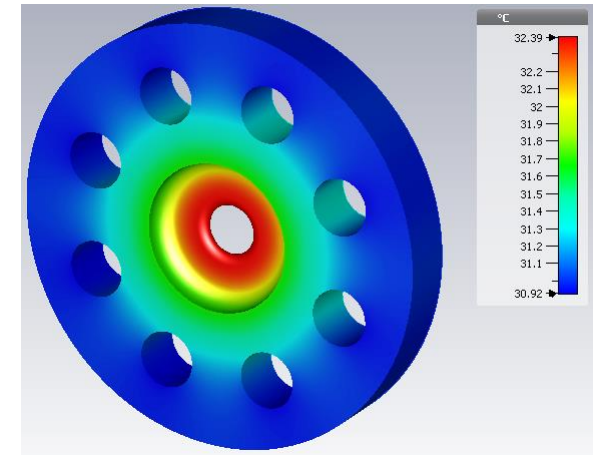
100 Hz

$P_{\text{diss}}=19 \text{ W}$



1 kHz

$P_{\text{diss}}=19 \text{ W}$



1 kHz

Water temperature: 30° C

Total detune of the structure: 3.5° in phase advance
(reduction in terms of accelerating gradient <0.5%)

Collaboration with Luigi Faillace (INFN)

CONCLUSIONS

The **design of the RF linacs** of EuPRAXIA@SPARC_LAB and CompactLight has been completed. **Thermal analysis** has been performed and the **mechanical design of the cell** has been done. A preliminary study on **high repetition rate operation** has been performed.

NEXT STEPS

For both the projects

- Integrate in the optimization tool an **exact solution algorithm** (Shumail-Dolgashev) and perform **simulations with particle tracking codes** like ELEGANT to calculate the **transverse dynamics of the beam** along the linac.

For EuPRAXIA@SPARC_LAB

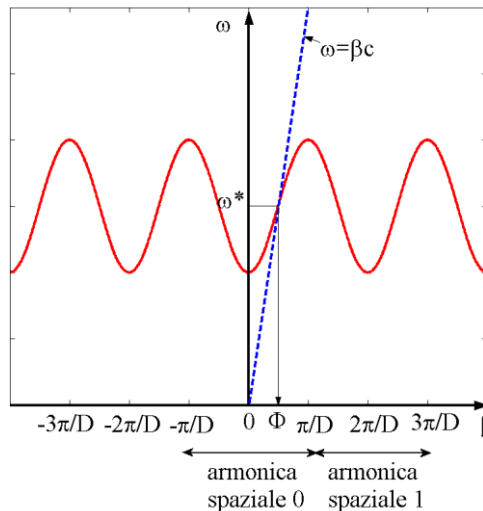
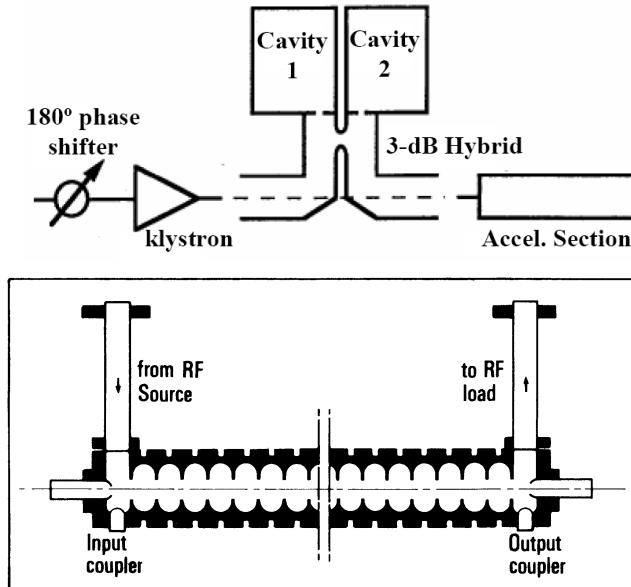
- **3 cells and structure prototypes** will be fabricated.
- A high power **test station** will be installed this year at LNF.

Thank you for your attention!

Traveling wave accelerating structures

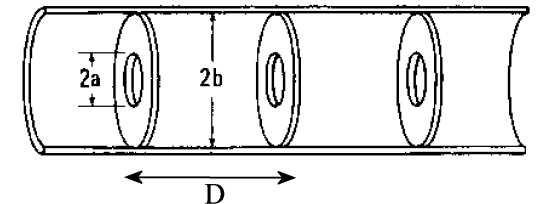
Propagation constant $\beta = \sqrt{\left(\frac{\omega}{c}\right)^2 - k_t^2} \Rightarrow v_{ph} = \frac{c}{\sqrt{1 - \left(\frac{k_t c}{\omega}\right)^2}} > c$ Phase velocity

dipendente dalla geometria della guida e dal modo considerato



Phase advance

$$\Phi = \beta D = \frac{\omega}{v_{ph}} D = \frac{\omega}{c} D$$



Basically, a TWAS is a **circular waveguide loaded by irises** in order to slow down the wave phase velocity. The spacing D between the irises determines the **phase advance per cell**.

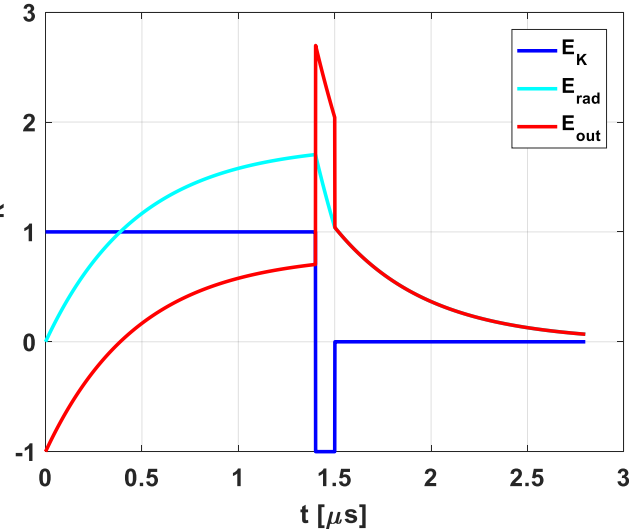
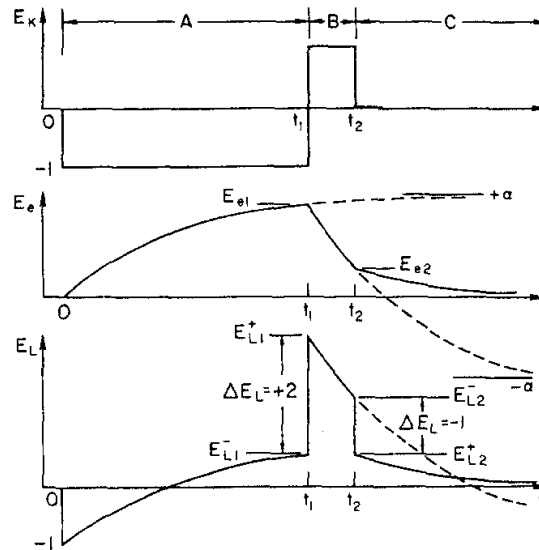
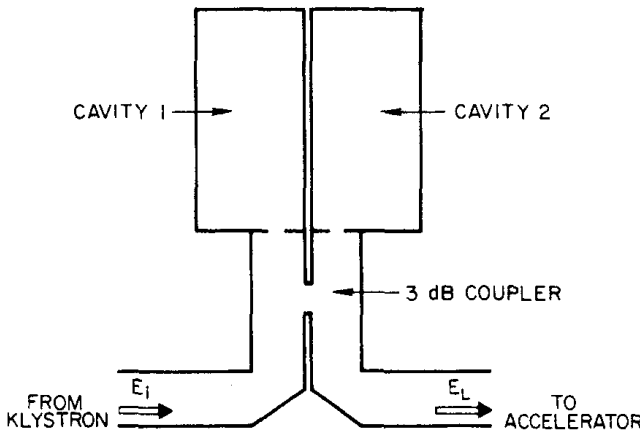
They are mainly used to accelerate electrons.

Courtesy of A. Gallo and D. Alesini

Pulse compressor: SLED

A **pulse compressor** is a component that allows to **increase the peak power** at the section input by reducing the pulse length. In a **SLED**, this is obtained by combing the power reflected by **2 high-Q cavities**.

Example: compressed pulse of 100 ns with a Q_e of 20000



$$\frac{E_{out}}{E_K}(t) = -\alpha e^{-\frac{t\omega}{2Q_L}} + (\alpha - 1), \quad 0 < t < t_1$$

$$\frac{E_{out}}{E_K}(t) = \gamma e^{-\frac{(t-t_1)\omega}{2Q_L}} - (\alpha - 1), \quad t_1 < t < t_2$$

$$\frac{E_{out}}{E_K}(t) = \left[\gamma e^{-\frac{(t_2-t_1)\omega}{2Q_L}} - \alpha \right] e^{-\frac{(t-t_2)\omega}{2Q_L}}, \quad t > t_2$$

$$\alpha = \frac{2\beta}{1+\beta} = 2 \frac{Q_l}{Q_e}, \quad \beta = \frac{Q_0}{Q_e}$$

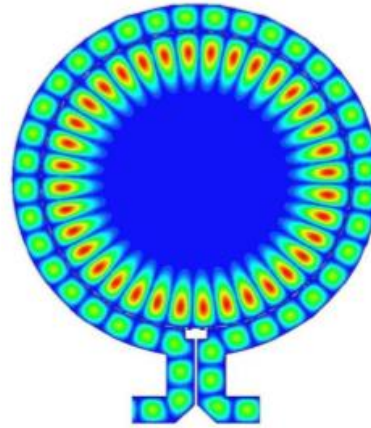
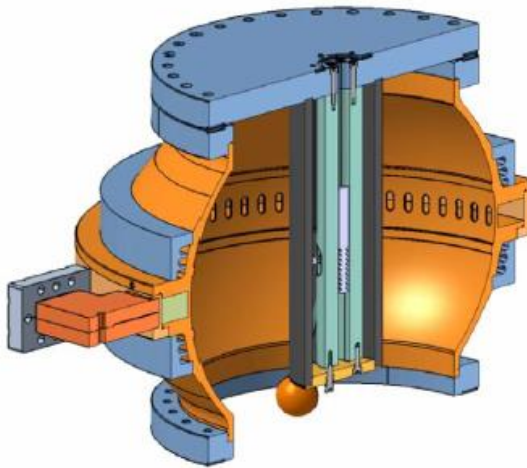
$$Q_L = \frac{Q_0}{1+\beta}, \quad \gamma = \alpha \left(2 - e^{-\frac{t_1\omega}{2Q_L}} \right) = 2 \frac{Q_l}{Q_e} \left(2 - e^{-\frac{t_1\omega}{2Q_L}} \right)$$

$$P_{out_SLED}(t) = P_K(t=0) \left(\frac{E_{out}}{E_K}(t) \right)^2 \quad [1]$$

Pulse compressor: BOC

For a BOC (Barrel-shape Open Cavity) the equations are the same but it's possible to obtain higher values of the unloaded quality factor. This allows to obtain better performances.

BOC



- ❖ Cavity is surrounded by rectangular waveguide to couple power.
- ❖ Power is coupled through coupling apertures.

Cell and structure parameters

Quality factor

$$Q = \omega_{RF} \frac{W}{p_{diss}}$$

It measures the merit of a cell as a resonator

Shunt impedance per unit length

$$R = \frac{E_{acc}^2}{p_{diss}} \left[\frac{\Omega}{m} \right]$$

It defines the efficiency of an accelerating mode

Group velocity

$$v_g = \frac{P_{in}}{W} \left[\frac{m}{s} \right]$$

It is the velocity at which the RF energy flows

R upon Q

$$\frac{R}{Q} = \frac{E_{acc}^2}{\omega W} \left[\frac{\Omega}{m} \right]$$

It is a qualification parameter of the cavity geometrical design

Time - dependent accelerating gradient : $E_{acc}(z, t') = G(z, t') = G_0[t' - \tau(z)]g(z)$

Signal time delay : $\tau(z) = \int_0^z \frac{dz'}{v_g(z')}$; Filling time : $t_f = \tau(L_s)$; $t' = t - t_1$;

$$G_0(t') = G(z=0, t') = \sqrt{\frac{\omega}{v_{g0}} \frac{R(0)}{Q(0)} P_{in-s}(t')} = \sqrt{\frac{\omega}{v_{g0}} \frac{R}{Q} P_{in-s}(t')} = \sqrt{\frac{\omega}{v_{g0}} \frac{R}{Q} P_K(t=0)} \frac{E_{out}}{E_K}(t)$$

with R shunt impedance per unit length and Q quality factor

$$\text{Attenuation per unit length : } \alpha(z) = \frac{1}{2} \left[\frac{1}{v_g} \frac{dv_g}{dz} - \frac{1}{R/Q} \frac{d(R/Q)}{dz} + \frac{\omega}{v_g Q} \right]$$

$$g(z) = e^{-\int_0^z \alpha(z') dz'} = \sqrt{\frac{v_g(0)}{v_g(z)}} \sqrt{\frac{R(z)}{Q(z)} \frac{Q(0)}{R(0)}} e^{-\frac{1}{2} \int_0^z \frac{\omega}{v_g(z') Q(z')} dz'}$$

$$\text{Hyp : } \frac{R}{Q} \text{ constant along } z \Rightarrow g(z) = \sqrt{\frac{v_{g0}}{v_g(z)}} e^{-\frac{1}{2} \int_0^z \frac{\omega}{v_g(z') Q(z')} dz'} = \sqrt{\frac{v_{g0}}{v_g(z)}} e^{-\frac{1}{2} \frac{\omega}{Q} \tau(z)}$$

$$\text{Section attenuation : } \tau_s = \int_0^{L_s} \alpha(z) dz$$

$$\text{Accelerating Voltage : } V_a = \int_0^{L_s} dz' G(z', t' = t_f = t_2 - t_1);$$

$$\text{Effective shunt impedance : } R_s = \frac{V_a^2}{P_K(t=0)L_s} [\Omega / m]$$

It defines the efficiency of the structure

$$\text{Total Power : } P_{tot} = \frac{V_{tot} \langle G \rangle}{R_s}$$

A. Lunin, V. Yakovlev, A. Grudiev, PRST-AB 14, 052001, (2011)

R. B. Neal, Journal of Applied Physics, V.29, pp. 1019-1024, (1958)

Single cell formulas

$$V_z = \left| \int_0^D E_z \cdot e^{j\omega_{RF} \frac{z}{c}} dz \right|$$

single cell accelerating voltage [V]:

$$E_{acc} = \frac{V_z}{D}$$

average accelerating field in the cell [$\frac{V}{m}$]

$$P_{in} = \int_{Section} \frac{1}{2} \text{Re}(\vec{E} \times \vec{H}^*) \cdot \hat{z} dS$$

average input power (flux power) [W]

$$P_{diss} = \frac{1}{2} R_s \int_{\substack{cavity \\ wall}} |H_{tan}|^2 dS$$

average dissipated power in the cell [W]

$$R_s = \sqrt{\frac{\pi f_{RF} \mu_0}{\sigma}} = \frac{1}{\sigma \delta}$$

surface resistance [Ω]

$$\delta = \frac{1}{\sqrt{\pi f_{RF} \mu_0 \sigma}}$$

skin depth [m]

$$p_{diss} = \frac{P_{diss}}{D}$$

average dissipated power per unit length [$\frac{W}{m}$]

$$W = \int_{\substack{cavity \\ volume}} \overbrace{\left(\frac{1}{4} \epsilon |\vec{E}|^2 + \frac{1}{4} \mu |\vec{H}|^2 \right)}^{\text{energy density}} dV$$

stored energy in the cell [J]

$$w = \frac{W}{D}$$

average stored energy per unit length [$\frac{J}{m}$]

$$Q = \omega_{RF} \frac{w}{p_{diss}}$$

quality factor [arb. units]

Breakdown

The major obstacle to high gradient is **RF breakdown**. It is a phenomenon that abruptly changes transmission and reflection RF power directed towards the structure. A local field quantity which predicts the high gradient performance of an accelerating structure is the **modified Poynting vector S_c** :

$$S_c = \text{Re}\{\bar{S}\} + g_c \text{Im}\{\bar{S}\} \left[\frac{W}{m^2} \right], \text{ with } g_c = \frac{1}{6}$$

The dependence of the modified Poynting vector on RF pulse length t_p at a fixed breakdown rate (BDR) has a well established **scaling law** observed in many experiments:

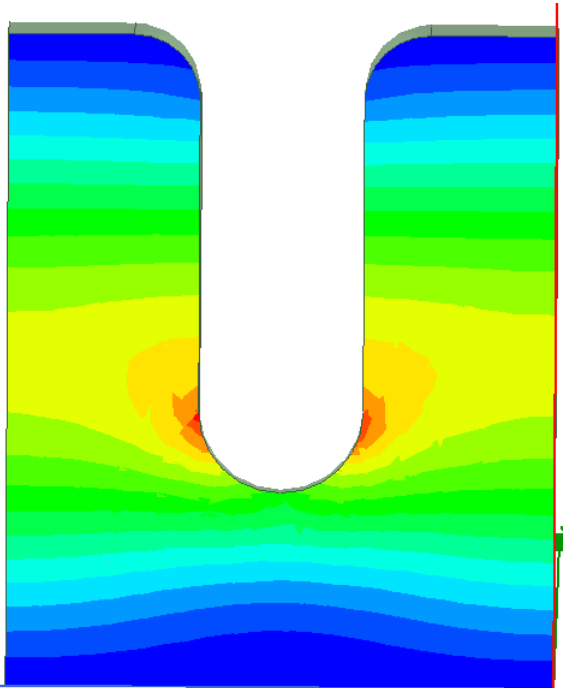
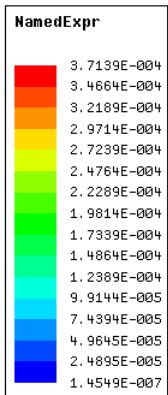
$$\frac{S_c^{15} t_p^5}{BDR} = \text{const}$$

The **BDR** is defined as the probability of having a breakdown and it is typically measured in breakdown per pulse for 1 m long structure. As design guideline for a new RF structure, S_c should not exceeds **4 MW/mm²** if the structure is supposed to operate at a breakdown rate smaller than **10⁻⁶ bpp/m** and a pulse length of **200 ns**.

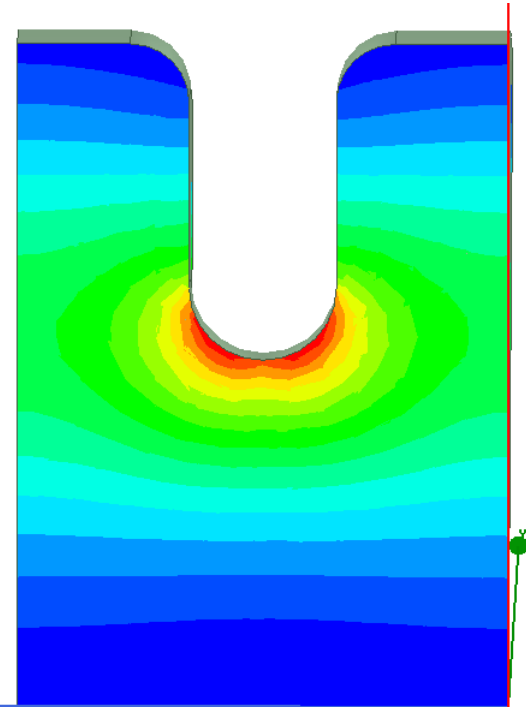
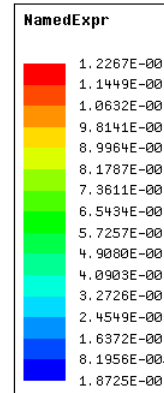
A. Grudiev, S. Calatroni, and W. Wuensch, PhysRevSTAB.12.102001 (2009)
K. Sjobak, E. Adli, A. Grudiev, MOPP028, Proc. of LINAC2014 (2014)

Breakdown

Maximum value of normalized modified Poynting vector



a=3 mm



a=6 mm

COUPLER MAIN PARAMETERS

For couplers, an important parameter is the **RF pulsed heating**. It is a process by which a metal is heated from magnetic fields on its surface due to high-power pulsed RF. The **temperature rise** is defined as (for **copper**):

$$\Delta T[^\circ\text{C}] = 127 |H_{\parallel}[\text{MA}/\text{m}]|^2 \sqrt{f_{\text{RF}}[\text{GHz}]} \sqrt{t_p[\mu\text{s}]}$$

As a general experimental rule, if the pulsed heating is **below 50 °C** damage to the couplers is practically avoided.

Coupling slots introduce a **distortion in the field distribution** and **multi-pole components** of the field can appear and affect the beam dynamics.

The multi-pole field components in the coupler are completely dominated by the **magnetic field asymmetry**. Odd components can be avoided with a symmetric feeding.

First order development of the **azimuthal magnetic field** near the beam axis:

$$B_{\phi}(r, \phi, z) \cong A_0(z)r + \sum_{n=1}^{\infty} A_n(z) \cos(n\phi) r^{n-1}$$

The **quadrupolar component** is the component associated to the term with $n=2$ and the gradient of the quadrupole component is exactly the term **A₂**.

V. A. Dolgashev, High magnetic fields in couplers of X-band accelerating structures (2003)

L. Laurent, Experimental study of rf pulsed heating (2011)

D. Alesini et al., 10.1103/PhysRevAccelBeams.20.032004 (2017).

Analytical study:

- Constant impedance w/ and w/o pulse compression
- Constant gradient w/ and w/o pulse compression

Constant Impedance (CI) AS formulas

$$v_g(z) = v_{g0}; \quad \tau(z) = \int_0^z \frac{dz'}{v_g(z')} = \frac{z}{v_{g0}}$$

$$t' = t - t_1; \quad \tau_s = \alpha L_s = \frac{\omega}{2v_{g0}Q} L_s; \quad t_f = \tau(L_s) = \frac{L_s}{v_{g0}} = \frac{2Q\tau_s}{\omega} \quad [5];$$

$$g(z) = \sqrt{\frac{v_{g0}}{v_g(z)}} e^{-\frac{1}{2Q}\omega\tau(z)} = e^{-\tau_s \frac{z}{L_s}}, \quad G_0(t') = \sqrt{2\tau_s \frac{R}{L_s} P_K(t=0)} \frac{E_{out}}{E_K}(t')$$

$$G(z, t') = \sqrt{2\tau_s \frac{R}{L_s} P_K(t=0)} \frac{E_{out}}{E_K}(t' - \tau(z)) e^{-\tau_s \frac{z}{L}}$$

[5] T. P. Wangler, RF Linear Accelerators, John Wiley & Sons, 2008

Constant Impedance (CI) AS – With pulse compression

$$\boxed{\frac{E_{out}}{E_K}(t') = \gamma e^{-\frac{t'\omega}{2Q_L}} - (\alpha - 1);} \quad G(z, t') = \sqrt{2\tau_s \frac{R}{L_s}} P_K(t=0) \left(\gamma e^{-\left(t' - \frac{z}{v_g}\right) \frac{\omega}{2Q_L}} - (\alpha - 1) \right) e^{-\tau_s \frac{z}{L_s}} = G_0 \left(\gamma e^{-\left(t' - \frac{z}{v_g}\right) \frac{\omega}{2Q_L}} - (\alpha - 1) \right) e^{-\tau_s \frac{z}{L_s}}$$

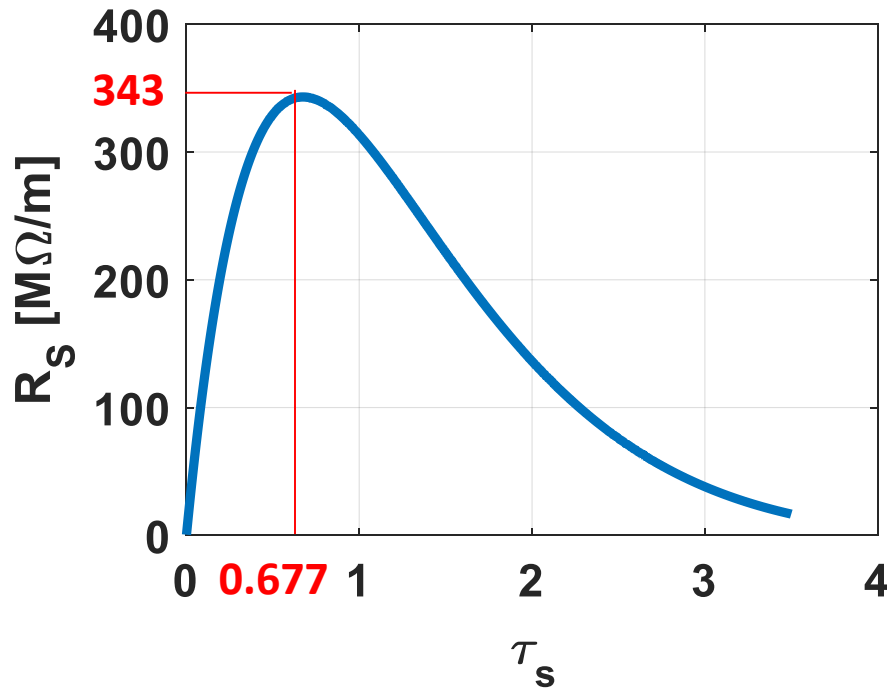
$$V_a = \int_0^{L_s} dz' G(z', t' = t_f = t_2 - t_1) = \sqrt{P_K(t=0)RL_s} \sqrt{\frac{2}{\tau_s}} \left[\gamma \left(\frac{1}{\frac{Q}{Q_L} - 1} \right) \left(e^{-\tau_s} - e^{-\frac{Q}{Q_L}\tau_s} \right) + (\alpha - 1)(e^{-\tau_s} - 1) \right] = \sqrt{P_K(t=0)RL_s} \sqrt{\frac{R_s}{R}} \quad [6]$$

$$\frac{R_s}{R} = \frac{V_a^2}{P_K(t=0)RL_s} = \left\{ \sqrt{\frac{2}{\tau_s}} \left[\gamma \left(\frac{1}{\frac{Q}{Q_L} - 1} \right) \left(e^{-\tau_s} - e^{-\frac{Q}{Q_L}\tau_s} \right) + (\alpha - 1)(e^{-\tau_s} - 1) \right] \right\}^2$$

$$\frac{G\left(\frac{z}{L_s}, t_F, \tau_{s0}\right)}{\left\langle G\left(\frac{z}{L_s}, t_F, \tau_{s0}\right) \right\rangle} = L_s \frac{\left(\gamma e^{-\left(1 - \frac{z}{L_s}\right) \frac{Q}{Q_L} \tau_{s0}} - (\alpha - 1) \right) e^{-\tau_{s0} \frac{z}{L_s}}}{\int_0^{L_s} \left(\gamma e^{-\left(1 - \frac{z}{L_s}\right) \frac{Q}{Q_L} \tau_{s0}} - (\alpha - 1) \right) e^{-\tau_{s0} \frac{z}{L_s}} dz}$$

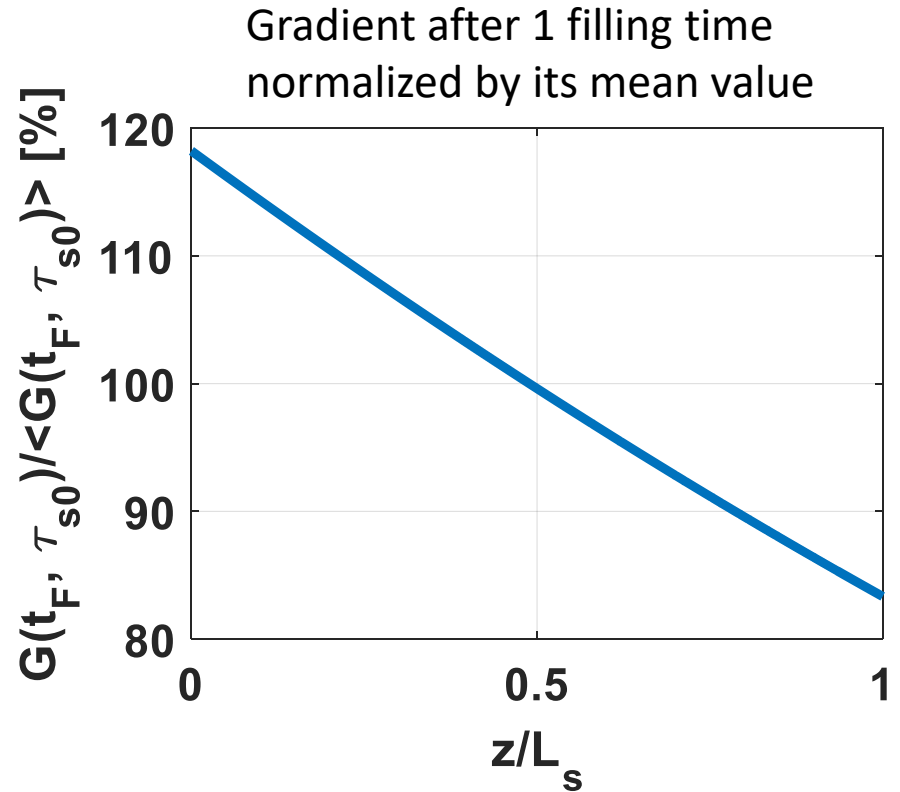
[6] J. Le Duff, High-field electron linacs, CERN 95-06, (1995)

Constant Impedance (CI) AS – With pulse compression



Reference formula

$$R_s = 2\tau_s R \left[\frac{\left(1 - \frac{2Q_l}{Q_e}\right)}{\tau_s} \left(1 - e^{-\tau_s}\right) + \frac{\left(\frac{2Q_l}{Q_e} \left[2 - e^{-(\tau_k - \tau_p)}\right]\right)}{\tau_s \left(1 - \frac{Q}{Q_l}\right)} \left(e^{-\tau_s \frac{Q}{Q_l}} - e^{-\tau_s}\right) \right]^2$$



Reference formula

$$G(z, t' = t_f) = \sqrt{\frac{\omega}{v_g} \frac{R}{Q} P_{in}} e^{-\tau_s / L_s z} \cdot \left\{ 1 + \frac{2Q_l}{Q_e} \left[\exp\left(-\frac{\omega(L_s - z)}{2v_g Q_l}\right) \left[2 - \exp\left(-\frac{\omega t_0}{2Q_l}\right) \right] - 1 \right] \right\}$$

Effective Shunt impedance in Const Gradient (CG) AS

$$v_g(z) = \frac{\omega L_s}{Q} \frac{\left[1 - \left(1 - e^{-2\tau_s} \right) \frac{z}{L_s} \right]}{\left(1 - e^{-2\tau_s} \right)}; \quad \tau(z) = \int_0^z \frac{dz'}{v_g(z')} = -\frac{Q}{\omega} \ln \left[1 - \left(1 - e^{-2\tau_s} \right) \frac{z}{L_s} \right] \quad [5]$$

$$\tau_s = \int_0^L \alpha(z) dz; \quad t_f = \tau(L_s) = \frac{2Q\tau_s}{\omega} \quad [5];$$

$$g(z) = 1, \quad G_0(t') = \sqrt{\frac{R}{L_s} P_K(t=0) \left(1 - e^{-2\tau_s} \right)} \frac{E_{out}}{E_K}(t') \quad [5]$$

$$G(z, t') = \sqrt{\frac{R}{L_s} P_K(t=0) \left(1 - e^{-2\tau_s} \right)} \frac{E_{out}}{E_K}(t' - \tau(z)) = G_0 \frac{E_{out}}{E_K}(t' - \tau(z))$$

[5] T. P. Wangler, RF Linear Accelerators, John Wiley & Sons, 2008

Constant Gradient (CG) AS – With pulse compression

$$\frac{E_{out}}{E_K}(t') = \gamma e^{-\frac{t'\omega}{2Q_L}} - (\alpha - 1);$$

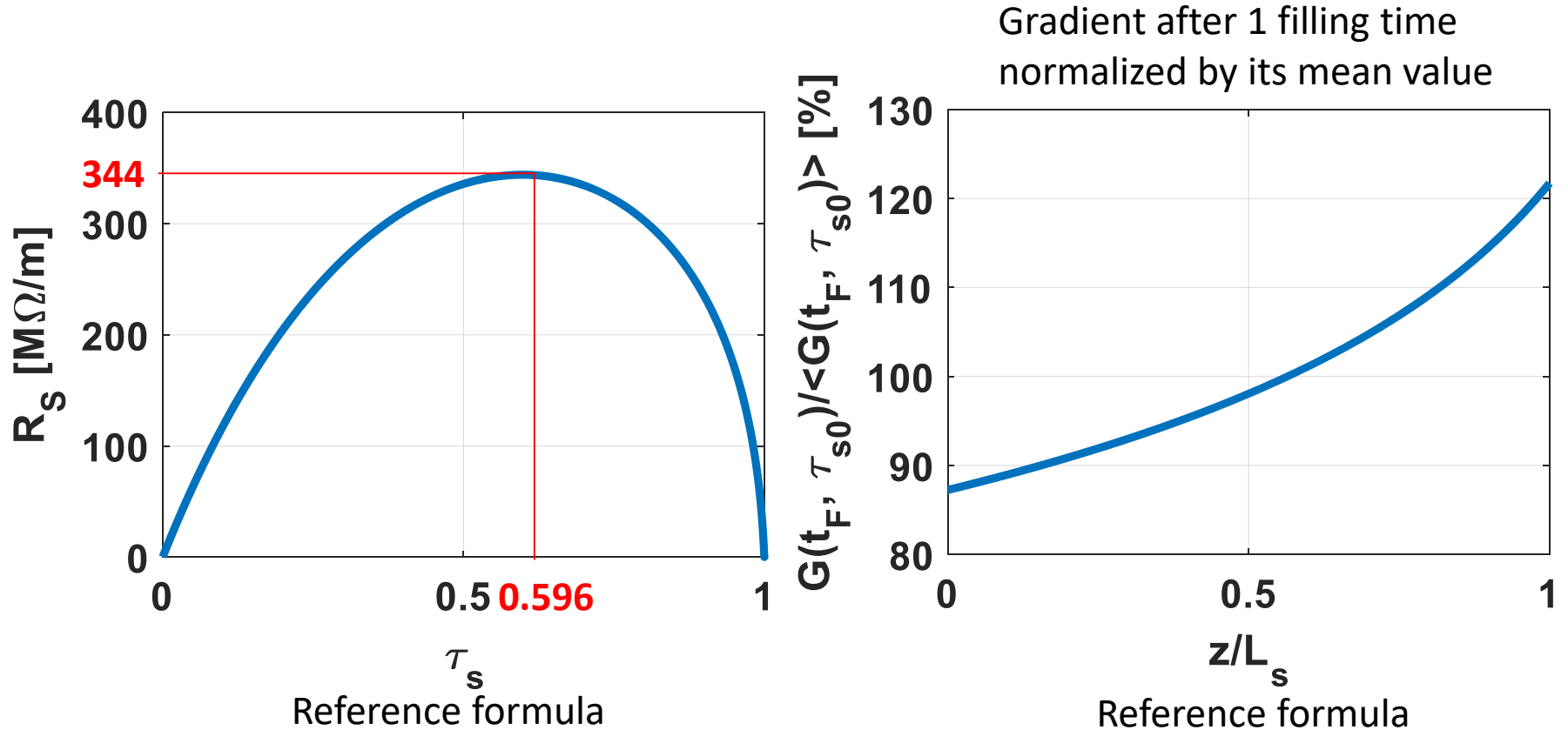
$$G(z, t') = \sqrt{\frac{R}{L_s} P_K(t=0)(1-e^{-2\tau_s})} \left\{ \gamma e^{-\frac{t'\omega}{2Q_L}} \left[1 - \left(1 - e^{-2\tau_s}\right) \frac{z}{L_s} \right]^{-\frac{Q}{2Q_L}} - (\alpha - 1) \right\} = G_0 \left\{ \gamma e^{-\frac{t'\omega}{2Q_L}} \left[1 - \left(1 - e^{-2\tau_s}\right) \frac{z}{L_s} \right]^{-\frac{Q}{2Q_L}} - (\alpha - 1) \right\}$$

$$V_a = \int_0^{L_s} dz' G(z', t' = t_f = t_2 - t_1) = \sqrt{P_K(t=0)RL_s(1-e^{-2\tau_s})} \left\{ \gamma e^{-\frac{Q}{Q_L}\tau_s} \left[\frac{1 - (e^{-2\tau_s})^{(1-\frac{Q}{2Q_L})}}{(1-\frac{Q}{2Q_L})(1-e^{-2\tau_s})} \right] - (\alpha - 1) \right\} = \sqrt{P_K(t=0)RL_s} \sqrt{\frac{R_s}{R}} \quad [1]$$

$$\frac{R_s}{R} = \frac{V_a^2}{P_K(t=0)RL_s} = (1-e^{-2\tau_s}) \left\{ \gamma e^{-\frac{Q}{Q_L}\tau_s} \left[\frac{1 - (e^{-2\tau_s})^{(1-\frac{Q}{2Q_L})}}{(1-\frac{Q}{2Q_L})(1-e^{-2\tau_s})} \right] - (\alpha - 1) \right\}^2$$

$$\frac{G\left(\frac{z}{L_s}, t_F, \tau_{s0}\right)}{\left\langle G\left(\frac{z}{L_s}, t_F, \tau_{s0}\right) \right\rangle} = L_s \frac{\gamma e^{-\frac{Q}{Q_L}\tau_{s0}} \left[1 - \left(1 - e^{-2\tau_{s0}}\right) \frac{z}{L_s} \right]^{-\frac{Q}{2Q_L}} - (\alpha - 1)}{\int_0^{L_s} \left\{ \gamma e^{-\frac{Q}{Q_L}\tau_{s0}} \left[1 - \left(1 - e^{-2\tau_{s0}}\right) \frac{z}{L_s} \right]^{-\frac{Q}{2Q_L}} - (\alpha - 1) \right\} dz}$$

Constant Gradient (CG) AS – With pulse compression



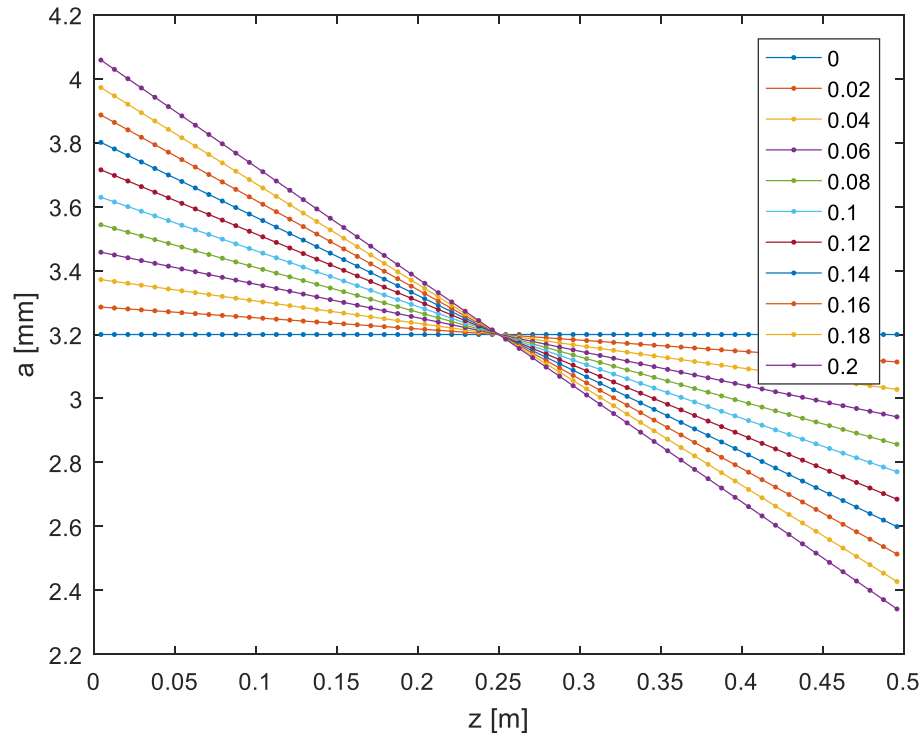
$$R_s = R \frac{2\tau_s}{1+\tau_s} \left\{ 1 - \frac{2Q_l}{Q_e} + \frac{2Q_l}{Q_e} \left[2 - \exp\left(-\frac{\omega t_k}{2Q_l}\right) \cdot \left(\frac{1+\tau_s}{1-\tau_s}\right)^{Q/2Q_l} \right] \right. \\ \left. \cdot \frac{1-\tau_s}{2\tau_s} \frac{1}{1-Q/2Q_l} \left[\left(\frac{1+\tau_s}{1-\tau_s}\right)^{1-Q/2Q_l} - 1 \right] \right\}^2$$

$$G(z, t' = t_f) = \sqrt{\frac{2\tau_s / L_s R}{1+\tau_s}} P_{in} \cdot$$

$$\left\{ 1 + \frac{2Q_l}{Q_e} \left[\left(\frac{1+\tau_s - \tau_s / L_s z}{1-\tau_s} \right)^{-\frac{Q}{2Q_l}} \left[2 - \exp\left(-\frac{\omega t_0}{2Q_l}\right) \right] - 1 \right] \right\}$$

$L_s=0.5\text{m}$ (60 cells), $N_s=32$

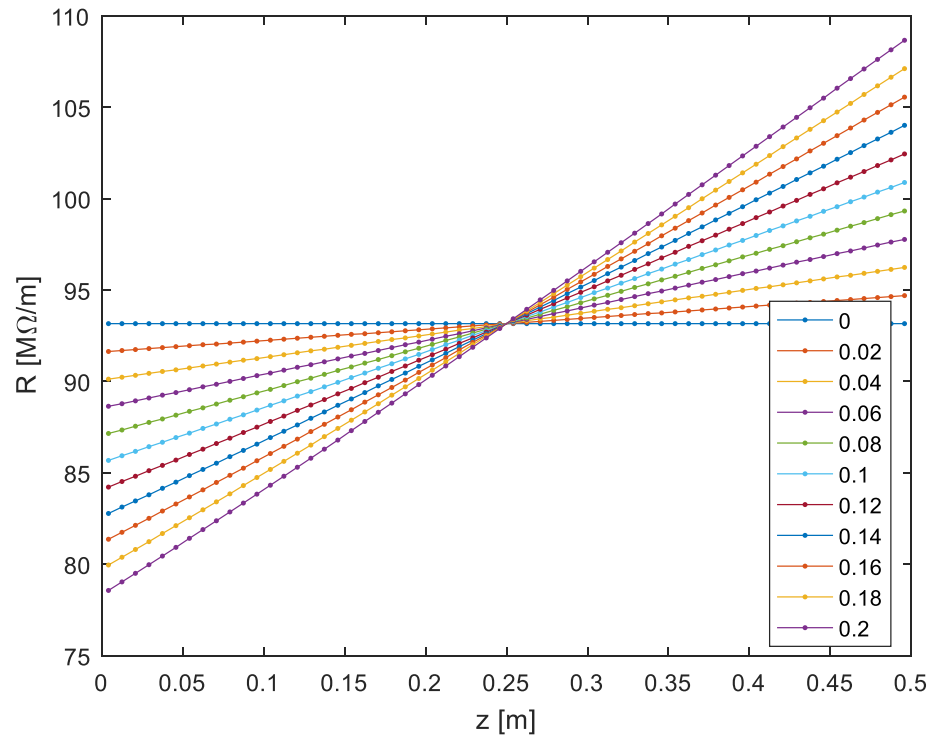
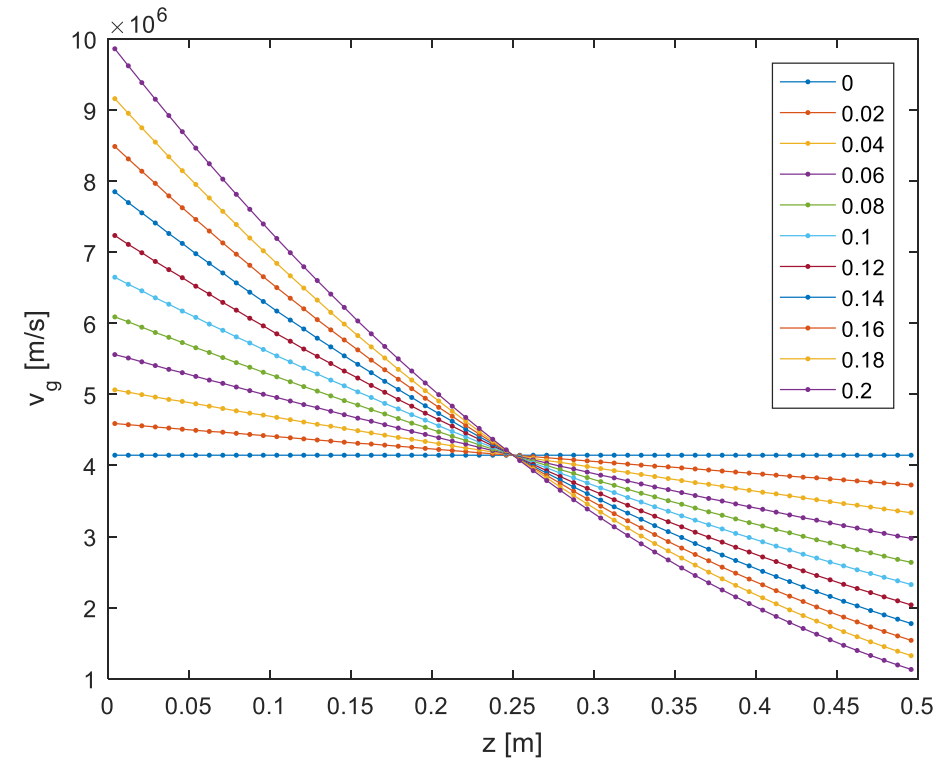
Slope from 0° to 0.2°
(step 0.02°)



With an active length of 16 m we can have 32 structures of 0.5 m

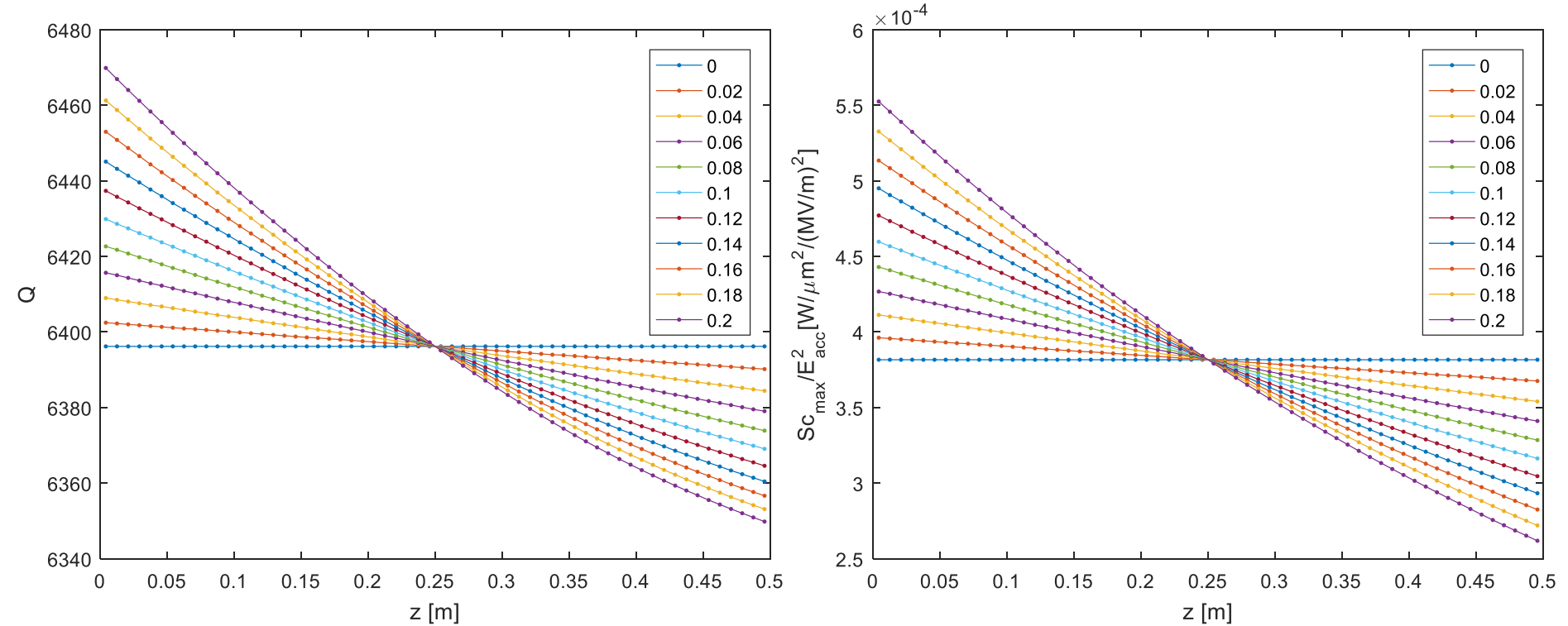
Fixing the length of the structure (60 cells for example) and the slope of the tapering (from 0° to 0.2° for the moment, $\langle a \rangle = 3.2$ mm) it is possible to find the iris radius of each cell (every \cdot is a cell) and then the related values of v_g , R , Q , normalized modified Poynting vector using the polynomial fits.

$L_s=0.5\text{m}$ (60 cells), $N_s=32$



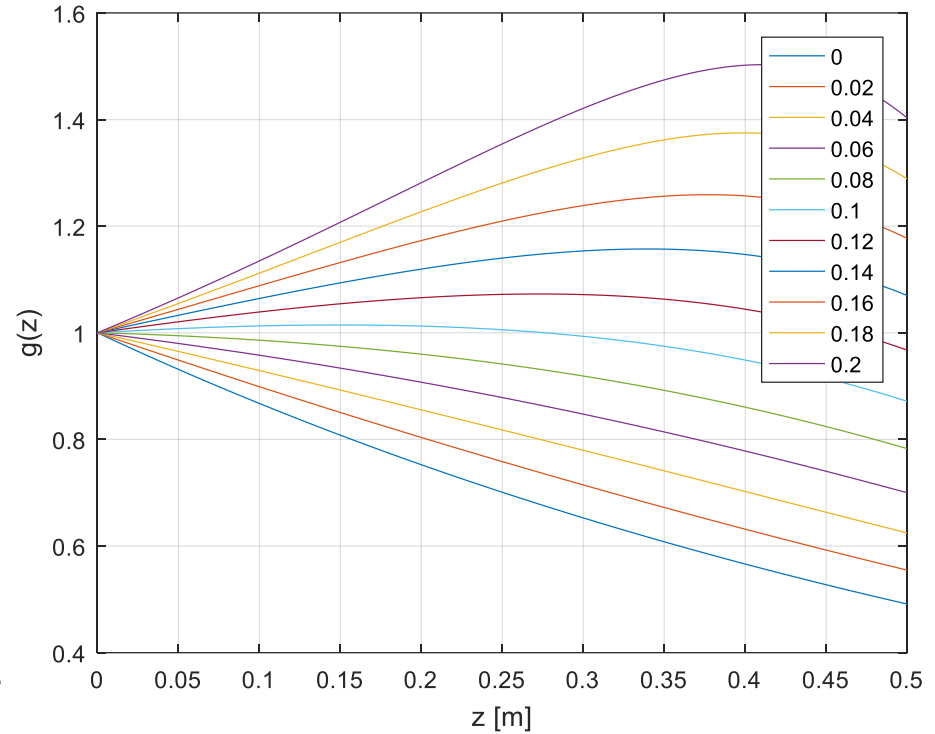
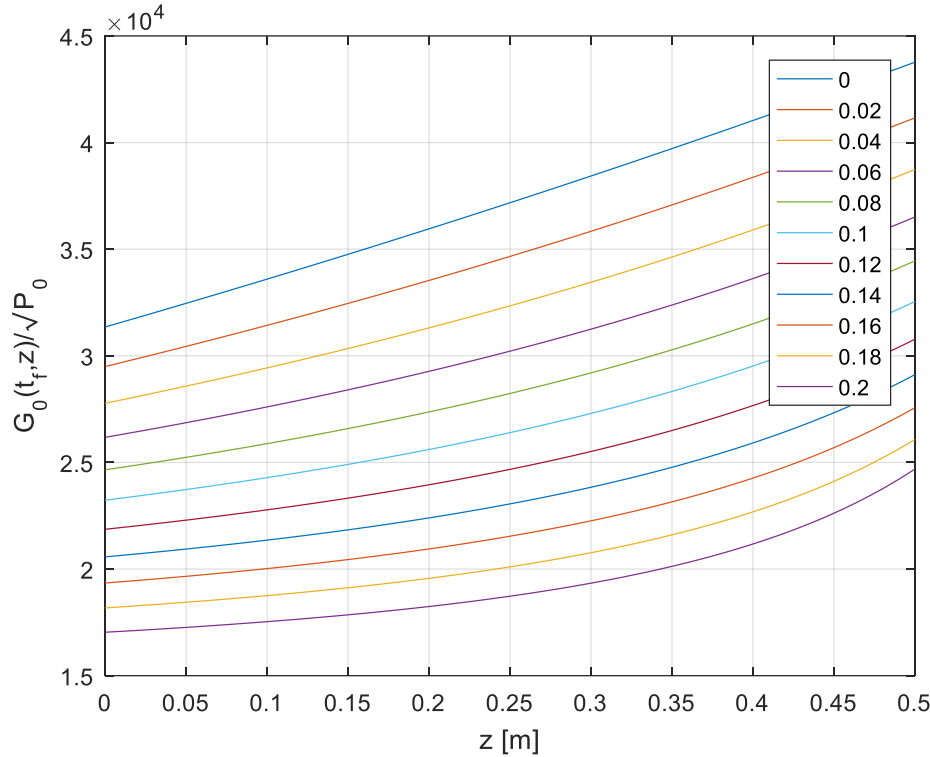
With a linear tapering there is a non-linear behavior of the group velocity along z .

$L_s=0.5\text{m}$ (60 cells), $N_s=32$



Since now we have the parameters of every cell it is possible to apply the general formulas in order to find the optimal slope for every fixed length (finding for each slope the optimal value of Q_e for the SLED).

Ls=0.5m (60 cells), Ns=32, Q0=180000



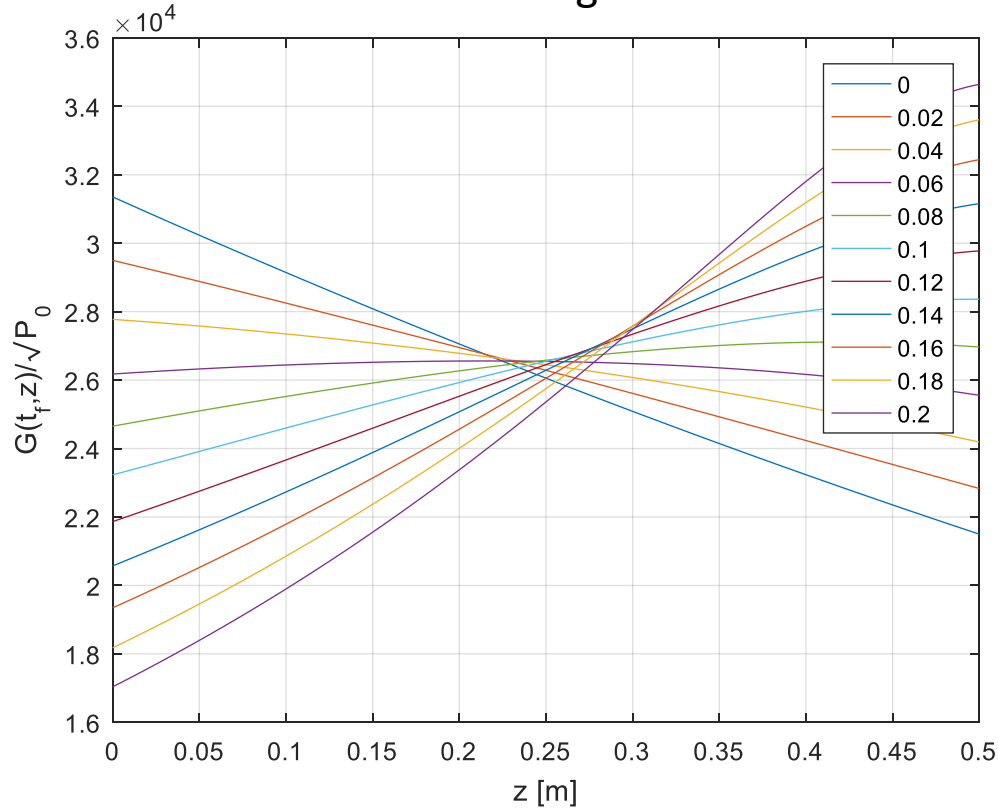
$$G_0[t_f - \tau(z)] = \sqrt{\frac{\omega}{v_g(0)} \frac{R(0)}{Q(0)}} P_0 \frac{E_{out}}{E_K} (t_f - \tau(z))$$

$$g(z) = e^{-\int_0^z \alpha(z') dz'} = \sqrt{\frac{v_g(0)}{v_g(z)}} \sqrt{\frac{R(z)}{Q(z)} \frac{Q(0)}{R(0)}} e^{-\frac{1}{2} \int_0^z \frac{\omega}{v_g(z') Q(z')} dz'}$$

$$\alpha(z) = \frac{1}{2} \left[\frac{1}{v_g} \frac{dv_g}{dz} - \frac{1}{R/Q} \frac{d(R/Q)}{dz} + \frac{\omega}{v_g Q} \right]$$

$L_s=0.5\text{m}$ (60 cells), $N_s=32$, $Q_0=180000$

Normalized gradient vs z
after 1 filling time

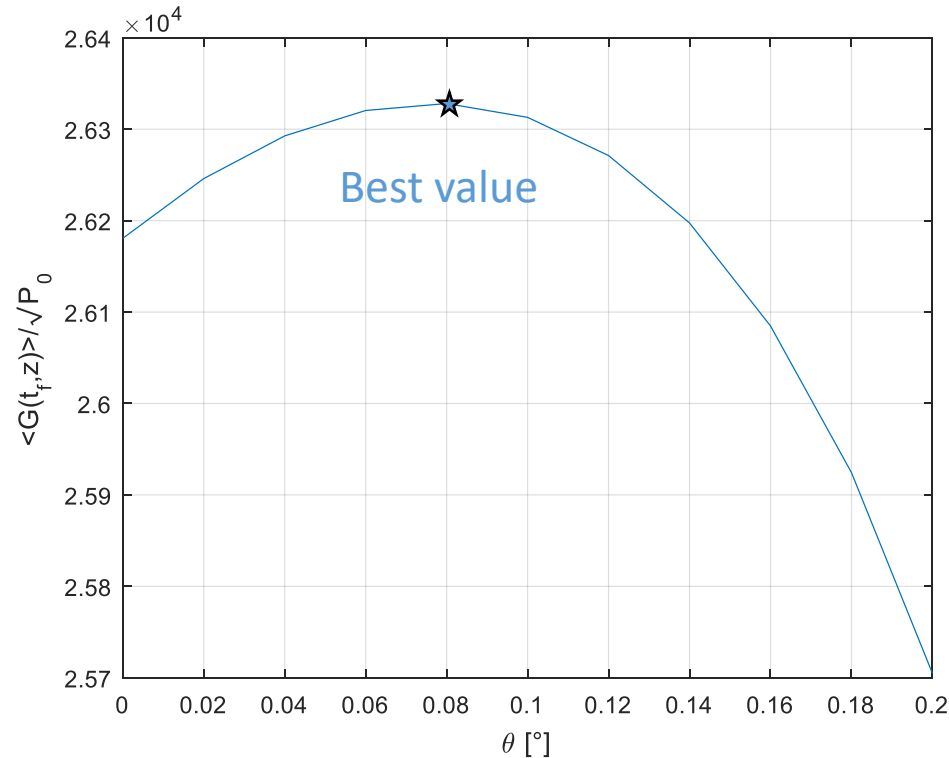


It is possible to observe that for each slope we obtain different profiles of the gradient.

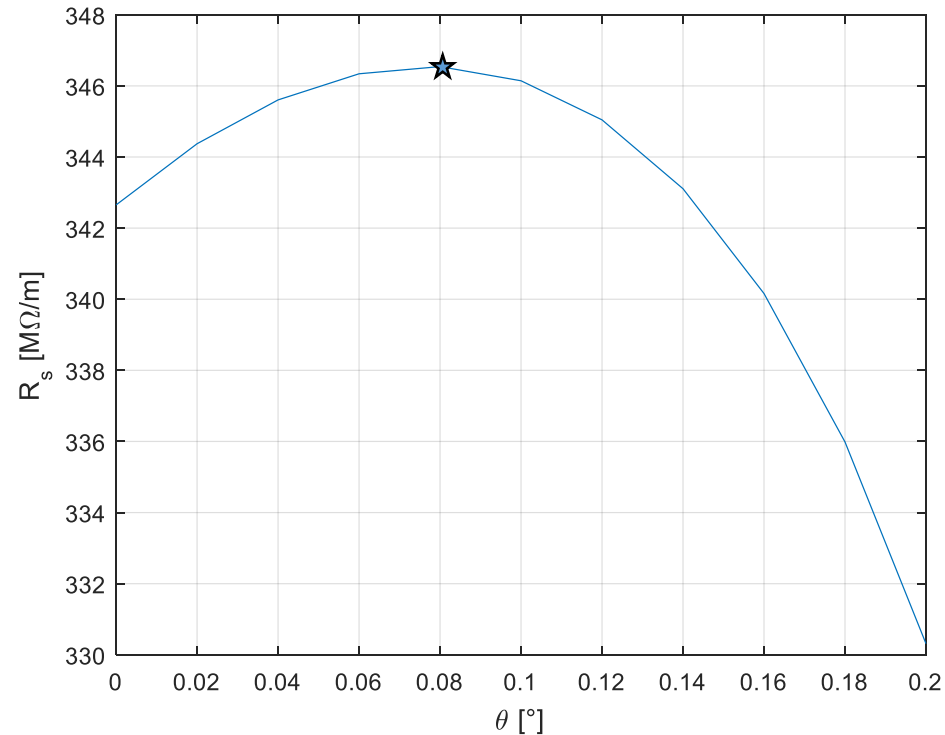
$$G(z, t_f) = G_0[t_f - \tau(z)]g(z) = \sqrt{\frac{\omega}{v_g(0)} \frac{R(0)}{Q(0)}} P_0 \frac{E_{out}}{E_K} (t_f - \tau(z)) \sqrt{\frac{v_g(0)}{v_g(z)}} \sqrt{\frac{R(z)}{Q(z)} \frac{Q(0)}{R(0)}} e^{-\frac{1}{2} \int_0^z \frac{\omega}{v_g(z') Q(z')} dz'}$$

$L_s=0.5\text{m}$ (60 cells), $N_s=32$, $Q_0=180000$

Average normalized gradient



Effective shunt impedance

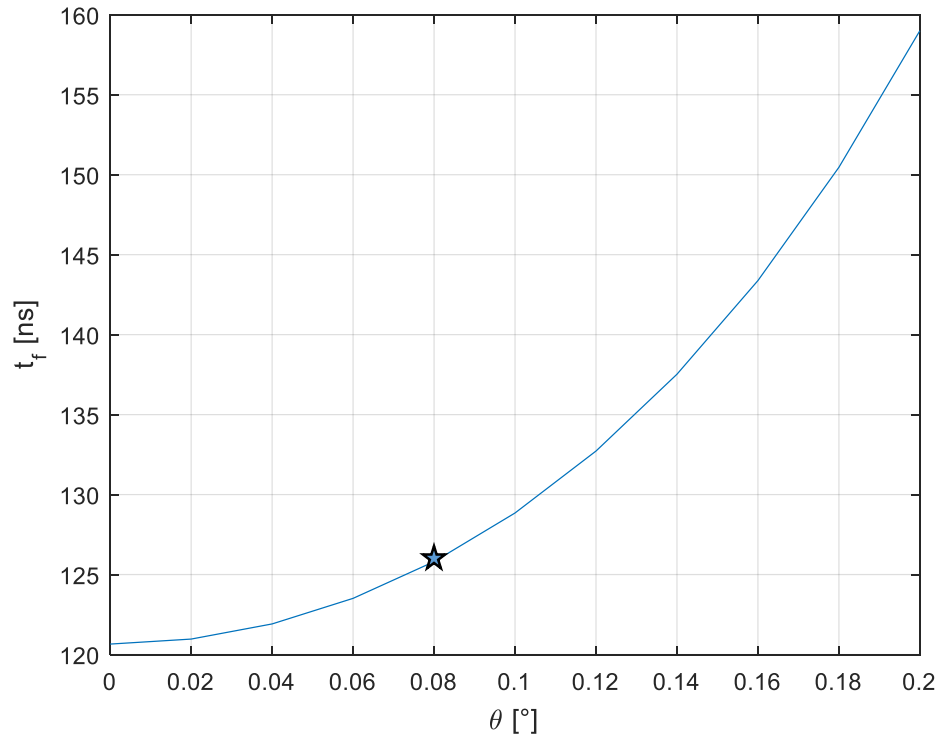


$$R_s = \frac{V_a^2}{P_0 L_s} \quad V_a = \int_0^{L_s} dz' G(z', t' = t_f)$$

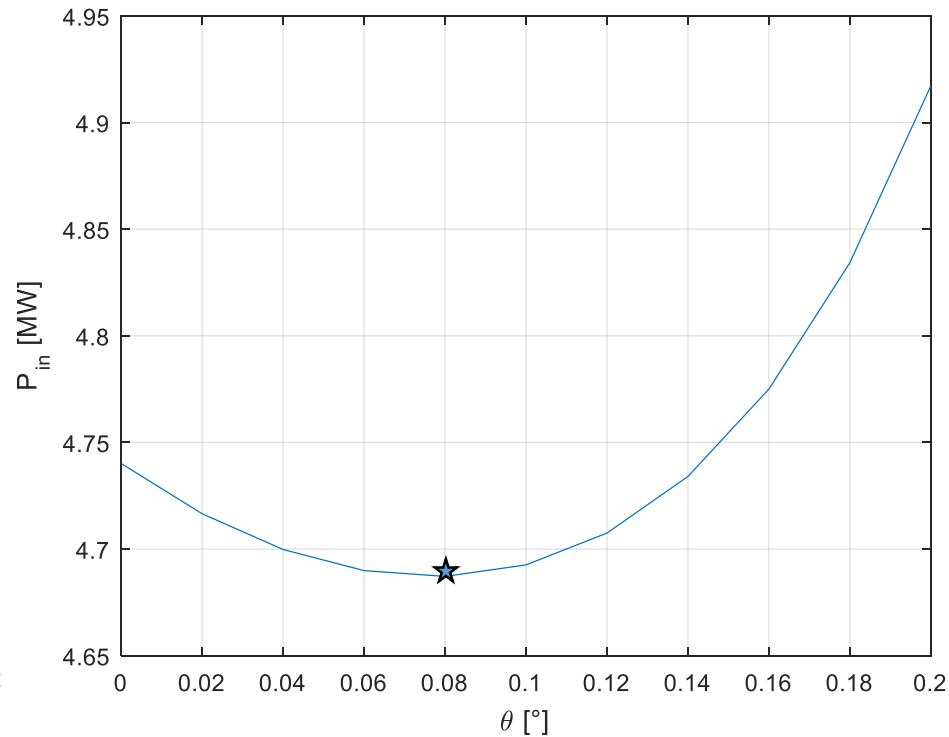
Considering the average (normalized to the input power) gradient or the effective shunt impedance we find that the optimal slope is 0.8° (corresponding to an iris radius variation from 3.5 mm to 2.9 mm).

$L_s=0.5\text{m}$ (60 cells), $N_s=32$, $Q_0=180000$

Filling time



Input power for each structure
(in order to obtain 57 MV/m)



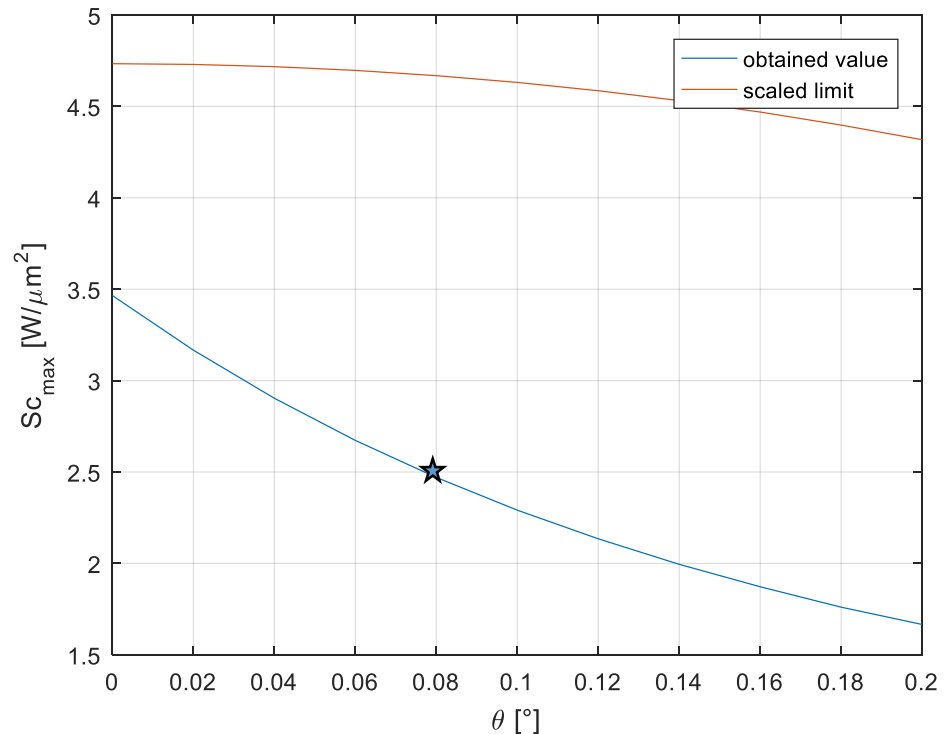
$$\tau(L_s) = \int_0^{L_s} \frac{dz'}{v_g(z')}$$

$L_s=0.5\text{m}$ (60 cells), $N_s=32$, $Q_0=180000$, $\langle G \rangle=57\text{ MV/m}$

Modified Poynting vector (calculated at the first cell)

The modified Poynting vector should not exceed $4\text{ W}/\mu\text{m}^2$ in order to have BDR below 1×10^{-6} bpp/m at pulse length of 200 ns

For each slope we are below the scaled limit (for an average gradient of 57 MV/m)

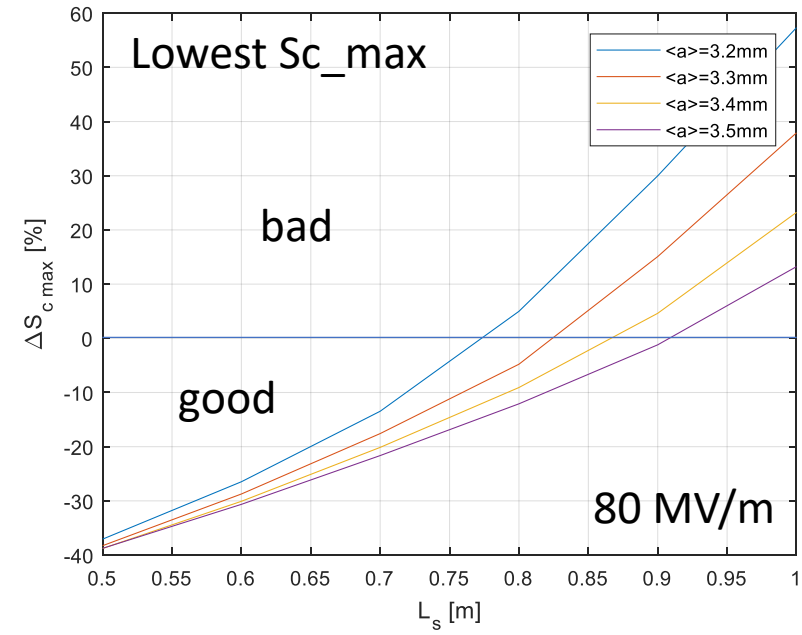
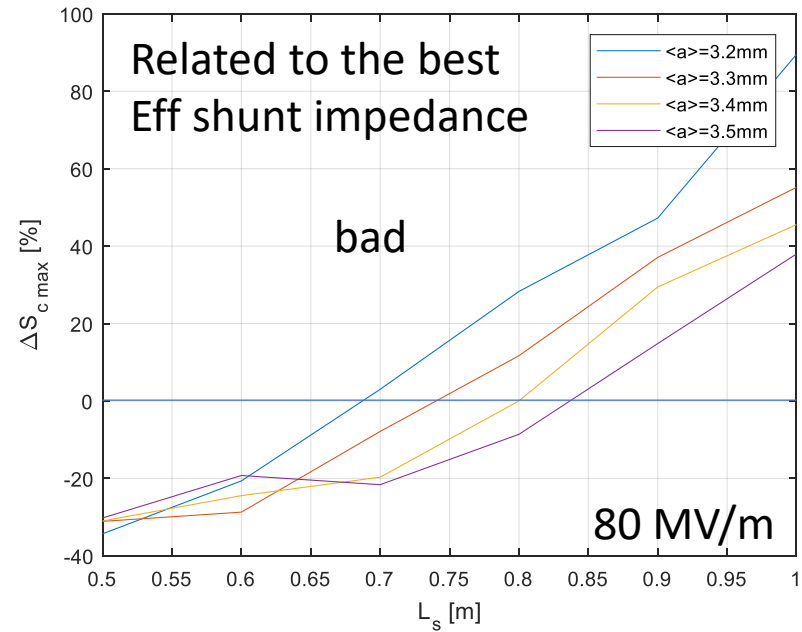
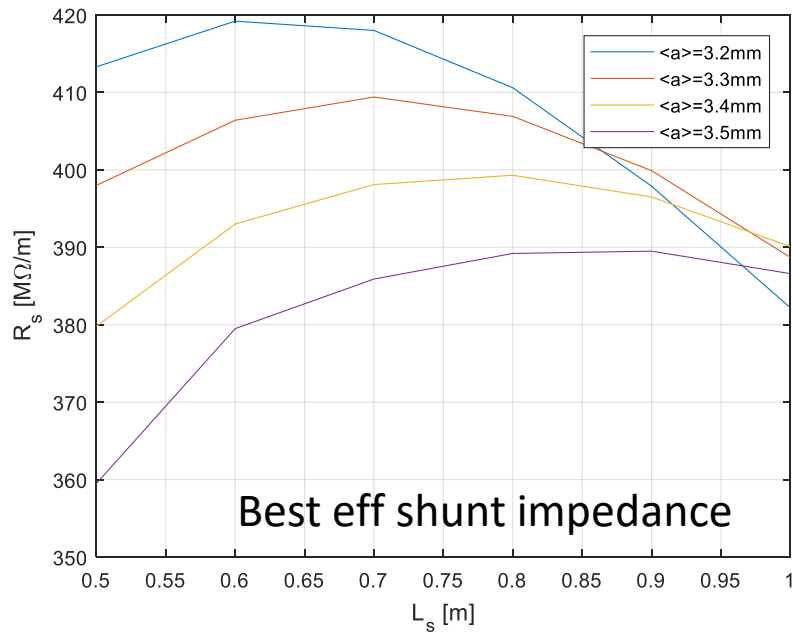


With this formula we take into account the fact that for every slope the filling time is slightly different

$$S_{c_{\text{scaled}}} = 4\text{ W} / \mu\text{m}^2 \frac{(200\text{ ns})^{1/3}}{t_p^{1/3}} \quad [4]$$

[4] A. Grudiev, S. Calatroni, and W. Wuensch, New local field quantity describing the high gradient limit of accelerating structures, PhysRevSTAB.12.102001 (2009)

STRUCTURE NUMERICAL OPTIMIZATION



$$\Delta S_{c_max} = (S_{c_max} - S_{c_limit}(10^{-6} \text{ bpp/m})) / S_{c_limit} * 100$$

MINIMUM IRIS RADIUS

Growth rate of the BBU due to wakefield kick from head to tail (Alexej Grudiev):

$$\gamma = \left| - \int_0^{L_t} \frac{Ne^2 W'_\perp(s)}{4k_\beta E(z)} dz \right| * \quad k_\beta \sim \frac{1}{\langle \beta \rangle}$$

$$W'_\perp(s) = \frac{4Z_0 c}{\pi a^4} s_1 \left[1 - \left(1 + \sqrt{\frac{s}{s_1}} \right) e^{-\sqrt{\frac{s}{s_1}}} \right] **$$

$$\frac{dW'_\perp(s)}{ds} = \frac{2Z_0 c}{\pi a^4} e^{-\sqrt{\frac{s}{s_1}}}$$

$$W'_\perp(\sigma_z) = \left. \frac{dW'_\perp(s)}{ds} \right|_{s=0} \sigma_z = \frac{2Z_0 c}{\pi a^4} \sigma_z$$

$$E(z) = E_0 + eGz$$

$$\gamma = \frac{Z_0 c}{2\pi a^4} \frac{eN\sigma_z \langle \beta \rangle}{a^4 G} \ln \left(\frac{E_L}{E_0} \right)$$

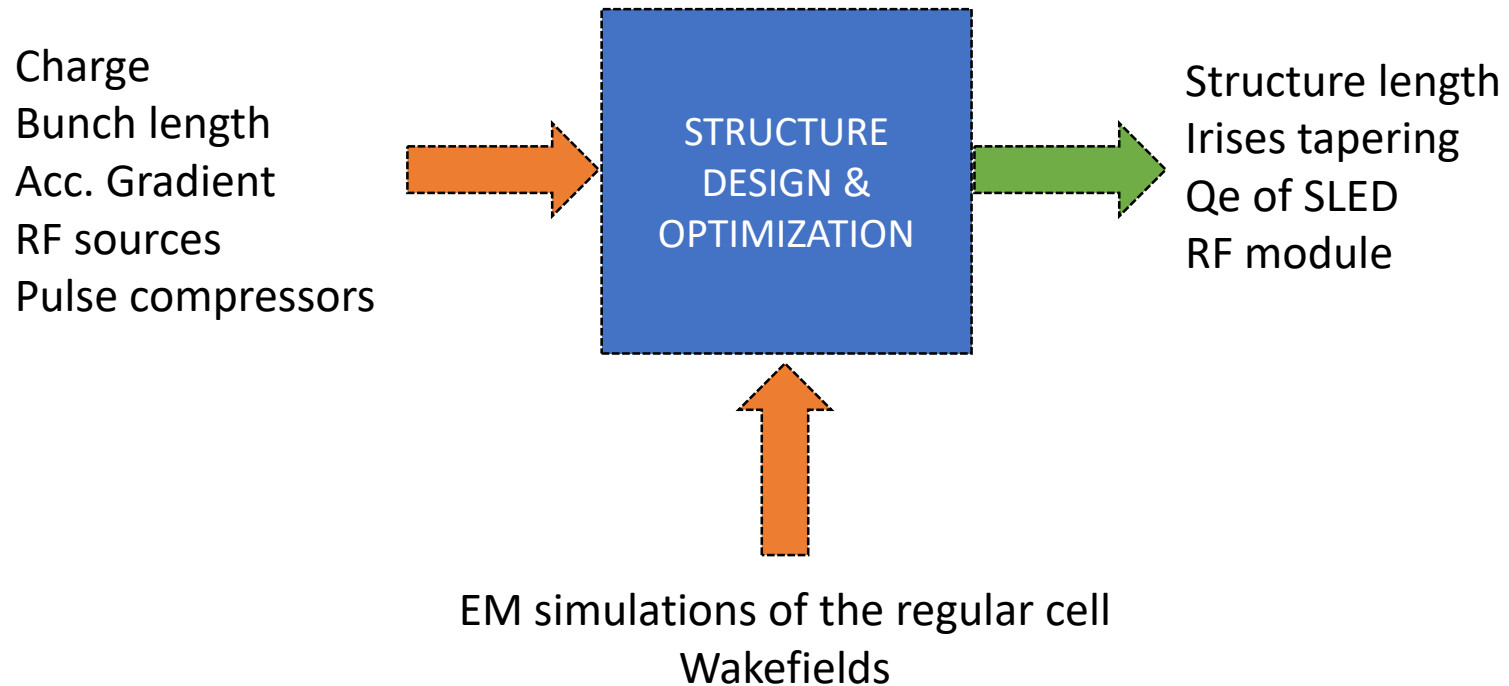
	PWFA	Full X-band
<G> [MV/m]	20	57
<β> [m]	~30	~30
E ₀ [MeV]	102	171
E _{L1} [MeV]	222	502
σ _z [μm]	50	112
eN [pC]	200	200
γ	2	2
a [mm]	3.2	

The critical part is the LINAC1, where beta is higher and the gradient is low.

* Alex Chao, "Physics of collective beam instabilities in high energy accelerators", 1993

** Karl Bane, "Short-range Dipole Wakefields in Accelerating structures for the NLC", SLAC-PUB-9663, 2003

STRUCTURE DESIGN & OPTIMIZATION



MATLAB code

- SLED plot $f(tf, Q_0, Q_e)$
- Import cell parameters from HFSS
- CI w/ SLED (analytical)
 - Contour plot $R_s/r=f(Q, Q_e) \rightarrow Q_{e_opt}=f(Q)$
 - Contour plot $\tau=f(Q, Q_e) \rightarrow \tau_{opt}=f(Q, \text{best } Q_e)$
 - (w/ HFSS data) Finds R_s max, τ_{opt} , G profile, L_{opt} , N_s , P_{tot} , N_k , Sc_{max} for every $\langle a \rangle$
- CG w/ SLED (analytical)
 - Contour plot $R_s/r=f(Q, Q_e) \rightarrow Q_{e_opt}=f(Q)$
 - Contour plot $\tau=f(Q, Q_e) \rightarrow \tau_{opt}=f(Q, \text{best } Q_e)$
 - (w/ HFSS data) Finds R_s max, τ_{opt} , G profile, L_{opt} , a first/last cells, vg first/last cells, equivalent linear tapering θ_{opt} , N_s , P_{tot} , N_k , Sc_{max} for every $\langle a \rangle$ (book and Grudiev's formulas)
 - Grudiev's formulas: new definition of τ that allows to plot vg vs τ

MATLAB code

- Numerical Approach
 - Fixed parameters: avg. iris radius, no. of cells, kly. Power, wg attenuation, avg. gradient
 - Design parameters: Q_e , theta of the linear tapering
 - It calculates the values of a , b , R , Q , v_g , Sc vs theta for every cell
 - It calculates the mean value of b between two cells, the $\tau(z)$ and then the filling time, $\alpha(z)$, τ_s , P_{out}/P_{in} , $g(z)$ for every slope
 - It calculates $EG_SLED(Q_e)$, $G_0(tf,z,Q_e)$, $G_0(tf,z,Q_e)$ and the Q_e that maximize V_a and then R_s for every slope
 - It calculates the slope that maximise R_s and the corresponding Sc_max , Kly. Power needed (considering attenuation) and peak Rf power in input of the cavity, the loss of $SLED_EG$ due to binary tree wg distribution

BEAM DYNAMICS SIMULATIONS

We have performed **beam dynamics simulations** with the tracking particle code **Elegant**. As a first approach, we have considered **Constant Impedance** structures with **wakefields** calculated with **Bane's formulas**.

The **energy spread** and the **distribution of the energy and current** along the electron bunch obtained with the simulation at the linac exit **satisfy the requirements***.

Next step: more accurate calculations considering the real tapering of the structure with **Shumail-Dolgashev's algorithm****.

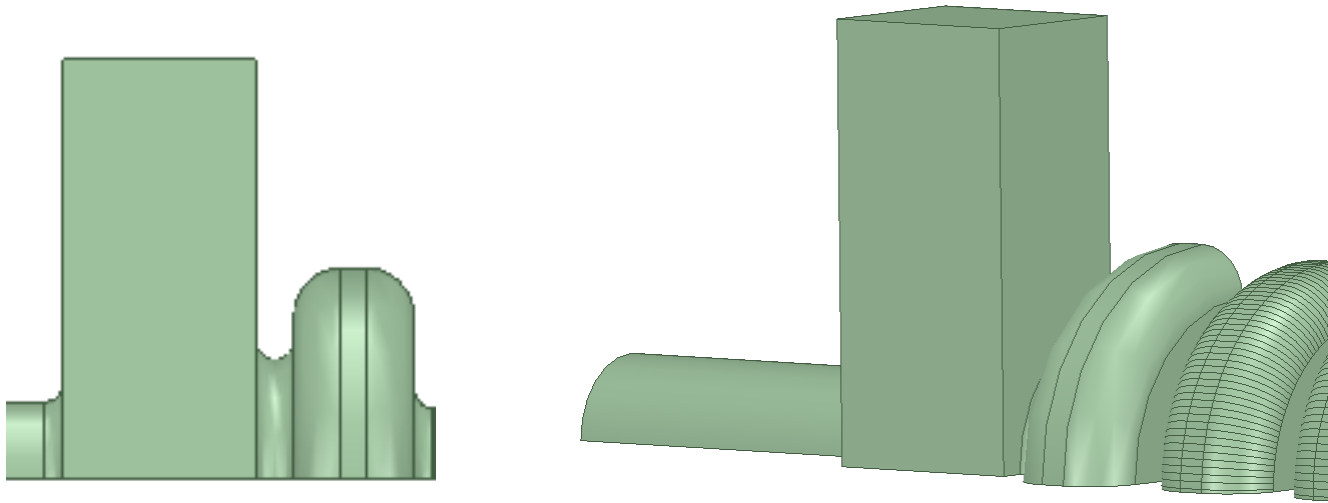
**C. Vaccarezza et al., EUPRAXIA@SPARC_LAB: Beam dynamics studies for the X-band Linac, NIM A 909 (2018) 314–317*

***M. Shumail and V. A. Dolgashev, Exact solution of multi-bunch instabilities for ultra-relativistic constant energy bunches in particle accelerators, Phys. Scr. 94 065208 (2019)*

COUPLERS DESIGN

Also a waveguide coupler has been designed. A **tapered waveguide** has been implemented in order to minimize the residual quadrupole field components.

The calculated **pulsed heating** on the input coupler is **<11 °C** (in the 80 MV/m case), the obtained **reflection coefficient** is **<-30 dB**.

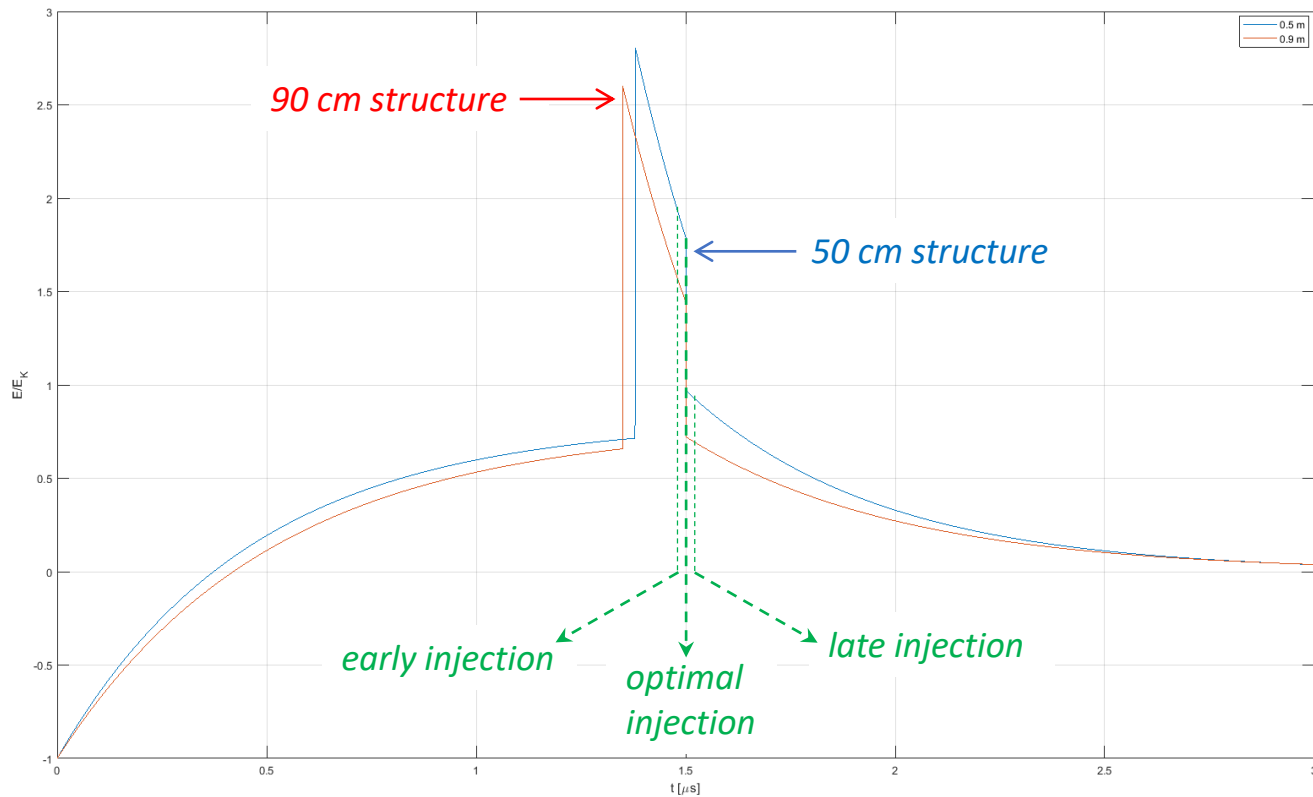


Work in progress:

- Calculate the equivalent quadrupole gradients g_B (and g_E) along z
- Calculate the integrated gradients

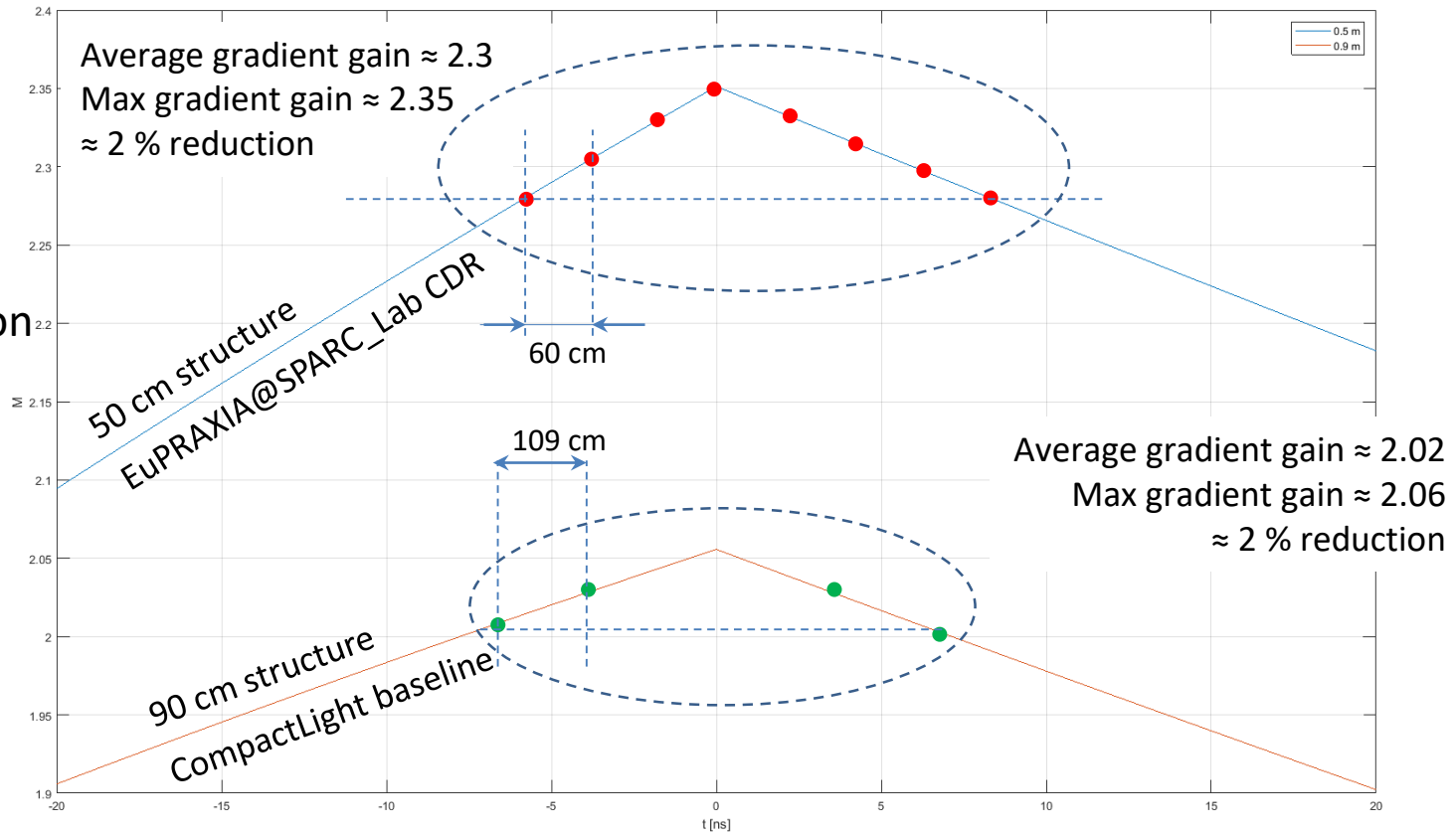
RF MODULE

The waveguide distribution is fully symmetric. This means that all cavities are filled simultaneously while the beam transit time between the first and the last cavity is 14 ns.



RF MODULE

Multiplication
Factor of
SLED



The plots represent the **average gradient gain for bunch injection timing errors** in the ± 20 ns range for the 2 considered modules: 8 x 50 cm (without magnets and diagnostics) and 4 x 90 cm structures. It is obtained by integrating the SLED compressed pulse in a **sliding time window whose width is constant and matches the structure filling time** (100 ns and 130 ns respectively). The module average gradient is slightly reduced because of the timing errors ($\approx 2\%$).

COMPARISON BETWEEN EuPRAXIA@SPARC_LAB AND CompactLight

	EuPRAXIA@SPARC_LAB	CompactLight
Frequency [GHz]	11.9942	
RF pulse [μ s]	1.5	
Net kly. power [MW]	≈ 40	
Average iris radius $\langle a \rangle$	3.2	3.5
Average gradient $\langle G \rangle$ [MV/m]	80 MV/m	65 MV/m
Linac Energy gain E_{gain} [GeV]	1.3	4.5
Structure length L_s [m]	0.5	0.9
Linac active length L_{act} [m]	16	69
Unloaded SLED Q-factor Q_0	180000	
External SLED Q-factor Q_E	19300	23000
Iris radius a [mm]	3.6-2.8	4.3-2.7
Group velocity v_g [%]	2.8-1.0	4.7-1.0
Section attenuation τ_s	0.534	0.767
Shunt impedance R [$M\Omega/m$]	105-130	90-131
Effective shunt Imp. R_s [$M\Omega/m$]	410	387
Filling time t_f [ns]	100	144
Structures per module N_m	8	4
Klystron power per module P_{k_m} [MW]	54	39
Peak input power [MW]	58	68
Input power averaged over the pulse [MW]	42	44
Total number of structures N_{tot}	32	80
Total number of klystrons N_k	8	20

Towards higher rep rate operation of the RF power sources (by Alessandro Gallo)

Any klystron model is optimized by design to be operated in a **specific working point** characterized by 3 parameters:

- **Max RF power** in saturation P_{RFsat} ;
- **Pulse duration** $\tau_{pulse} + \tau_{trans}$ (flat top + transient);
- **Repetition rate** f_{rep} .

The **tube efficiency** is defined as : $\eta = \frac{P_{RFsat}}{V \cdot I_k}$

and it is maximum when the tube is operated at the nominal working point.

The klystron operational **rep rate** can be **increased** at expenses of the **saturated RF power** (by decreasing the tube HV) and/or the **pulse duration**.

The **main limitation** for the rep rate increasing comes from the **power released** on the **tube collector** P_{coll} which can **not exceed** a **limit value** corresponding to the **nominal working point** (with some margin).

$$P_0 = V_0 I_0 = 410 kV \cdot 310 A = 127 MW; \quad \eta_{kly} = \frac{P_{RFmax}}{P_0} \square 40\%$$

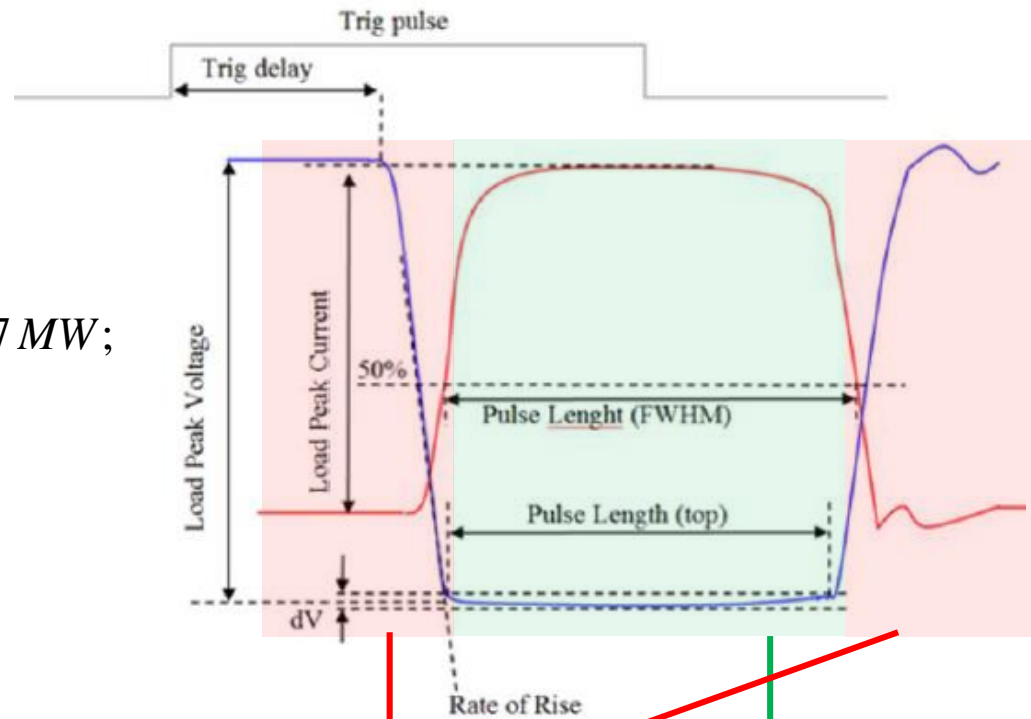
CPI VKX-8311A

OPERATIONAL PARAMETERS

	Unit	Value
RF frequency	MHz	11 994
RF peak power (max)	MW	50
RF average power (max)	kW	5.0
Modulator peak power	MW	127
Modulator average power (max)	kW	3.2
Operational voltage	kV	0 - 410
Operational current	A	0 - 310
PRF range	Hz	1 - 100
Pulse length (top)	μs	0.5 - 2.0
Top flatness (dV)	%	<±0.25
Rate of rise	kV/μs	300 - 450
Pulse to pulse stability	ppm	<50
Trig delay	μs	~1.2
Pulse to Pulse time jitter	ns	<±5
Pulse width time jitter	ns	<±8

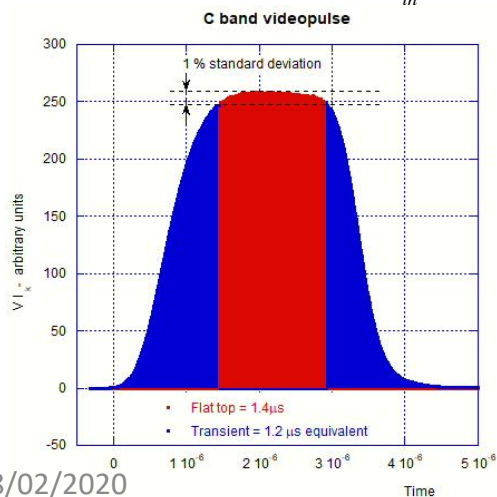
$$P_0 = V_0 I_0 = 410 \text{ kV} \cdot 310 \text{ A} = 127 \text{ MW};$$

$$\eta_{kly} = \frac{P_{RF_{max}}}{P_0} \approx 40\%$$



$$P_{coll} = U_{coll} f_{rep} = f_{rep} \int_{t_{in}}^{t_{fin}} V(t) I_k(t) dt = f_{rep} \left[\int_{trans} V(t) I_k(t) dt + \int_{flat\ top} V(t) I_k(t) dt \right]$$

$$\approx V_0 I_0 \tau_{trans} \quad \approx V_0 I_0 \tau_{pulse}$$



*Scandinova
modulator
pulse for C-
band klystron*

$$\text{with } \tau_{trans} = \frac{1}{V_0 I_0} \int_{trans} V(t) I_k(t) dt \approx 0.5 \div 2 \mu s$$

It mainly depends on the modulator characteristics

Klystron collector power limits are conservatively specified by manufacturers assuming transient durations longer than those provided by state-of-the-art solid state modulators. **Canon** (formerly Toshiba) specifies tubes (E37113 - X band and E37212 – C band) assume $\tau_{trans} \approx 2.5 \mu s$.

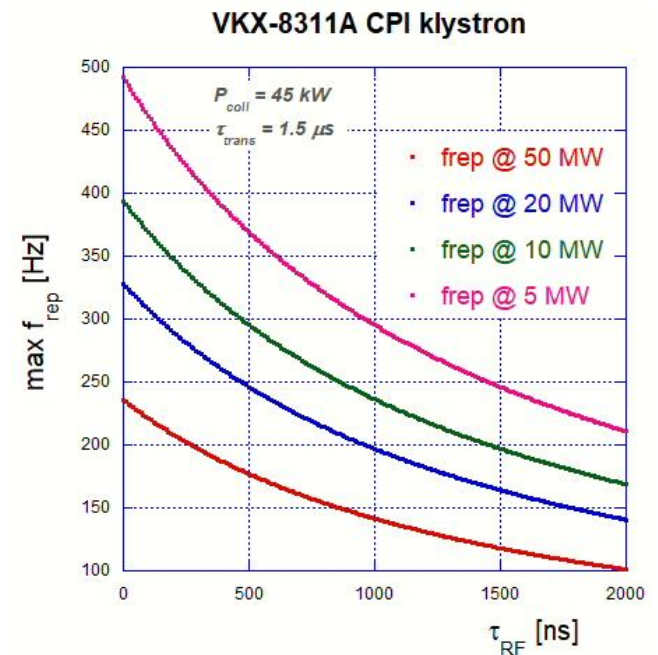
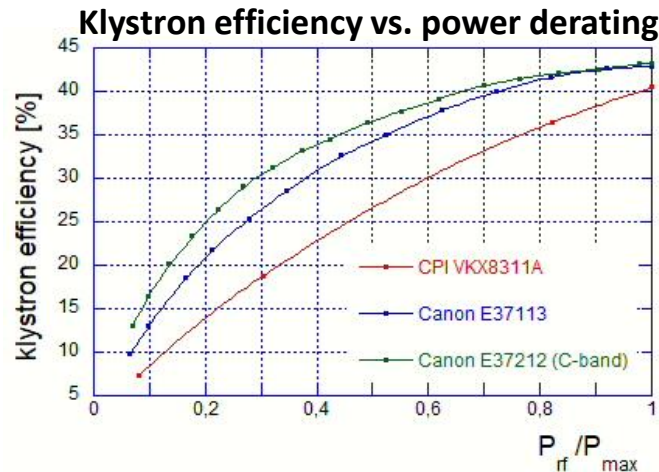
Assuming the same τ_{trans} value for the CPI VKX-8311A klystron (to be verified with CPI), we got:

$$P_{coll} \simeq V_0 I_{k_0} (\tau_{flat\ top} + \tau_{trans}) f_{rep} \simeq \frac{P_{RFsat}}{\eta} (\tau_{flat\ top} + \tau_{trans}) f_{rep} \simeq 127 MW \cdot (1.5 \mu s + 2.5 \mu s) \cdot 100 Hz \simeq 50.8 kW$$

Since the limit imposed by P_{coll} can not be overcome, the rep rate can only be increased at the expenses of the RF saturation power (HV working point) and/or RF pulse duration.

The amount of **rep rate increase** obtainable by reducing the pulse duration depends very much on the actual value of the **dead time τ_{trans}** , which is a **characteristics of the modulator**.

The amount of rep rate increase obtainable by **reducing the HV** and the RF saturation power P_{RFsat} is limited by the **tube efficiency decrease**.



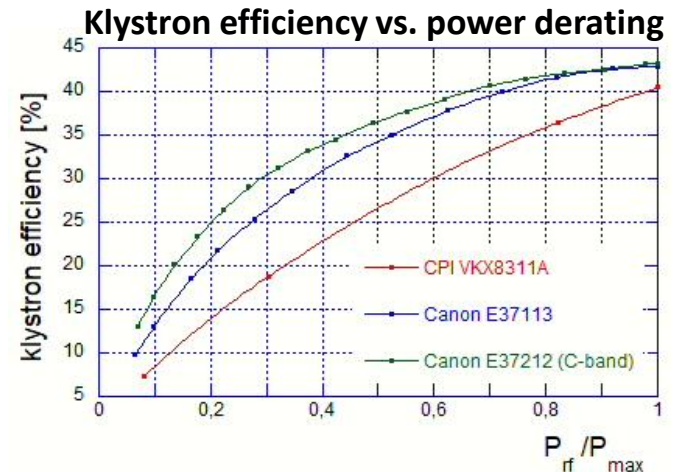
Towards higher rep rate operation of the RF power sources

The **main limitation** for the rep rate increasing comes from the **power released** on the **tube collector** P_{coll} which can **not exceed** a **limit value** corresponding to the **nominal working point** (with some margin).

The klystron operational **rep rate** can be **increased** at expenses of the **saturated RF power** (by decreasing the tube HV) and/or the **pulse duration**.

$$P_{coll} \simeq \frac{P_{RFsat}}{\eta} (\tau_{flat\ top} + \tau_{trans}) f_{rep}$$

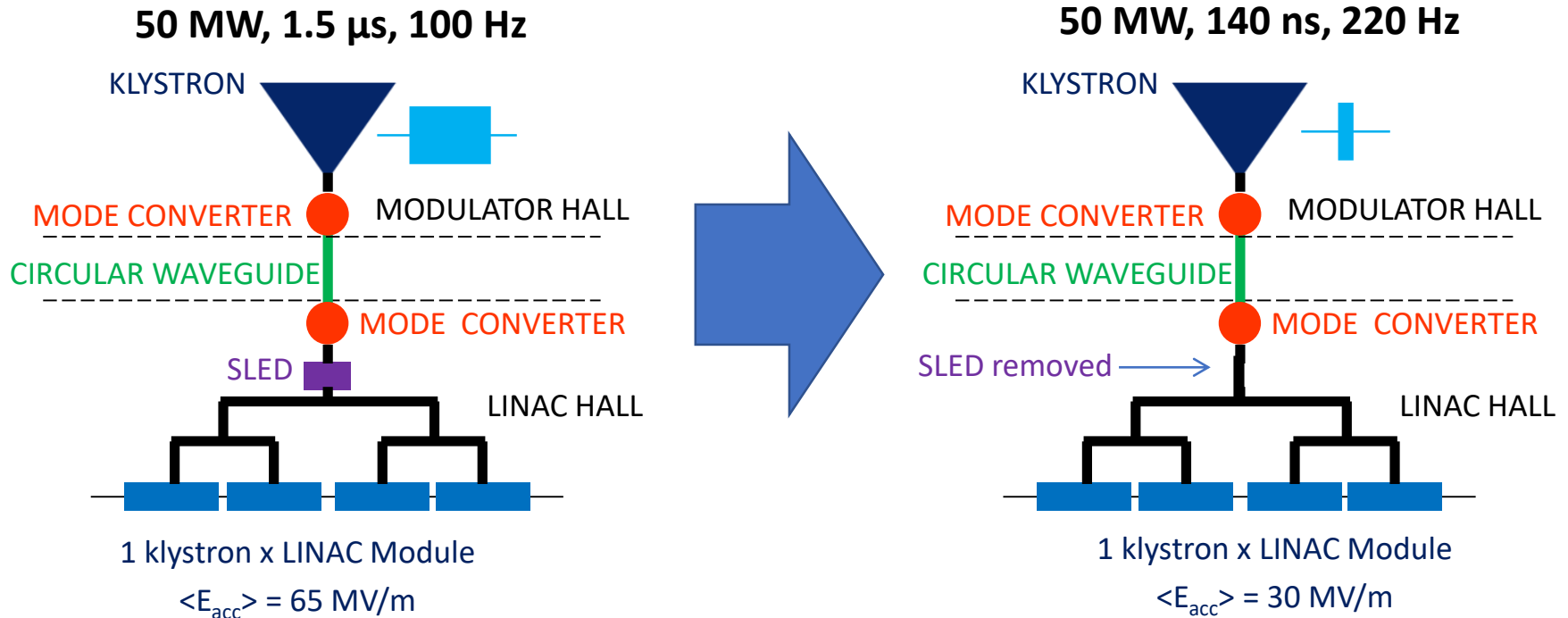
The amount of rep rate increase obtainable by **reducing the HV** and the RF saturation power P_{RFsat} is limited by the **tube efficiency decrease**.



The amount of rep rate increase obtained by **reducing the pulse duration** depends very much on the actual value of the **dead time** τ_{trans} , which is a **characteristics of the modulator**.

1st scenario: pulse shortening

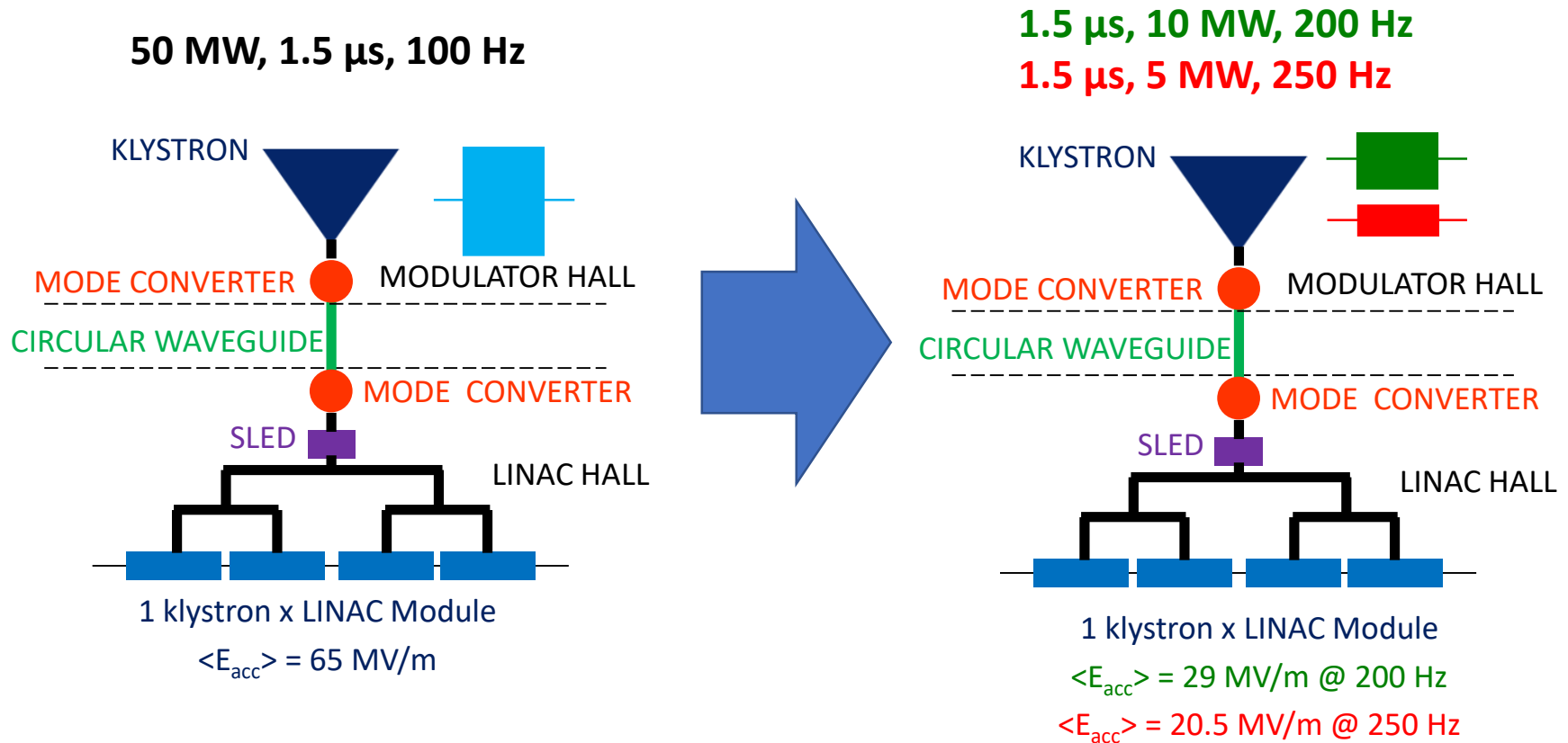
rep rate increase limited by modulator dead time ($\approx 1.5 \mu\text{s}$)



- **Linac energy downgraded to $\approx 45\%$ of the max value @ 220 Hz rep rate;**
- **Not flexible:** as soon as the SLED is removed the gradient is reduced by a factor ≈ 2.2 ;
- Klystron operated always at its nominal working point (good!);
- **Max rep rate very much dependent on modulator dead time τ_{trans}**

2nd scenario: klystron peak power reduced

rep rate increase limited by klystron inefficiency at reduced HV values



- Linac energy downgraded to $\approx 30\%$ of the max value @ 250 Hz rep rate;
- **Flexible**: different compromises between rep rate and RF peak power explorable;
- Klystron operated in a **wide range of working points (realistic?)**

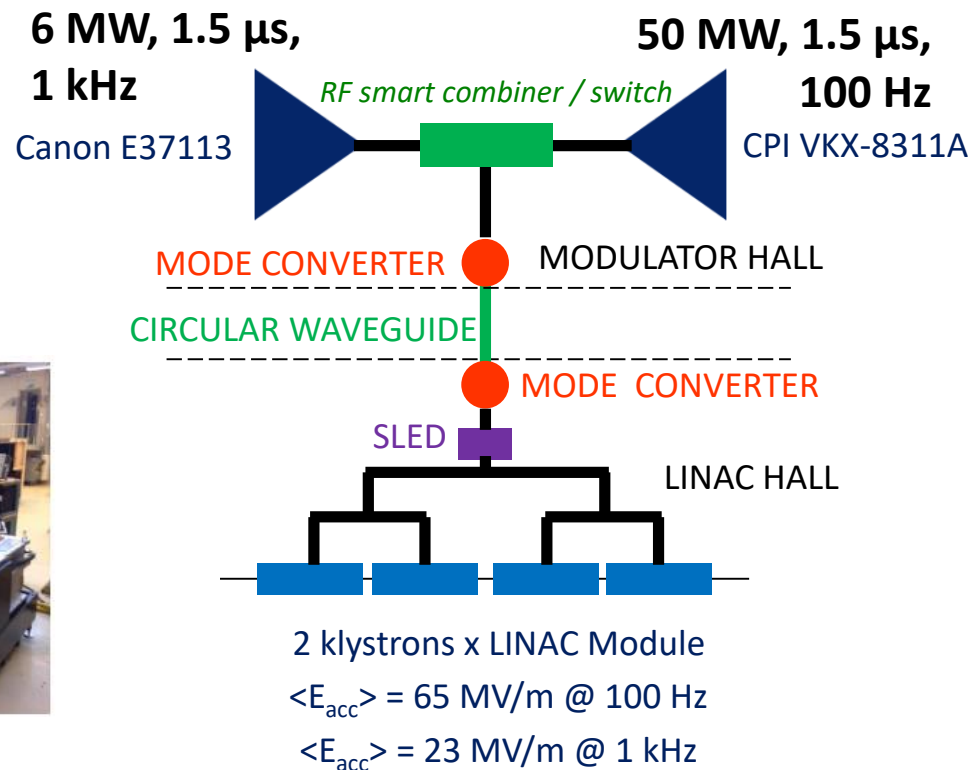
3rd scenario: high rep rate – reduced peak power klystrons

rep rate increase based on dedicated tubes, in substitution of or in addition to high peak power ones

Canon E37113 klystrons

Scandinova solid state modulators

Parameters	Specifications	units
	E37113	
RF Frequency	11.9942	GHz
Peak RF power	6	MW
RF pulse length	5	μ s
Pulse repetition rate	400	Hz
Klystron voltage	150	kV
Micro perveance	1.5	

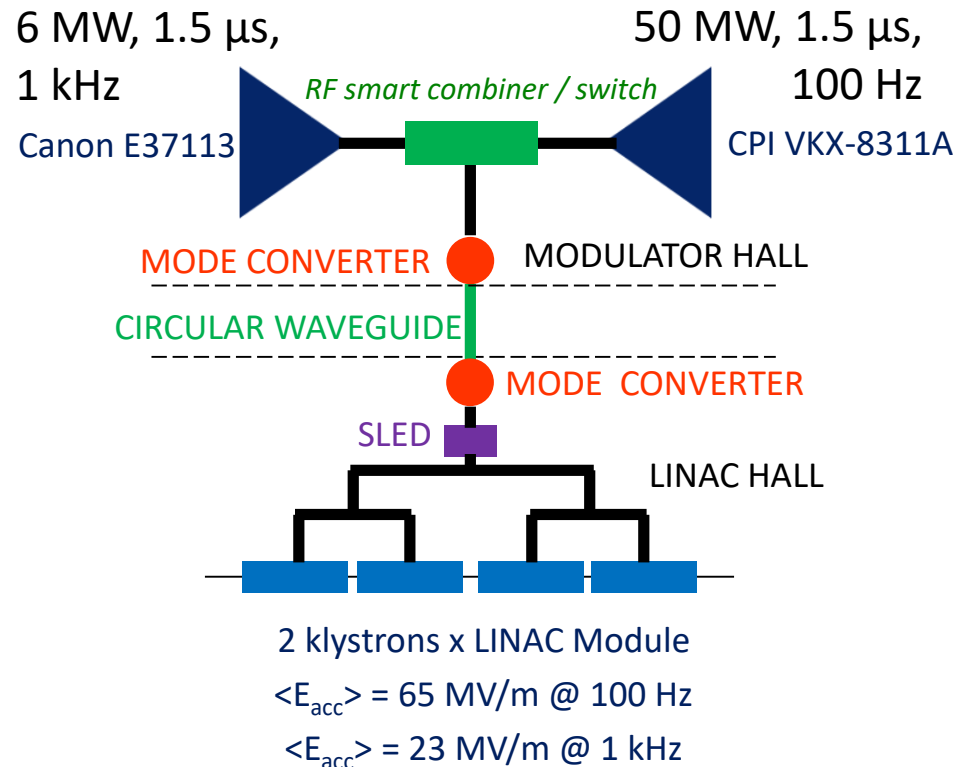
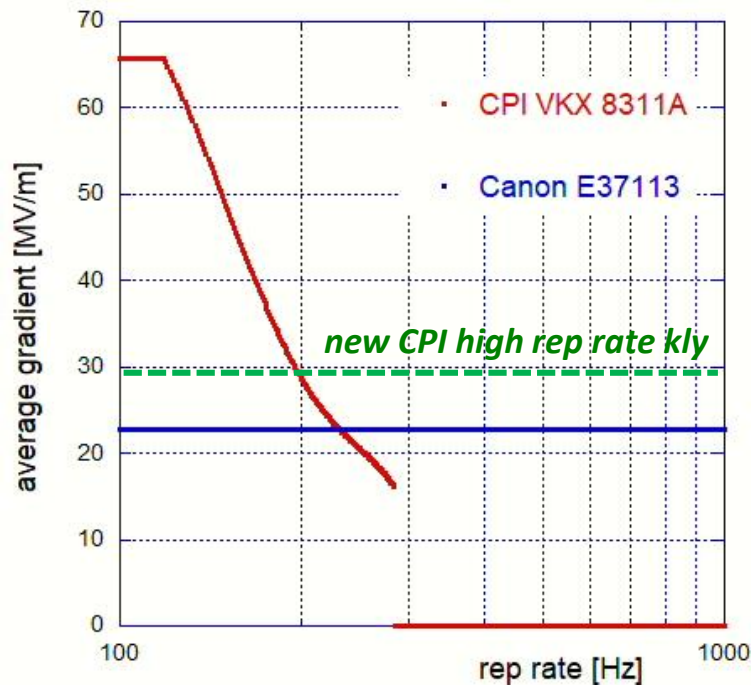


6 MW, 1.5 μ s, 1 kHz operation probably possible

- **1 kHz rep rate capability, with linac energy up to \approx 35% of the max value;**
- Switching or combining 2 sources would preserve **high gradient at low rep rate;**
- If source combination is possible, **gradients > 30 MV/m available at rep rates \leq 250 Hz;**
- **CPI will probably announce a new tube capable of delivering 10 MW, 1.5 μ s, 1 kHz (gradient of 30 MV/m)**

3rd scenario: high rep rate – reduced peak power klystrons

rep rate increase based on dedicated tubes, in substitution for or in addition to high peak power ones



This study is very rough and need to be continued more rigorously, but we need:

- more precise requests and **specifications by FEL users**
- more **technical data from klystron producer**
- more **experimental data** from existing power plants (high rep rate tests @ Xboxes?)
- maybe **new creative ideas** to better exploit the existing hardware...

ACCELERATING STRUCTURE AND MODULE: PARAMETERS

Parameter	Value
Frequency [GHz]	11.9942
Phase advance per cell [rad]	$2\pi/3$
Shunt impedance R [MΩ/m]	90-131
Effective shunt Imp. R_s [MΩ/m]	387
Group velocity v_g [%]	4.7-1.0
P_{out}/P_{in}	0.215
Filling time [ns]	144
Number of cells per structure	108
Unloaded SLED Q-factor Q_0	180000
External SLED Q-factor Q_E	23000
# structures per module N_m	4
Module active length L_{mod} [m]	3.6
Average iris radius $\langle a \rangle$	3.5
Iris radius input-output [mm]	4.3-2.7
Structure length L_s [m]	0.9
Accelerating cell length [mm]	8.332

	Rep. rate [Hz]		
	100	250	1000
Average gradient $\langle G \rangle$ [MV/m]	65	32	30.4
Max klystron available output power [MW]	50	50	10
Required input power per module P_K [MW]	39	42.5	8.5
RF pulse [μs]	1.5	0.15	1.5
SLED	ON	OFF	ON
Av. diss. power per structure [kW]	1	0.31	2.2
Peak input power per structure [MW]	68	10.6	14.8
Av. Input power per structure [MW]	44	10.6	9.6
Module energy gain [MeV]	234	115	109

CONTRIBUTORS

INFN

David Alesini

Marco Bellaveglia

Simone Bini

Bruno Buonomo

Fabio Cardelli

Enrica Chiadroni

Gianluca di Raddo

Roberto di Raddo

Massimo Ferrario

Alessandro Gallo

Andrea Ghigo

Anna Giribono

Valerio Lollo

Luca Piersanti

Bruno Spataro

Cristina Vaccarezza

CERN

Nuria Catalan Lasheras

Alexej Grudiev

Matteo Volpi

Walter Wuensch

SLAC

Valery Dolgashev

Muhammad Shumail

Filippos Toufexis